OIL SPILL SCIENCE *and* TECHNOLOGY

Edited by
Mervin Fingas

G P
P

Oil Spill Science and Technology

Oil Spill Science and Technology

Prevention, Response, and Cleanup

Edited by
Mervin Fingas

ELSEVIER

Amsterdam • Boston • Heidelberg • London • New York • Oxford
Paris • San Diego • San Francisco • Singapore • Sydney • Tokyo

Gulf Professional Publishing is an imprint of Elsevier

Gulf Professional Publishing is an imprint of Elsevier
30 Corporate Drive, Suite 400, Burlington, MA 01803, USA
The Boulevard, Langford Lane, Kidlington, Oxford, OX5 1GB, UK

Notices

Knowledge and best practice in this field are constantly changing. As new research and experience broaden our understanding, changes in research methods, professional practices, or medical treatment may become necessary.

Practitioners and researchers must always rely on their own experience and knowledge in evaluating and using any information, methods, compounds, or experiments described herein. In using such information or methods they should be mindful of their own safety and the safety of others, including parties for whom they have a professional responsibility.

To the fullest extent of the law, neither the Publisher nor the authors, contributors, or editors, assume any liability for any injury and/or damage to persons or property as a matter of products liability, negligence or otherwise, or from any use or operation of any methods, products, instructions, or ideas contained in the material herein.

Library of Congress Cataloging in Publication Data

Oil spill science and technology : prevention, response, and clean up / edited by Mervin Fingas. – 1st ed.
p. cm.
Summary: "The National Academy of Sciences estimate that 1.7 to 8.8 million tons of oil are released into world's water every year, of which more than 70% is directly related to human activities. The effects of these spills are all too apparent: dead wildlife, oil covered marshlands and contaminated water chief among them. This reference will provide scientists, engineers and practitioners with the latest methods use for identify and eliminating spills before they occur and develop the best available techniques, equipment and materials for dealing with oil spills in every environment. Topics covered include: spill dynamics and behaviour, spill treating agents, and cleanup techniques such as: in situ burning, mechanical containment or recovery, chemical and biological methods and physical methods are used to clean up shorelines. Also included are the fate and effects of oil spills and means to assess damage"– Provided by publisher.
ISBN 978-1-85617-943-0
1. Oil spills–Prevention. 2. Oil spills–Cleanup. 3. Oil spils–Managements. I. Fingas, Mervin F.
TD427.P4O38785 2010
628.1'6833–dc22

2010033465

British Library Cataloguing in Publication Data

A catalogue record for this book is available from the British Library.

ISBN: 978-1-85617-943-0

11 12 13 10 9 8 7 6 5 4 3 2 1
Printed and bound in the USA

Contents

Chapter 6

Oil Spill Remote Sensing: A Review

Merv Fingas and Carl E. Brown

Chapter Outline

6.1. INTRODUCTION

Large spills of oil and related petroleum products in the marine environment can have serious biological and economic impacts. Public and media scrutiny is usually intense following a spill, with demands that the location and extent of the oil spill be determined. Remote sensing is playing an increasingly important role in oil spill response efforts. Through the use of modern remote-sensing instrumentation, oil can be monitored on the open ocean around the clock. With knowledge of slick locations and movement, response personnel can more effectively plan countermeasures in an effort to lessen the effects of the pollution. In recent years, there has been a strong interest in detection of illegal discharges, especially in view of the large seabird mortality associated with such discharges.[1]

Even though sensor design and electronics are becoming increasingly sophisticated and much less expensive, the operational use of remote-sensing

Oil Spill Science and Technology. DOI: 10.1016/B978-1-85617-943-0.10006-1

equipment lags behind the technology. In remote sensing, a sensor, other than the eye or conventional photography, is used to detect the target of interest at a distance. The most common forms of oil spill surveillance and mapping are still sometimes carried out with simple still or video photography. Remote sensing from an aircraft is still the most common form of oil spill tracking. Attempts to use satellite remote sensing for oil spills continue, although success is not necessarily as claimed and is generally limited to identifying features at sites where known oil spills have occurred or for mapping discharges or known spills.

It is important to divide the uses of remote sensing into the end use or objective, as the utility of the sensor or sensor system is best defined that way. Remote-sensing systems for oil spills used for routine surveillance certainly differ from those used to detect oil on shorelines or land. A single tool does not serve for all functions. For a given nation and several functions, many types of systems may, in fact, be needed. Furthermore, it is necessary to consider the end use of the data. The end use of the data, be it location of the spill, enforcement, or support to cleanup, may also dictate the resolution or character of the data needed.

Several general reviews of oil spill remote sensing have been prepared.[2-7] These reviews show that although progress has been made in oil spill remote sensing, this progress has been slow. Furthermore, these reviews show that specialized sensors offer advantages to oil spill remote sensing. Off-the-shelf sensors have very limited application to oil spills.

6.2. VISIBLE INDICATIONS OF OIL

Under many circumstances oil on the surface is not visible to the eye.[8] Other than the obvious situations of nighttime and fog, in many situations oil cannot be seen. A very common situation is that of thin oil, such as from ship discharges, or

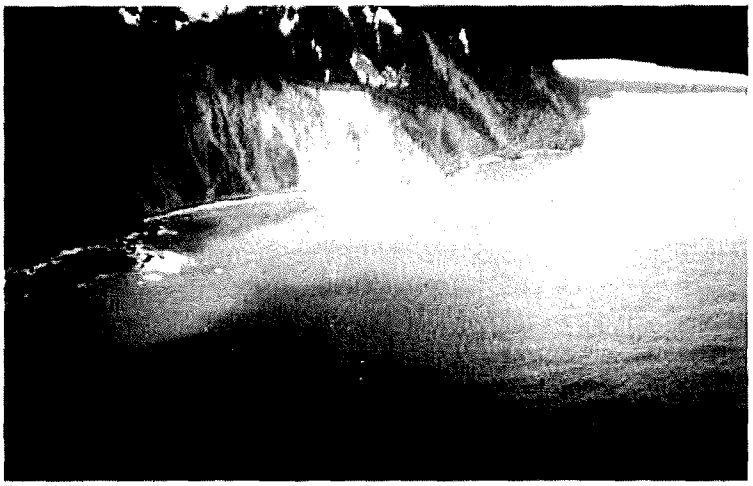

FIGURE 6.1 An example of problems in detecting slicks visually. There is no oil in this image. The differences in water color are caused by mineral fines at the top of the pictures and the meeting of darker water from the open ocean.

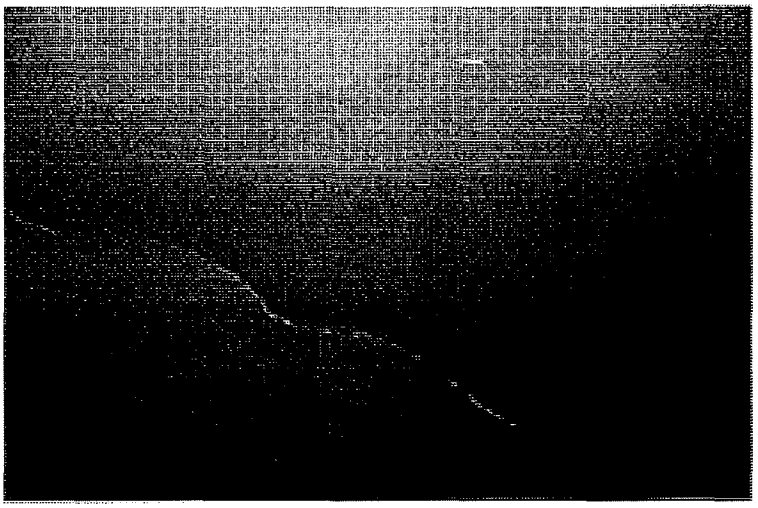

FIGURE 6.2 Another example of confusion in the visible region. This anomaly is caused by the front between a river and seawater. Again there is no oil in this image.

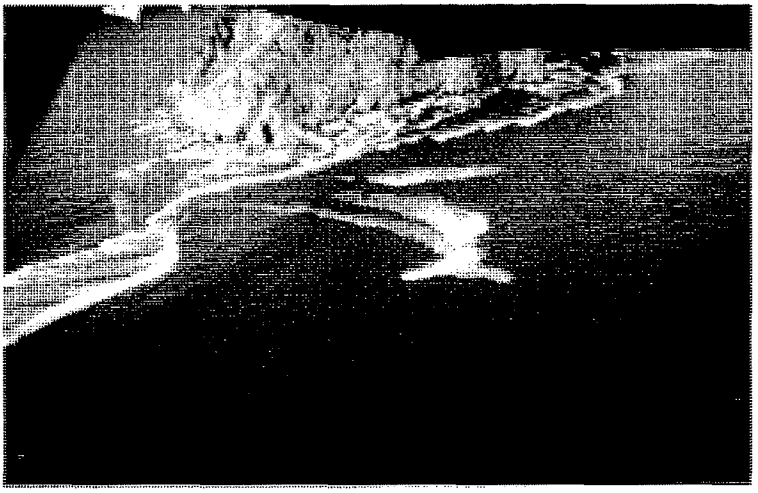

FIGURE 6.3 An image of Herring "milk" on the water surface. This is often mistaken for oil in various sensors, and again there is no oil in this image.

the presence of materials, such as sea weed, ice, and debris, that mask oil presence. Often there are conditions on the sea that may appear like oil, when indeed there is no oil. These include wind shadows from land forms, surface wind patterns on the sea, surface dampening by submerged objects or weed beds, natural oils or biogenic material, and oceanic fronts. In the case of large spills, the area may be too great to be mapped visually. Several of these cases are illustrated in Figures 6.1 to 6.12. All of these factors dictate that remote-sensing systems be used to assist in the task of mapping and identifying oil. In many cases, aerial observation and remote sensing are necessary to direct cleanup crews to slicks. Figure 6.13 shows a case where no aerial direction

FIGURE 6.4 This image again shows no oil and shows open seawater at a front with mineral-laden bay water.

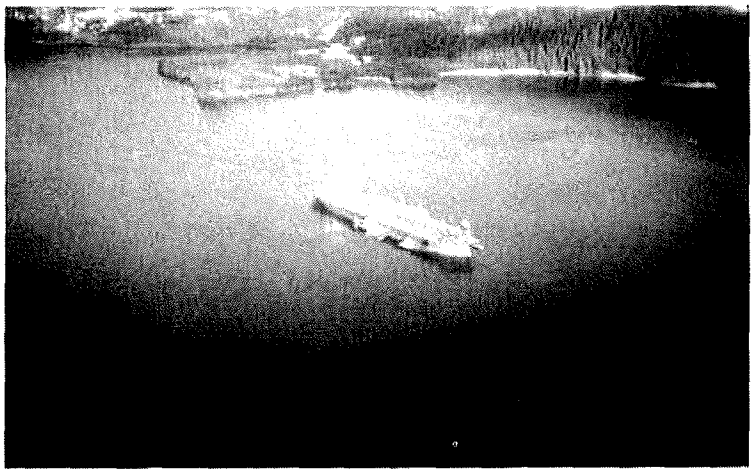

FIGURE 6.5 An image of the *Exxon Valdez* tanker at Naked Island. The apparent oil is actually reflections from clean water and some wind ruffles on the sea. There is no oil in this image.

was given and a skimmer crew is missing the slick by about half a kilometer. Figure 6.14 shows a skimmer crew that was directed to the thicker slick in the area.

6.3. OPTICAL SENSORS

6.3.1. Visible

The use of human vision alone is not considered remote sensing; however, it still represents the most common technique for oil spill surveillance. In the

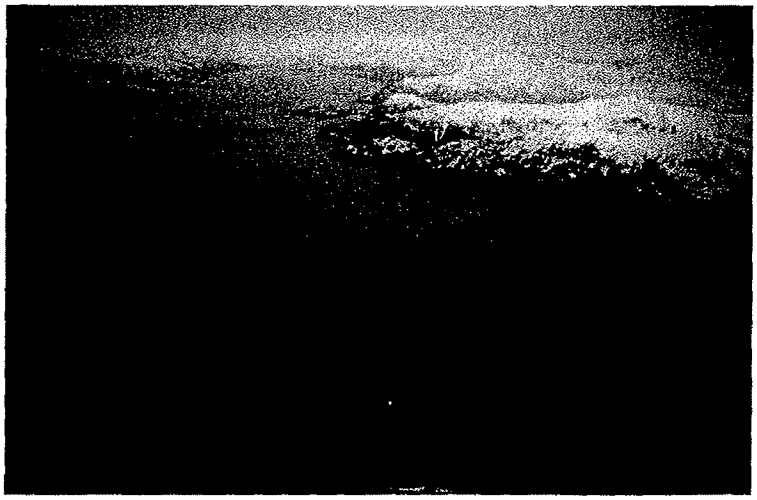

FIGURE 6.6 An image looking into a bay. The foreground material is oil; however what appears somewhat like oil further into the bay are actually surface wind calms.

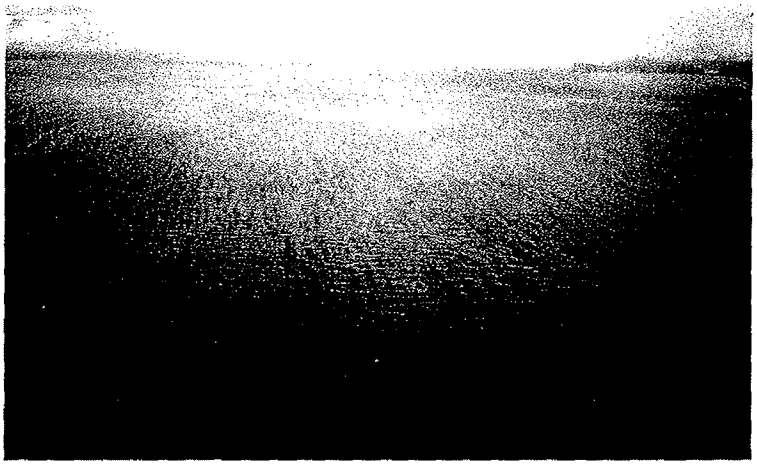

FIGURE 6.7 An image of sheen from a major spill. One can see sheen to a distance of about 30 km and about 10 km wide. Large areas like this are hard to map without the aid of remote sensing.

past, major campaigns using only human vision were mounted with varying degrees of success.[9] Optical techniques, using the same range of the visible spectrum detection, are the most common means of remote sensing. Cameras, both still and video, are common because of their low price and commercial availability. In recent years, visual or camera observation has been enhanced by the use of GPS (Global Positioning Systems).[10] Systems are now available to directly map remote-sensing data onto base maps.

In the visible region of the electromagnetic spectrum (approximately 400 to 700 nm), oil has a higher surface reflectance than water, but shows limited nonspecific absorption tendencies. Oil generally manifests throughout the

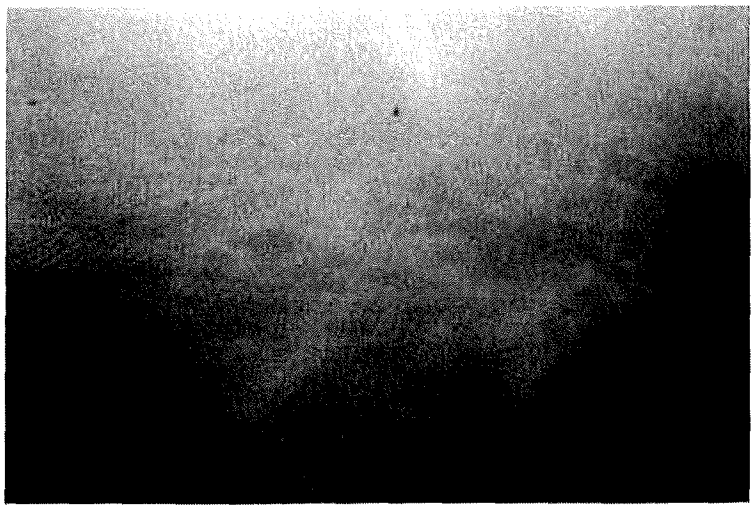

FIGURE 6.8 An image of water from an airplane during foggy conditions. There is no oil in this image.

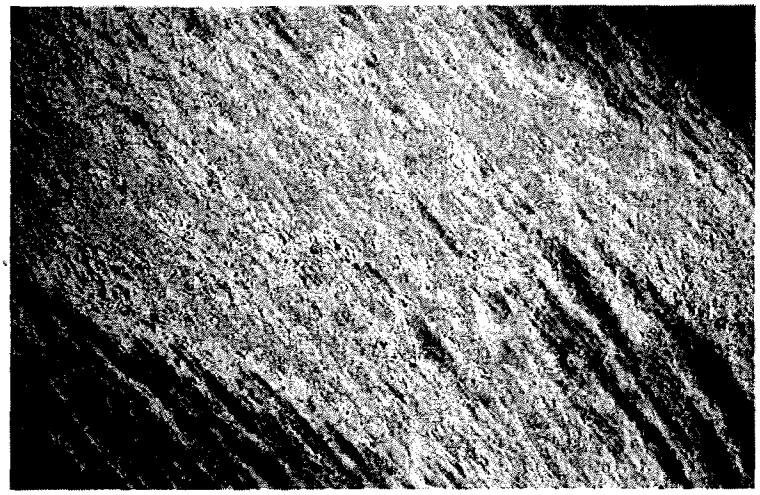

FIGURE 6.9 A visible image of a slick that had just been illegally discharged from a ship. The multiple colors are due to the light path interference and indicates a thickness of about 1 μm.

entire visible spectrum. Sheen shows up silvery and reflects light over a wide spectral region down to the blue. As there is no strong information in the 500 to 600 nm region, this region is often filtered out to improve contrast.[11] Overall, however, oil has no specific characteristics that distinguish it from the background.[12] Taylor studied oil spectra in the laboratory and the field and observed flat spectra with no usable features distinguishing it from the background.[13] Therefore, techniques that separate specific spectral regions do not increase detection capability. Some researchers noted that while the oil spectra is flat, the presence of oil may slightly alter water spectra.[14] It has been suggested that

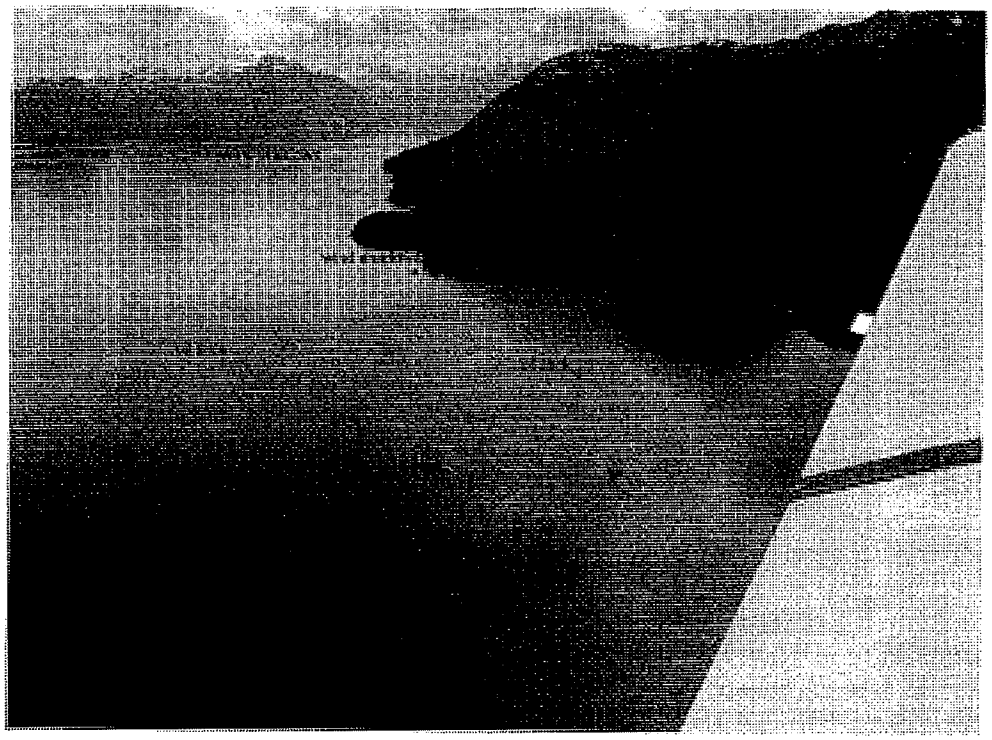

FIGURE 6.10 A visible image of a cleanup operation. Notice the various false indications of oil further away from the scene. *Photography by Environment Canada.*

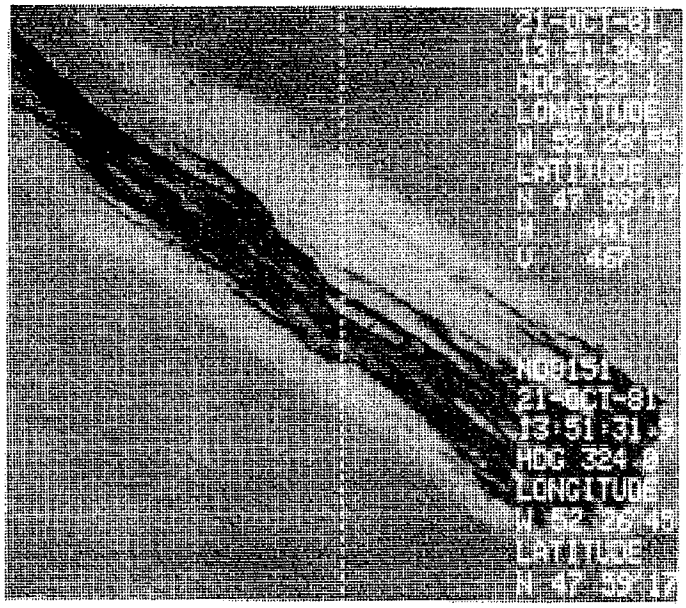

FIGURE 6.11 An infrared image of a slick as taken in 1981. Note the annotation providing essential times and positions.

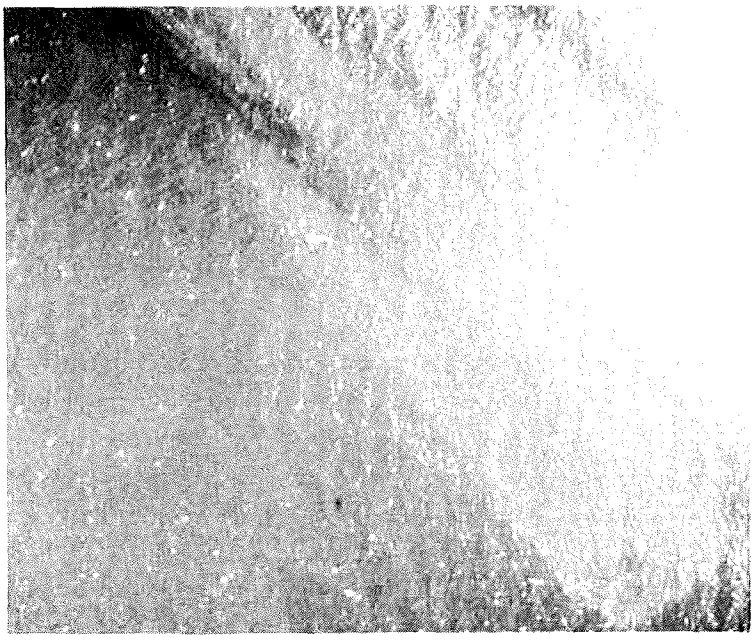

FIGURE 6.12 A visible image of the same slick and at the same time as the one shown in Figure 6.11. This illustrates the higher capability that infrared imaging has under these specific conditions.

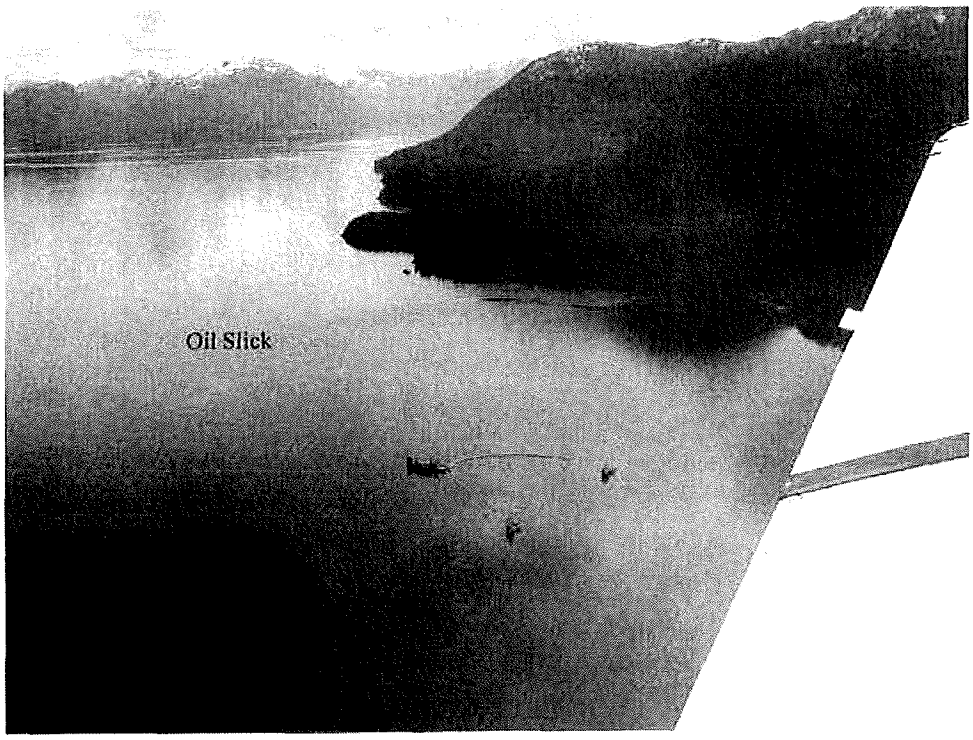

FIGURE 6.13 A visible image of a cleanup crew missing a slick by at least a half kilometer. The actual slick is noted on the image. Aerial direction of cleanup crews is not only desirable but necessary in many cases. *Photography by Environment Canada.*

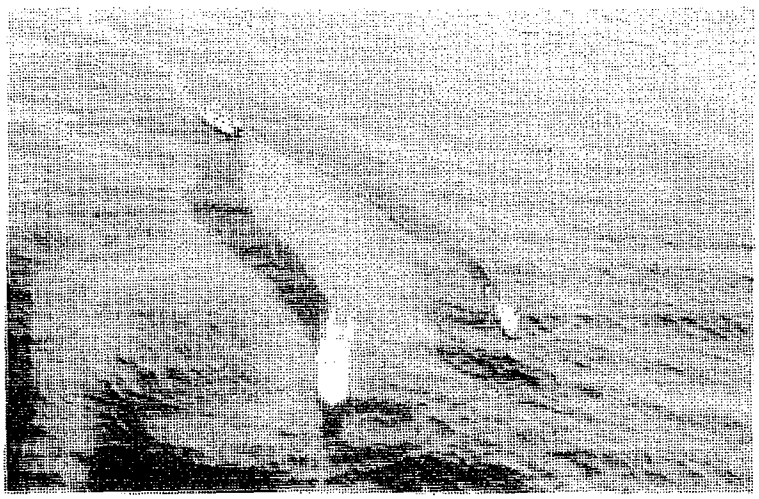

FIGURE 6.14 A visible image of a cleanup crew aiming toward the thickest slicks in the area as directed by an aerial surveillance team.

the water peaks are raised slightly at 570 to 590, 780 to 710, and 810 to 710 nm. At the same time there are depressions or troughs at 650 to 680 nm and 740 to 760 nm. It has been found that high contrast in visible imagery can be achieved by setting the camera at the Brewster angle (53 degrees from vertical) and using a horizontally aligned polarizing filter that passes only that light reflected from the water surface.[15] This is the component that contains the information on surface oil.[11] It has been reported that this technique increases contrast by up to 100%. Filters with band-pass below 450 nm can be used to improve contrast. View angle is important, and some researchers have noted that the thickness changes the optimal view angle.[16]

On land, hyperspectral data (use of multiple bands, typically 10 to 100) has been used to delineate the extent of an oil well blowout.[17] The technique used was spectral reflectance in the various channels, as well as the usual black coloration.

Video cameras are often used in conjunction with filters to improve the contrast in a manner similar to that noted for still cameras. This technique has had limited success for oil spill remote sensing because of poor contrast and lack of positive discrimination. Despite this, video systems have been proposed as remote-sensing systems.[18] With new light-enhancement technology (low lux), video cameras can be operated even in darkness. Tests of a generation III night vision camera shows that this technology is capable of providing imagery in very dark night conditions.[19,20]

Scanners were used in the past as sensors in the visible region of the spectrum. A rotating mirror or prism sweeps the field-of-view (FOV) and directs the light toward a detector. Before the advent of CCD (charge-coupled device) detectors, this sensor provided much more sensitivity and selectivity than a video camera. Another advantage of scanners was that signals were

digitized and processed before display. Recently, newer technology has evolved, and similar digitization can now be achieved without scanning by using a CCD imager and continually recording all elements, each of which is directed to a different FOV on the ground. This type of sensor, known as a push-broom scanner, has many advantages over the older scanning types. It can overcome several types of aberrations and errors, the units are more reliable than mechanical ones, and all data are collected simultaneously for a given line perpendicular to the direction of the aircraft's flight. Several types of scanners were developed. In Canada, the MEIS (Multidetector Electro-optical Imaging Scanner) and the CASI (Compact Airborne Spectrographic Imager) have been developed, and in the Netherlands, the Caesar system was developed.[11, 21, 22]

Digital photography has enabled the combination of photographs and the processing of images. Locke et al. used digital photography from vertical images to form a mosaic for an area impacted by an oil spill.[23] It was then possible to form a singular image and to classify oil types by color within the image. The area impacted by the spill was also carried out. Video cameras are often used in conjunction with filters to improve the contrast in a manner similar to that noted for still cameras. This technique has had limited success for oil spill remote sensing because of poor contrast and lack of positive discrimination.

The detection or measurement of oil in water has never been successfully accomplished using remote visible technology. There may be potential for light scattering technology. Stelmaszewski and coworkers measured the light scattering of crude oil in water emulsions and noted that scattering increases with wavelength in the UV range and decreases slightly with the wavelength of visible light.[24]

The use of visible techniques in oil spill remote sensing is largely restricted to documentation of the spill because there is no mechanism for positive oil detection. Furthermore, there are many interferences or false alarms. Sun glint and wind sheens can be mistaken for oil sheens. Biogenic material such as surface seaweeds or sunken kelp beds can be mistaken for oil. Oil on shorelines is difficult to identify positively because seaweeds look similar to oil and oil cannot be detected on darker shorelines. In summary, the usefulness of the visible spectrum for oil detection is limited. It is, however, an economical way to document spills and provide baseline data on shorelines or relative positions.

6.3.2. Infrared

Oil, which is optically thick, absorbs solar radiation and reemits a portion of this radiation as thermal energy, primarily in the 8 to 14 μm region. In infrared (IR) images, thick oil appears hot, intermediate thicknesses of oil appear cool, and thin oil or sheens are not detected. The thicknesses at which these transitions occur are poorly understood, but evidence indicates that the transition between the hot and cold layer lies between 50 and 150 μm and the minimum

detectable layer is between 10 and 70 μm.[25-28] The reason for the appearance of the "cool" slick is not fully understood. A plausible theory is that a moderately thin layer of oil on the water surface causes destructive interference of the thermal radiation waves emitted by the water, thereby reducing the amount of thermal radiation emitted.[8] This may be analogous to the appearance of the rainbow sheen, which is explained in Section 6.2. The cool slick would correspond to the thicknesses as observed above because the minimum destructive thickness would be about two times the wavelength, which is between 8 and 10 μm. This would yield a destructive onset of about 16 to 20 μm to about 4 wavelengths or about 32 to 40 μm. The destructive area is usually only seen with test slicks, which is explained by the fact that the more rapidly spreading oil is more transparent than the remaining oil. The onset of the hot thermal layer would in theory then be at thicknesses greater than this or at about 50 μm.

IR devices cannot detect emulsions (water-in-oil emulsions) under most circumstances.[29] This is probably a result of the high thermal conductivity of emulsions as they typically contain 70% water and thus do not show a temperature difference.

IR cameras are now very common, and commercial units are available from several manufacturers. In the past, scanners with IR detectors were largely used. A disadvantage of the older type of IR detector, however, is that they required cooling to avoid thermal noise, which would overwhelm any useful signal. Liquid nitrogen, which provides about 4 hours of service, had traditionally been used to cool the detector. Some, smaller sensors use closed-cycle or Sterling coolers, which operate on the cooling effect created by expanding gas. While a gas cylinder or compressor must be transported with this type of cooler, refills or servicing may not be required for days at a time.[30] In recent times, uncooled detectors are commonplace and have entirely replaced the older, cooled detectors.

Most IR sensing of oil spills takes place in the thermal IR at wavelengths of 8 to 14 μm. A slightly different sensor, which is designed as a fixed-mounted unit, uses the differential reflectance of oil and water at 2.5 and 3.1 μm.[31] Tests of a mid-band IR system (3.4 to 5.4 μm) over the *Tenyo Maru* oil spill showed no detection in this range, but ship scars were visible.[32-34] Specific studies in the thermal IR (8 to 14 μm) show that there is no spectral structure in this region.[35] Tests of a number of IR systems show that spatial resolution is extremely important when the oil is distributed in windrows and patches, emulsions are not always visible in the IR, and cameras operating in the 3 to 5 μm range are only marginally useful.[36] Nighttime tests of IR sensors show that there is detection of oil (oil appears cold on a warmer ocean), however, the contrast is not as good as during daytime.[36-38]

The relative thickness information in the thermal IR can be used to direct skimmers and other countermeasure equipment to thicker portions of the slick. Figures 6.11, 6.12, 6.15, and 6.16 illustrate the utility of IR oil imaging. Oil

FIGURE 6.15 An image of an oil slick formed from a composite of infrared and ultraviolet images. The red represents the thermal infrared and the thickest oil. The darker spots are intermediate thicknesses. The light blue area represents thin oil or sheen and is taken from the ultraviolet image.

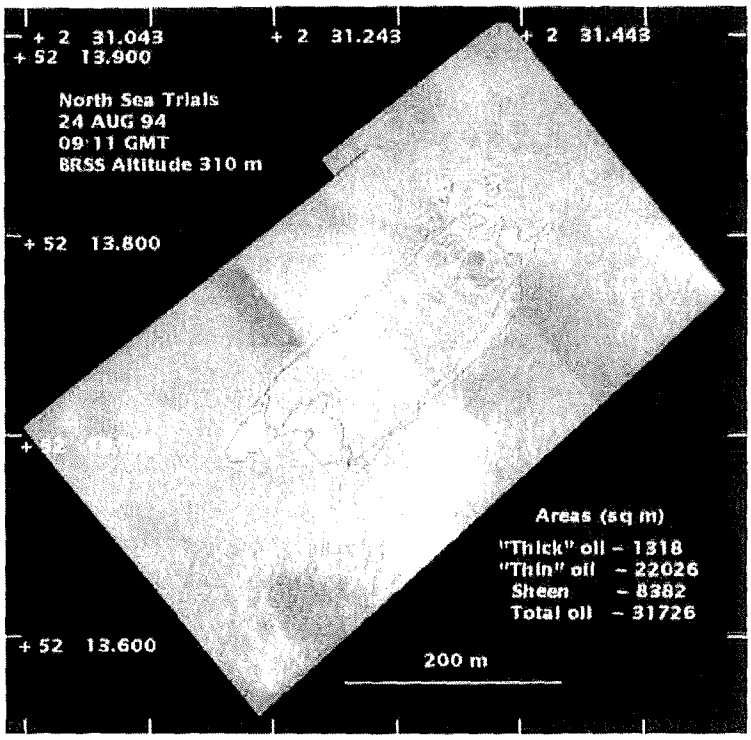

FIGURE 6.16 A composite image of the infrared and ultraviolet images of a slick similar to that in Figure 6.11. The outlined areas are from the infrared sensor and represent the thicker oil. Areas of the infrared and ultraviolet sensors are also annotated.

detection in the IR is not positive, however, as several false targets can interfere, including seaweed, shoreline, and oceanic fronts.[39] IR is reasonably inexpensive, however, and is currently the prime tool used by the spill remote-sensor operator.

6.3.3. Ultraviolet

Ultraviolet (UV) sensors can be used to map sheens of oil as oil slicks display high reflectivity of UV radiation even at thin layers (<0.1 μm). Overlaid UV and IR images are often used to produce a relative thickness map of oil spills. This has been illustrated in Figures 6.15 and 6.16. UV cameras, though inexpensive, are not often used in this process, however, as it is difficult to overlay camera images.[30] Data from IR scanners and derived from push-broom scanners can be easily superimposed to produce these IR/UV overlay maps. UV data are also subject to many interferences or false images such as wind slicks, sun glints, and biogenic material. Since these interferences are often different from those for IR sensing, combining IR and UV can provide a more positive indication of oil than using either technique alone.

6.4. LASER FLUOROSENSORS

Laser fluorosensors are sensors that take advantage of the fact that certain compounds in petroleum oils absorb UV light and become electronically excited. This excitation is rapidly removed through the process of fluorescence emission, primarily in the visible region of the spectrum. Since very few other compounds show this tendency, fluorescence is a strong indication of the presence of oil. Natural fluorescing substances, such as chlorophyll, fluoresce at sufficiently different wavelengths than oil to avoid confusion. As different types of oil yield slightly different fluorescent intensities and spectral signatures, it is possible to differentiate between classes of oil under ideal conditions.[40-50] Readers are referred to a separate subsection in this book for a review of laser fluorosensors. This section on remote sensing will just give a brief introduction.

Most laser fluorosensors used for oil spill detection employ a laser operating in the UV region of 300 to 355 nm.[40,50-52] With this wavelength of activation, there exists a broad range of fluorescent response for organic matter, centered at 420 nm. This is referred to as Gelbstoff or yellow matter, which can be easily annulled. Chlorophyll yields a sharp peak at 685 nm. The fluorescent response of crude oil ranges from 400 to 650 nm with peak centers in the 480 nm region. The use of laser fluorosensors for chlorophyll and other applications has been well documented.[53] One laser fluorosensor operating at 488 nm from an Argon ion laser was successful in detecting oil from a ship platform.[54]

Another phenomenon, known as Raman scattering, involves energy transfer between the incident light and the water molecules. When the incident UV light interacts with the water molecules, Raman scattering occurs. This involves an energy transfer between the incident light and the water molecules. The water molecules absorb some of the energy as rotational-vibrational energy and emit light at wavelengths, which are the sum or difference between the incident radiation and the vibration-rotational energy of the molecule. The Raman signal for water occurs at 344 nm when the incident wavelength is 308 nm (XeCl laser). The water Raman signal is useful for maintaining wavelength calibration of the fluorosensor in operation, but it has also been used in a limited way to estimate oil thickness because the strong absorption by oil on the surface will suppress the water Raman signal in proportion to thickness.[55,56] The point at which the Raman signal is entirely suppressed depends on the type of oil, since each oil has a different absorption coefficient. The Raman signal suppression has led to estimates of sensor detection limits of about 0.05 to 0.1 μm.[57]

The principle of fluorescence can also be used on a smaller scale. A hand-held UV light has been developed to detect oil spills at night at short range.[58] Another related instrument is the Fraunhofer Line Discriminator, which is essentially a passive fluorosensor using solar irradiance instead of laser light.[11] This instrument was not very successful because of the limited discrimination and the low signal-to-noise ratio.

Laser fluorosensors have significant potential as they may be the only means to discriminate between oiled and unoiled seaweed and to detect oil on different types of beaches. Tests on shorelines show that this technique has been very successful.[59] Algorithms for the detection of oil on shorelines have been developed.[60] Work has been conducted on detecting oil in the water column, such as occurs with the product, Orimulsion.[61-65] The fluorosensor is also the only reliable means of detecting oil in certain ice and snow situations. Operational use shows that the laser fluorosensor is a powerful tool for oil spill remote sensing.[19,43]

6.5. MICROWAVE SENSORS

6.5.1. Radiometers

Microwave radiometers detect the presence of an oil film on water by measuring an interference pattern excited by the radiation from free space. The apparent emissivity factor of water is 0.4 compared to 0.8 for oil.[11,66] This passive device can detect this difference in emissivity and could therefore be used to detect oil. In addition, as the signal changes with thickness, in theory, the device could be used to measure thickness. This detection method has not been very successful in the field, however, as several environmental and oil-specific parameters must be known. In addition, the signal return is dependent

on oil thickness but in a cyclical fashion. A given signal strength can imply any one of two or three signal film thicknesses within a given slick. Microwave energy emission is greatest when the effective thickness of the oil equals an odd multiple of one quarter of the wavelength of the observed energy. Biogenic materials also interfere, and the signal-to-noise ratio is low. In addition, it is difficult to achieve high spatial resolution (might need resolution in meters rather than the typical tens of meters for a radiometer).[67]

The Swedish Space Agency has carried out work with different systems, including a dual-band, 22.4- and 31-GHz device, and a single band 37-GHz device.[68] Skou, Sorensen, and Poulson describe a two-channel device operating at 37.5 and 10.7 GHz.[69] Mussetto and coworkers at TRW described the tests of 44-94-GHz and 94-154-GHz, two-channel devices over oil slicks.[70] They showed that correlation with slick thickness is poor and suggest that factors other than thickness also change surface brightness. They suggest that a single-channel device might be useful as an all-weather, relative-thickness instrument. Tests of single-channel devices over oil slicks have also been described in the literature, specifically a 36-GHz and a 90-GHz device.[71,72] A new method of microwave radiometry has recently been developed in which the polarization contrasts at two orthogonal polarizations are measured in an attempt to measure oil slick thickness.[73] A series of frequency-scanning radiometers have been built and appear to have overcome the difficulties with the cyclical behavior.[74,75]

In summary, passive microwave radiometers may have potential as all-weather oil sensors. Their potential as a reliable device for measuring slick thickness, however, is uncertain at this time.

6.5.2. Radar

Capillary waves on the ocean reflect radar energy, producing a "bright" image known as sea clutter. Since oil on the sea surface dampens capillary waves, the presence of an oil slick can be detected as a "dark" sea or one with an absence of this sea clutter.[76] Unfortunately, the oil slick is not the only phenomenon detected in this way. There are many interferences or false targets, including freshwater slicks, wind slicks (calms), wave shadows behind land or structures, seaweed beds that calm the water just above them, glacial flour, biogenic oils, and whale and fish sperm.[77-81] As a result, radar can be ineffective in locations such as Prince William Sound, Alaska where dozens of islands, freshwater inflows, ice, and other features produce hundreds of such false targets. Despite these limitations, radar is an important tool for oil spill remote sensing because it is the only sensor that can be used for searches of large areas and it is one of the few sensors that can "see" at night and through clouds or fog.

Figures 6.17 to 6.23 illustrate the many slick look-alikes that appear in radar displays.

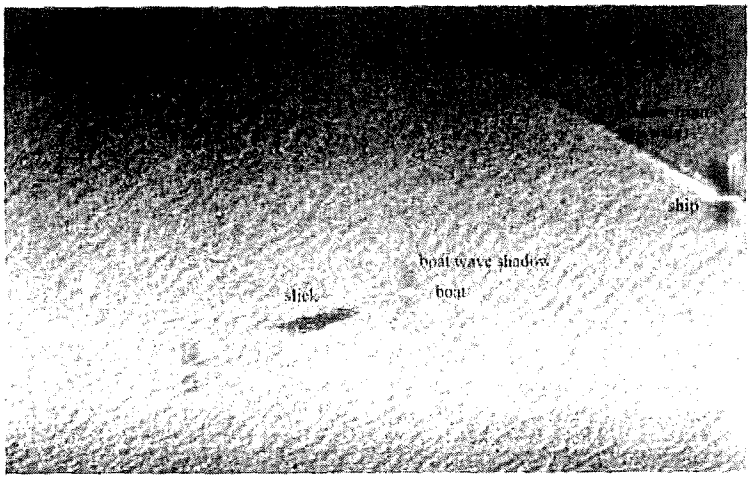

FIGURE 6.17 Airborne radar image of a small test slick attended by two boats. Note that the boats cast a radar shadow on both their sides. A ship is passing to the top right of the image, and the ship's wake also casts a radar shadow.

FIGURE 6.18 A satellite Radarsat-I image of a large area of sea during the raising of the Irving Whale barge. Note that the area to the left that appears darker is caused by wind shadows and low winds. Only the small areas noted are actually slicks. One might have to know beforehand where the slicks were before interpreting this image.

The two basic types of imaging radar that can be used to detect oil spills and for environmental remote sensing in general are Synthetic Aperture Radar (SAR) and Side-Looking Airborne Radar (SLAR). SLAR is an older but less expensive technology that uses a long antenna to achieve spatial resolution. SAR uses the forward motion of the aircraft to synthesize a very long antenna, thereby achieving very good spatial resolution, which is independent of range, with the disadvantage of requiring sophisticated electronic processing. Though inherently more expensive, the SAR has greater range and resolution than the

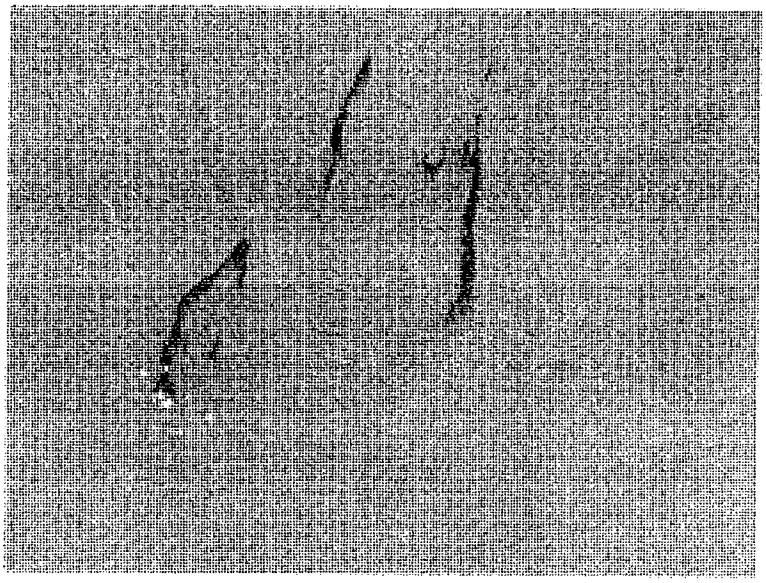

FIGURE 6.19 A close-up of the area shown in Figure 6.18 from radar satellite. These dark areas are actually oil, as confirmed by ground observation. The white spots in the center are ships.

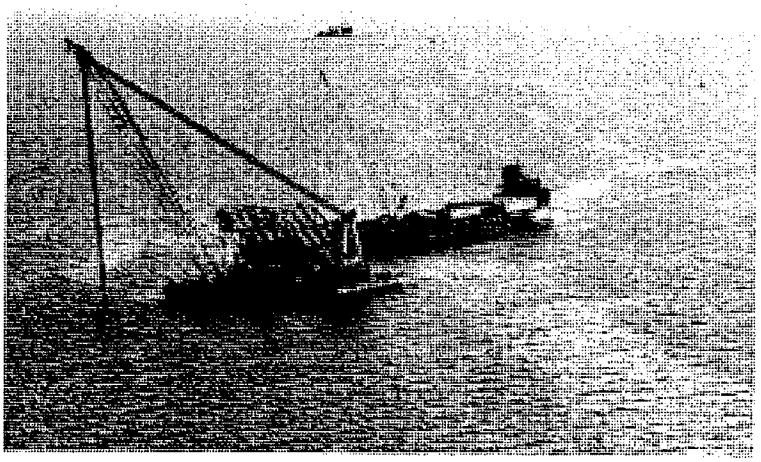

FIGURE 6.20 An image of the source of the oil shown in Figure 6.19. The ships shown here appear as white spots in the radar image in Figure 6.19. *Photography by Environment Canada.*

SLAR. In fact, comparative tests show that SAR is vastly superior.[82-84] Search radar systems, such as those frequently used by the military, cannot be used for oil spills because they usually remove the clutter signal, which is the primary signal of interest for oil spill detection. Furthermore, the signal processing of this type of radar is optimized to pinpoint small, hard objects, such as periscopes. This signal processing is very detrimental to oil spill detection.

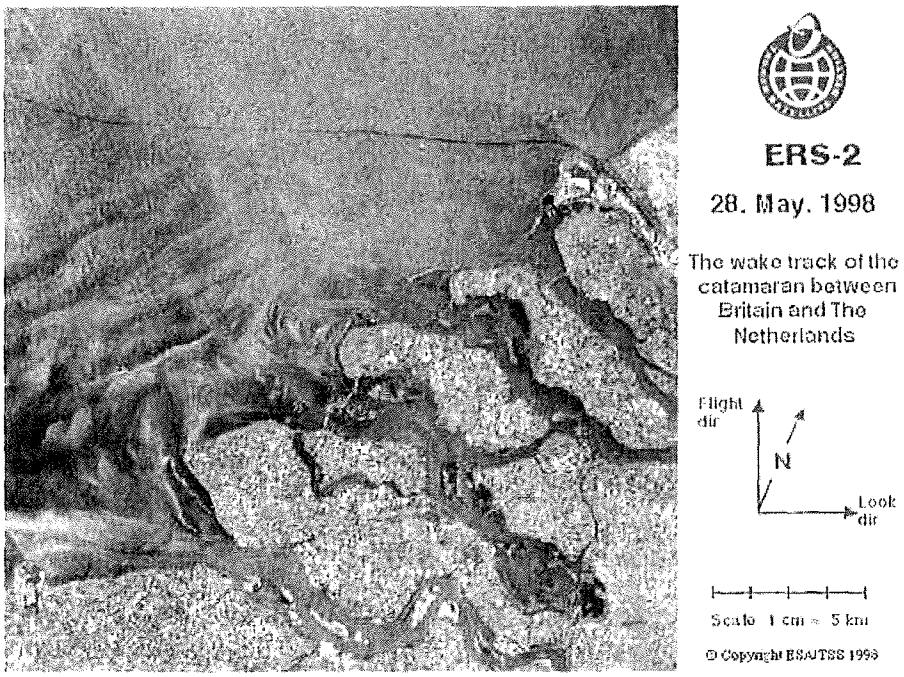

FIGURE 6.21 A radar satellite image of a coastline. There is no oil in this image. The track through the image is the wake of a vessel. It should be noted that all ship wakes leave a shadow like this, making it very hard to use radar to detect ship discharges. The dark areas near the coastline are low-wind areas, probably caused by the coast wind shadows.

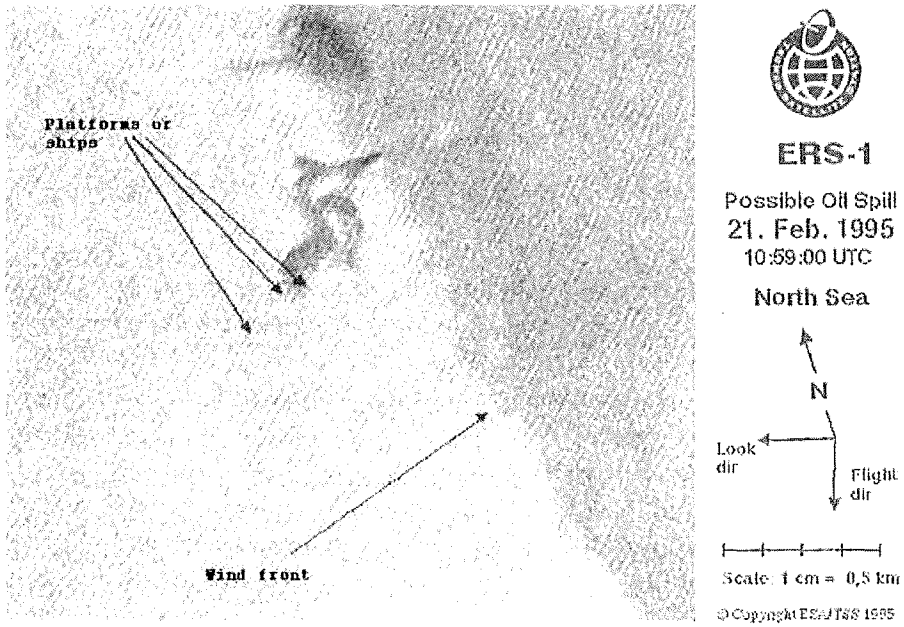

FIGURE 6.22 A view of an area near ships and platforms. A possible slick is pointed out; however, as it is very near a major low-wind area, it is difficult to say whether or not this is really a slick.

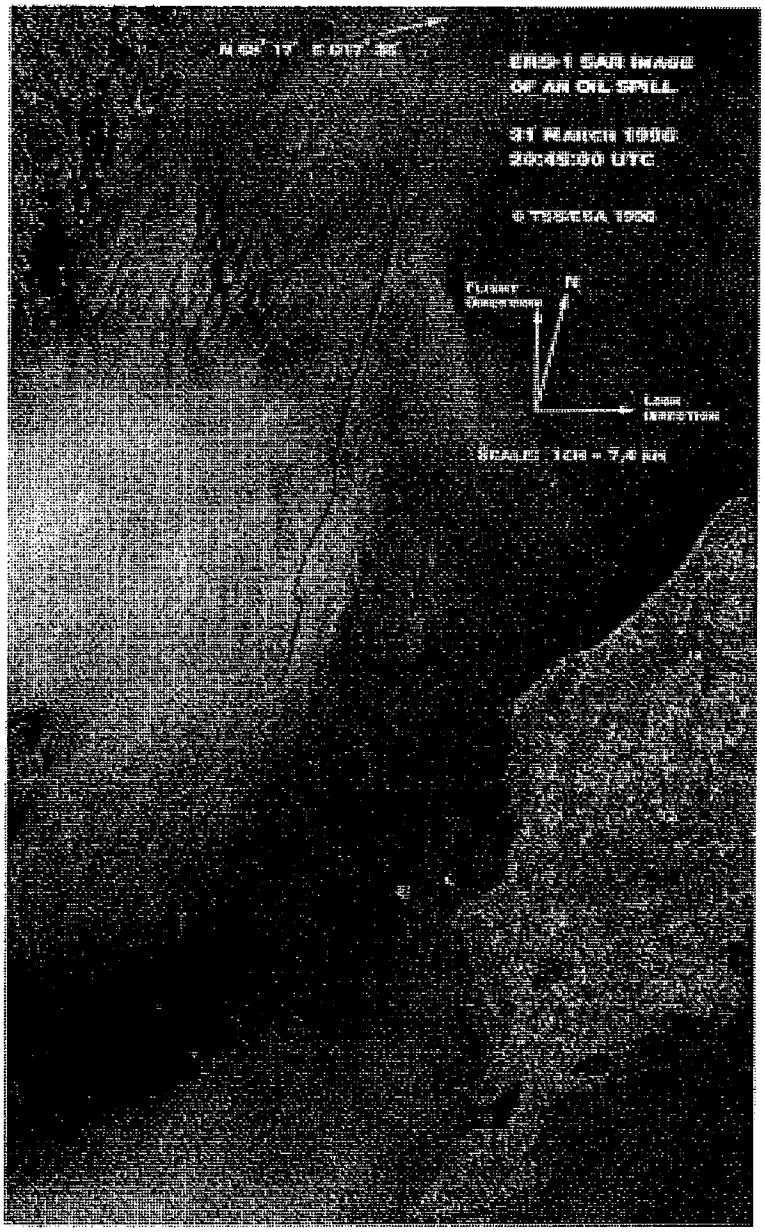

FIGURE 6.23 A view of the track of a vessel. Despite the interpretation that there was a slick behind the vessel, the black line may be simply a ship wake. Note also the other dark areas from low winds and coast wind shadows.

SLAR has predominated airborne oil spill remote sensing, primarily because of the lower price.[85,86] There is some recognition among the operators that SLAR is very subject to false hits, but solutions are not offered.

Experimental work on oil spills has shown that X-band radar yields better data than L- or C-band radar.[87,88] It has also been shown that vertical antenna

polarizations for both transmission and reception (VV) yield better results than other configurations.[82,89-91] The ability of radar to detect oil is also limited by sea state. Sea states that are too low will not produce enough sea clutter in the surrounding sea to contrast to the oil, and very high seas will scatter radar sufficiently to block detection inside the troughs. Indications are that minimum wind speeds of 1.5 m/s (~3 knots) are required to allow detectability, and a maximum wind speed of 6 m/s (~12 knots) will again remove the effect.[92-94] The most accepted limits are 1.5 m/s (~3 knots) to 10 m/s (~20 knots). This limits the environmental window of application of radar for detecting oil slicks. Gade et al. studied the difference between extensive systems from a space-borne mission and a helicopter-borne system.[95] They found that at high winds, it was not possible to discriminate biogenic slicks from oil. At low-wind speeds, it was found that images in the L-band showed discrimination. Under these conditions, the biogenic material showed greater damping behavior in the L-band. Okamoto et al. studied the use of ERS-1 using an artificial oil (oleyl alcohol) and found that an image was detected at a wind speed of 11m/s, but not at 13.7 m/s.[96]

SAR can be polarimetric imaging that is horizontal-horizontal (HH), vertical-vertical (VV), and cross combinations of these. Several researchers have shown that VV is best for oil spill detection and discrimination.[97-100] Migliaccio et al. showed that the co-polarized phase difference—for example, the difference between the HH and VV phases can be used to discriminate oil

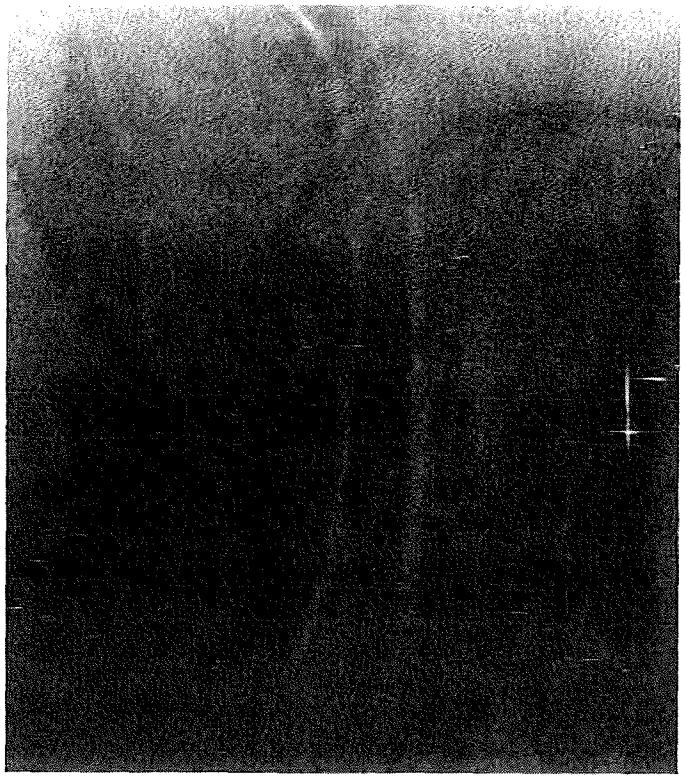

FIGURE 6.24 An HH polarized view of the sea surface.

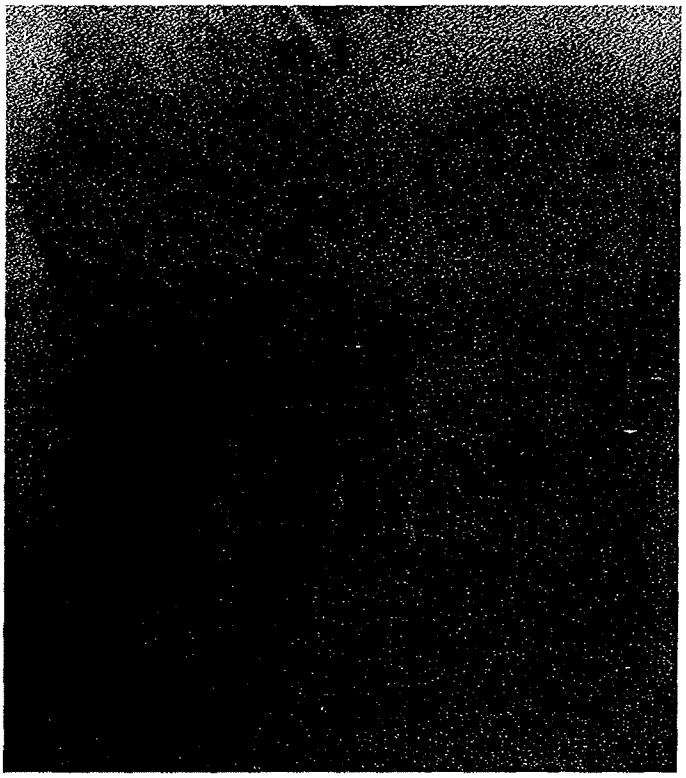

FIGURE 6.25 A VV polarized view of the same area of sea surface. Note that this polarization yields a slightly clearer image of sea-surface details than shown in Figure 6.24.

slicks from biogenic slicks.[97] A larger standard deviation for the slick, compared to the sea, typically indicates that it is oil. Figures 6.24 and 6.25 show the difference between a VV and HH polarization.

Radar has also been used to measure currents and predict oil spill movements by observing frontal movements.[101] Work has shown that frontal currents and other features can be detected by SAR.[102]

Shipborne radar has similar limitations and the additional handicap of low altitude, which restricts its range to between 8 and 30 km, depending on the height of the antenna. Ship radars can be adjusted to reduce the effect of sea clutter deenhancement. Shipborne radar successfully detected a surface slick in the Baltic Sea from 8 km away and during a trial off the coast of Canada at a maximum range of 17 km.[103] During the *Prestige* spill, a Netherlands vessel successfully used this technique to guide a recovery vessel into slicks. The technique is, however, very limited by sea state, and in all cases where it was used, the presence and location of the slick were already known or suspected. Recently, researchers have carried out work on improving the imaging of slicks from shipborne radars.[104] Today there are some commercial products that enhance the images from shipborne radar to enable some oil imaging.

Gangeskar has proposed an automatic system that can be mounted on oil drilling platforms.[105] This system would use standard X-band ship navigation units and would provide an alert if an oil spill was present. The system includes

an extensive postprocessing system to provide both a user-friendly GUI and an automatic detection and alert system. The system has not been fully tested to date.

In summary, radar optimized for oil spills is useful in oil spill remote sensing, particularly for searches of large areas and for nighttime or foul weather work. The technique is highly prone to false targets, however, and is limited to a narrow range of wind speeds. Because of the all-weather and day-night capability, radar is now the most common means of remote sensing.

6.5.2.1. Radar Processing

Because radar detection of oil spills is so highly susceptible to false images, much work has taken place on means to differentiate oil slicks and false targets, often called look-alikes. These look-alikes include: low-wind areas, areas sheltered by land, rain cells, organic films, grease ice, wind fronts, up-welling zones, oceanic fronts, algae blooms, current shear zones, and so on.[106] The discussion in this subsection is relevant to both satellite and airborne SAR systems.

Several "automatic" systems have been designed for slick detection.[107] Limited testing with actual satellite output has shown that many false signals are present in most locations.[108,109] Extensive effort on data processing appears to improve the chances of oil detection.[110] In recent years, automatic systems have given way to systems involving smart algorithms that are manipulated by operators.[111-113]

The most common way to eliminate wind-origin look-alikes is to map the wind fields in the same coordinates as the radar data.[110,114] The most common slick look-alikes are low-wind areas. One group of researchers used radar wind data calibrated to wind data from an ocean buoy to map oil seeps in the southern Gulf of Mexico.[114]

Most researchers used some form of neural networks or fuzzy logic to assist in the discrimination of look-alikes and the intended targets.[115-118] Others used various forms of models such as range dependence models.[119]

Topouzelis and coworkers developed several series of mathematical networks for differentiating slicks from look-alikes.[120-123] The basis of these networks is the idea that generally oil slicks are imaged through a complex series of processes and conditions. Thus imaging is not a simple statistical manipulation. The same group developed a fuzzy classification to differentiate look-alikes from oil spills. The methodology involved four procedures. The first is the segmentation of the image into large image segments with different statistical values. In the second procedure, a detailed scale segmentation is carried out, and statistical values of each segment are compared to the threshold of the large segment from which it came. Third, the dark portions are classified according to the properties of the surrounding areas. Finally, the dark areas are classified using knowlege bases. The group also examined the use of

forward-feed neural networks to discriminate slicks from look-alikes.[120,124] Several topologies of forward-feed neural networks were examined, and none were better than others. The networks yielded classification accuracies as high as 91.3 to 93.6% for the given example. A recent work by Topouzelis used the inputs of shape texture, asymmetry, mean difference to neighbours, and power to the mean images in a neural network.[106] The workers used forward-feed neural networks. It was found that the classification accuracy was 99.4% for the MLP network in the test case. Later, Topouzelis and co workers used a similar method to test a data set of 69 oil spills and 90 look-alikes.[122] They found a combination of 11 features out of a possible 25 features. The 11 features found to be best for discrimination are perimeter, shape factor object mean value, ratio of the power to mean ratios, local area contrast ratio, mean border gradient, maximum border gradient, standard deviation border gradient, maximum border gradient, mean difference to neighbors, and spectral texture. Use of these factors resulted in classification accuracies of 85.3% for oil spills and 84.4% for look-alikes.

A similar approach is to use a classification scheme that incorporates some of the same input parameters. Karantzalos and Argialas proposed a classification scheme involving processes and then a classification scheme. The first processing step involves filtering and levels.[125] The second step is segmentation of the images to include all suspected slicks. The final step is to classify the potential slicks according to area, perimeter, shape complexity eccentricity, orientation, segment mean border gradient, inside segment standard deviation, and outside segment standard deviation.

Several researchers have used Geographic Information System (GIS) databases to assist in the interpretation of SAR imagery.[125-131] The technique divides the area of interest into segments and notes data such as currents, proximity to land, wind, and sea lanes. These parameters are then correlated to the SAR images. For example, oil spills are much more likely under the correct wind conditions, in sea lanes, and far from land. Tahvonen used data sets including wind speed and direction, sea-surface temperature, heavy rain, and location of algae blooms to assist in the discrimination.[126] Muellenhoff proposed a data set consisting of wind information, sea-surface temperature, chlorophyll-a concentration, geostrophic currents, wave information, contextual background information, and existing oil spill databases.[129] The assigned influences were wind speed—30%; wind direction—12%; sea-surface temperature—14%, chlorophyll-a concentration—10%; oil ports—10%; and main traffic lines—20%. Wave and current direction only accounted for 2% each.

Migliaccio and group studied the processing of SAR images from an aircraft-based sensor.[132-134] It was noted that the main obstacle to analysis was speckle in the images. Speckle is caused by stray reflectances, such as from rough seas. Speckle is also caused by random constructive and destructive interference. Since speckle is temporary, multi-look imaging is one way to decrease speckle by a large amount. Further processing can then be achieved by

combining multi-look data with wind data, best obtained from satellite scatterometers. The technique proposed for multi-look data is to divide the SAR imagery into subbands and then generate lower-resolution imagery. Then the images are averaged. This results in reduction of speckle. To process single-look data with high speckle content, filters are used. First speckle is removed, and then an ROA (ratio of average) filter is used. In both techniques, edge detection is used to find the actual limits of the slicks or look-alikes.

Marghany and co workers used a fractal method to analyze SAR data.[135] The images are broken into fractals, and these fractals have dimensions that are different for oil spills and look-alikes. A further study under different wind speeds showed that there were differences only in the wide beam mode for low-wind zones and current shear features between real oil slicks.[136] Danisi et al. utilized a similar approach.[137]

Another method employed by researchers to separate oil slicks from look-alikes is to use textural analysis.[138,139] Direct statistical methods are also employed. Tello et al. noted that an algorithm characterizing the border between oil spill candidates and the surrounding sea allows for good classification.[139] Lounis et al. used a measure of similarity between the local probability density function of clean water and of the dark area to be examined.[140] Comparing the two values is said to result in discrimination between oil and look-alikes. Pelizzari employed a similar technique using graph cuts to estimate a smoothness factor.[141]

Ferraro et al. describe the development of an operational system for the Mediterranean Sea and show a procedure for identifying oil spills as (1) isolation and contouring of all dark signatures, (2) extraction of shape and backscattering contrast signatures, (3) test of these values against standard values, and (4) calculation of the probabilities of each patch.[142-144]

Another series of techniques involves the use of two streams of information. Several researchers used both SAR and visible information from the MODIS (Moderate Resolution Imaging Spectroradiometer) satellites to discriminate between look-alikes and oil slicks.[145] The visible imagery is subject to false images, but not the same ones as satellites, and thus discrimination can be achieved to a degree. Similarly, Sipelgas used visible imagery from the MODIS satellite to assist in discrimination of false images from oil slicks in the Gulf of Finland.[146] Adamo et al. used three streams for information—SAR data, MODIS, and MERIS data—to discriminate look-alikes from actual spills.[145]

6.5.3. Microwave Scatterometers

A microwave scatterometer is a device that measures the scattering of radar energy by a target. One radar scatterometer was flown over several oil slicks and used a low-power transmitter operating in the Ku band (13.3 GHz).[11] The scatterometer detected the oil, but discrimination was poor. The "Heliscat," a device with five frequencies, has been used to investigate capillary wave

damping.[92] The advantage of a microwave scatterometer is that it has an aerial coverage similar to optical sensors and it can look at several incident angles. The main disadvantages include the lack of discrimination for oil and the lack of imaging capability.

6.5.4. Surface Wave Radars

It is possible to send radio waves along the sea using high frequency. The conductivity of the sea acts as a form of wave guide. These radars can be used to detect ships as far out as 500 km.[147] Since these are surface wave phenomena, only targets above the surface are detected; thus slicks may not be detected by this technique.[148] Modeling of the technique does not show whether there is potential for this method.[149]

6.5.5. Interferometric Radar

Radars can be used to measure height, currents, and other surface elevation phenomena using interferometric techniques. Some radar systems on aircraft are fitted for this application, such as the government of Canada Convair 580. This can also be carried out in space using two satellites traveling in tandem. One research group employed the tandem satellite pairs of ERS-2 and ENVISAT to carry out such work, but there are no reports on the use on oil spills.[150]

6.6. SLICK THICKNESS DETERMINATION

There has long been a need to measure oil slick thickness; this need has been expressed both within the oil spill response community and among academics in the field. There are presently no reliable methods, either in the laboratory or in the field, for accurately measuring oil-on-water slick thickness. The ability to do so would significantly increase understanding of the dynamics of oil spreading and behavior. Knowledge of slick thickness would make it possible to determine the effectiveness of certain oil spill countermeasures, including dispersant application and *in-situ* burning. Indeed, the effectiveness of individual dispersants could be determined quantitatively if the oil remaining on the water surface following dispersant application could be accurately measured.[151,152]

6.6.1. Visual Thickness Indications

A very important tool for working with oil spills has been the relationship between appearance and thickness. Careful study of the literature on this relationship and comparison of this to field experience shows that there is limited potential to scale thicknesses to visual appearance.[8] The only physical-based appearances that occurs are thicknesses of about 0.7 to 2.5 μm

TABLE 6.1 Relationship of Thickness to Appearance

	Visibility Thresholds (μm)					
	Minimum	Silvery	Rainbow	Darkening Colors	Dull Colors	Dark
Typical thickness	0.09	0.1	0.6*	0.9	2.7	8.5

**Note this is the only physical-based appearance factor*

FIGURE 6.26 A rainbow sheen above a sunken vessel. The appearance of a rainbow sheen is the only strong visible indicator of slick thickness, and thickness may be between about 0.7 and 2.5 μm. *Photography by Environment Canada.*

at which the rainbow colors appear as a result of multiple constructive and destructive interferences by light. Table 6.1 presents a summation of the best knowledge on this phenomenon. Figures 6.26 and 6.27 show typical rainbow sheens for which we can estimate that the thickness is about 1 μm. This is the only color appearance that has a physical slick thickness associated with it.

6.6.2. Slick Thickness Relationships in Remote Sensors

A number of investigators tried to correlate slick thickness with appearance in various remote-sensing instruments. Hollinger and Mennella conducted a series of eight controlled oil spills off Virginia to investigate the use of microwave radiometry to delineate oil spills.[153] They used 19.4 and 69.8 GHz radiometers on the spills. Measurements using sorbents were used to calibrate the

FIGURE 6.27 A rainbow sheen above another sunken vessel. The appearance of a rainbow sheen is the only strong visible indicator of slick thickness, and thickness may be between about 0.7 and 2.5 μm. *Photography by Environment Canada.*

radiometer. It was noted that the sheens typically had a thickness of 2 to 4 μm. It was found that 90% of the oil was in 10% of the slick area and that the microwave threshold was about 0.1 mm (100 μm).

A series of experiments was carried out in 1979 to evaluate IR and SLAR for oil spill detection.[154] The imagery was correlated against visual and sorbent measurements, which were used to derive a thickness estimate. It was concluded that the IR threshold was between 25 and 50 μm and for SLAR 100 nm. Furthermore, manipulation of data showed that a mass balance could be achieved if the thickness at which the IR showed oil to be colder at the sea occurred at 100 μm and for the heated portion of the oil at 1,000 μm.

The United Kingdom conducted Isowake Experiments in 1982.[155,156] On the basis of estimations and calculations, it was concluded that the lowest detectable slick thickness for IR was between 10 and 50 μm, whereas hot spots in the IR image could be as much as 1,000 μm.

MacDonald et al. used photography from the space shuttle to define up to 124 slicks in an area of the Gulf of Mexico, offshore Louisiana.[157] Similarly, a thematic image from Landsat showed at least 66 slicks in one large area. Some of the thickness relationships were based on unpublished experimental data from Duckworth.

Brown et al. conducted experiments to measure the visibility of oil slicks. The observers and a visible UV camera were mounted in a crane basket 30 m over the slick.[12,158,159] It was found that the detection ability decreased by over 50% for most oils and for the cameras when the angle was changed from 90 to 55 degrees from the horizontal (equivalent incidence angle of 0 to 35 degrees). Detectability degraded to 70% and sometimes to nil as the viewing angle was

decreased past 55 through 35 degrees. Brown et al. conducted several experiments to ascertain the relationship between thickness of slicks and the density (or intensity) of the IR image.[39] The thicknesses varied between 1 and 10 mm, and thicknesses were measured using an acoustic system. No relationship between slick thickness and IR brightness was found.

6.6.3. Specific Thickness Sensors

The suppression of the water Raman peak in laser fluorosensor data has not been fully exploited or tested. This technique may work for thin slicks, but not necessarily for thick ones, at least not with a single excitation frequency. Attempts have been made to calibrate the thickness appearance of IR imagery, but also without success. It is suspected that the temperatures of the slick as seen in the IR are highly dependent on oil type, sun angle, and weather conditions. If so, it may not be possible to use IR as a calibrated tool for measuring thickness. Because accurate ground-truth methods do not exist, it is very difficult to calibrate existing equipment.[160,161] The use of sorbent techniques to measure surface thickness yields highly variable results.[151] As noted in the section on microwave radiometers, the signal strength measured by these instruments can imply one of several thicknesses. This methodology does not appear to have potential other than for measuring relative oil thickness.

A variety of electrical, optical, and acoustic techniques for measuring oil thickness have been investigated.[161,162] Two promising techniques were pursued in a series of laboratory measurements. In the first technique, known as thermal mapping, a laser is used to heat a region of oil, and the resultant temperature profiles created over a small region near this heating are examined using an IR camera.[163] The temperature profiles created are dependent on the oil thickness. A more promising technique involves laser acoustics.[164,165] The Laser Ultrasonic Remote Sensing of Oil Thickness (LURSOT) sensor consists of three lasers, one of which is coupled to an interferometer to accurately measure oil thickness.[160,165-168] The sensing process is initiated with a thermal pulse created in the oil layer by the absorption of a powerful CO_2 laser pulse. Rapid thermal expansion of the oil occurs near the surface where the laser beam was absorbed, which causes a steplike rise of the sample surface as well as an acoustic pulse of high frequency and large bandwidth (~15 MHz for oil). The acoustic pulse travels down through the oil until it reaches the oil–water interface where it is partially transmitted and partially reflected back toward the oil–air interface, where it slightly displaces the oil's surface. The time required for the acoustic pulse to travel through the oil and back to the surface again is a function of the thickness and the acoustic velocity of the oil. The displacement of the surface is measured by a second laser probe beam aimed at the surface. Motion of the surface induces a phase or frequency shift (Doppler shift) in the reflected probe beam. This phase or frequency modulation of the probe beam can then be demodulated with an interferometer.[169] The thickness

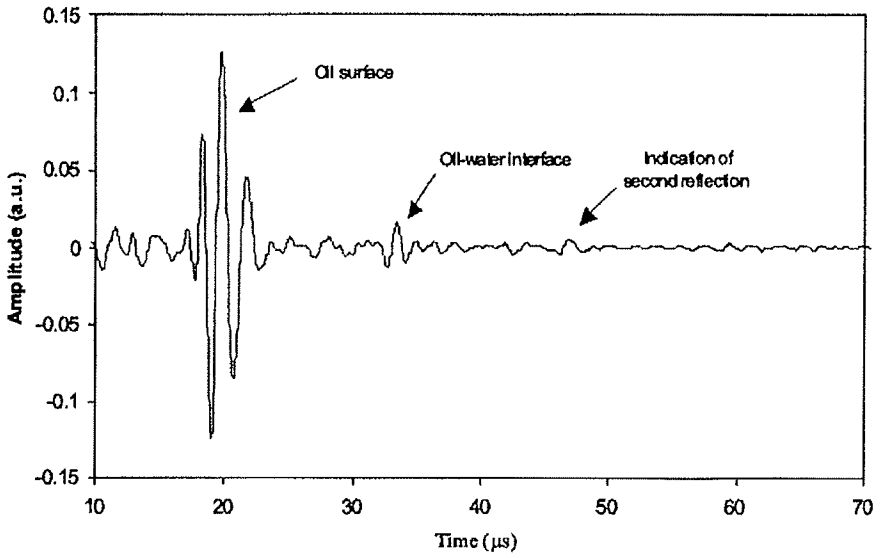

FIGURE 6.28 The signal from a 3-laser-thickness sensor. The time corresponds to a thickness of about 6 mm. This was measured by a prototype sensor mounted in an aircraft and flying over bins with various thicknesses of oil on water.

can be determined from the time of propagation of the acoustic wave between the upper and lower surfaces of the oil slick. This is a very reliable means of studying oil thickness and has great potential. Laboratory tests have confirmed the viability of the method, and a test unit has been flown to confirm its operability.[160] Figure 6.28 shows the first airborne measurement of slick thickness.

Several attempts have been made to measure thickness by using visible spectral imaging. As there are no visual indications other than the rainbow sheen area around 0.8 μm, these efforts are wasted.[8,170]

6.7. ACOUSTIC SYSTEMS

Pogorzelski has shown that acoustic means can be used to measure oil viscosities on the surface.[171] A directional acoustic system employing high-frequency forward specular scattering was used in the laboratory and at sea. Signals scattered are related to the rheological film properties. It is not known at this time if the system is scalable or exactly what the limitations are.

6.8. INTEGRATED AIRBORNE SENSOR SYSTEMS

Increasingly, a number of different types of airborne oil spill remote sensors are being consolidated into sensor systems. The reason for this integration is to take advantage of the different information provided by each of the specific sensors and combine the information to provide a more complete and comprehensive

information product. Although each of the individual sensors has specific inherent weaknesses such as false detections, these false detections are often different for each sensor type; hence a consolidation of information can help resolve and remove some of the uncertainties that exist from a single data source. Furthermore, additional information such as the relative thickness of the oil slick can be deduced from the overlaying of imagery from several sensor types. Although the absolute thickness of an oil slick remains the subject of continued research and scientific opinion, the ability to locate the thicker portions of the slick is essential in terms of operational spill cleanup and response. In addition to the integration of a number of remote sensors into a sensor system, information from other sources such as marine vessel traffic surveillance systems (i.e., automatic identification system, AIS) can be integrated and can play an essential role in identifying the source of the marine pollution.

Two commercially available airborne marine oil spill remote-sensing systems are the MEDUSA and the MSS 6000.[172-174] MEDUSA incorporates a number of sensor technologies such as laser fluorosensors, IR/UV line scanners, forward-looking IR sensors, microwave radiometers, SLAR systems, and camera systems, as well processing software into a flexible real-time data acquisition and processing system. The data from the various sensors are geo-referenced and fused with information from Airborne Information Systems (AIS) and marine surveillance radars into a GIS—based display output format. The processing software is known as the Oil Spill Scene Analysis System (OSSAS) and allows for the extraction of features such as the area of oil coverage, including areas of intermediate and thicker portions of the slick. The MSS 6000 Maritime Surveillance System is comprised of a flexible suite of sensors such as SLAR systems, IR/UV line scanners, forward-looking IR sensors, microwave radiometers, and camera systems, along with data processing and mission management software in order to perform the oil spill remote-sensing surveillance task. The MSS 6000 also focuses on sensor integration and includes AIS and marine search radar inputs. All sensor data, imagery, slick targets, vessels, and the like are annotated using navigation data from a single source to form an integrated part of a GIS). Both the MEDUSA and MSS 6000 can distribute their data in near—real time via direct downlink or satellite communications to vessels or shore-based communications centers. A large number of maritime nations are now employing integrated airborne sensor systems.[174,175]

6.9. SATELLITE REMOTE SENSING

The use of optical satellite remote sensing for oil spills has been attempted several times. The slick from the IXTOC I well blowout in Mexico was detected using GOES (Geostationary Operational Environmental Satellite) and by the AVHRR (Advanced Very High Resolution Radiometer) on the

LANDSAT satellite.[11] A blowout in the Persian Gulf was subsequently detected. The massive *Exxon Valdez* slick was detected on SPOT (Satellite Pour l'Observation de la Terre) satellite data.[176] Oiled ice in Gabarus Bay resulting from the *Kurdistan* spill was detected using LANDSAT data.[177,178] Several workers were able to detect the Arabian Gulf War Spill in 1991.[179-182] The *Haven* spill near Italy was also monitored by satellite.[183] A spill in the Barents Sea was tracked using an IR band on NOAA 10.[184] It is significant to note that, in all these cases, the position of the oil was known and data had to be processed to actually see the oil, which usually took several weeks. Newer findings show that the ability to detect oil may be a complex function of conditions, oil types, and view angles.[185-187] Figure 6.29 shows a visible satellite image of an area in Russia in which there was a massive pipeline spill. As noted in the caption for this image, the oil is not visible; however, a round lake in the image was mistaken for oil. Figure 6.30 shows an oiled ice area off Canada in which sediment and oil appear alike.

There are several problems associated with relying on satellites operating in optical ranges, for oil spill remote sensing. The first is the timing and frequency of overpasses and the absolute need for clear skies to perform optical work.[188] The chances of the overpass and the clear skies occurring at the same time give

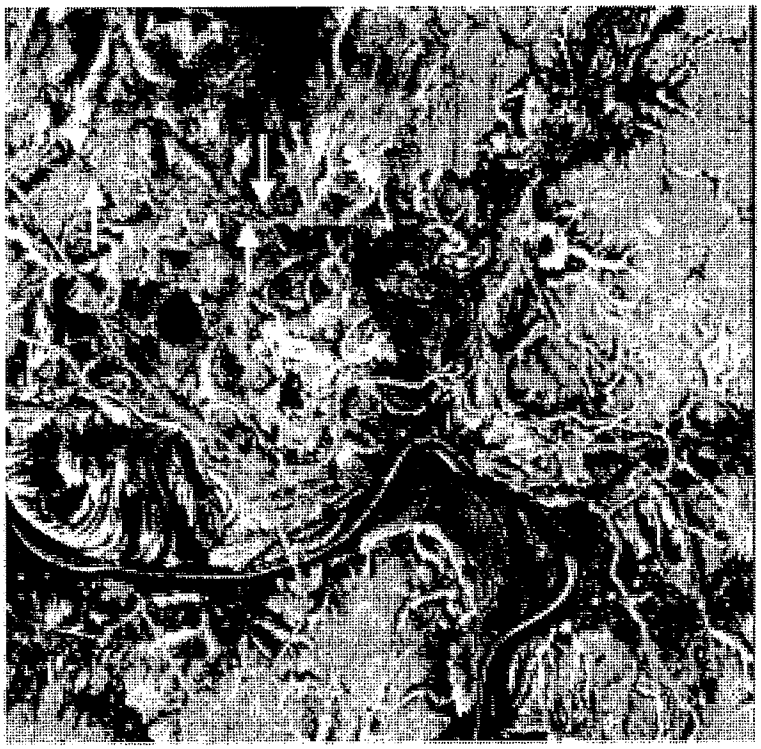

FIGURE 6.29 A SPOT satellite visible image of an area in Russia where a large oil spill occurred. The oil spill is shown by the arrows. The black round objects are lakes. This illustrates that satellite visible imagery is difficult to interpret.

FIGURE 6.30 A satellite visible image of an area off the east coast of Canada where an oil spill had occurred. Some of the black stripes in the white ice are oil mixed with sediment; others are sediment. The black on the right is land and the black on the left is sea. This image also illustrates the lack of discrimination of targets using visible satellite imagery.

a very low probability of seeing a spill on a satellite image. This point is well illustrated in the case of the *Exxon Valdez* spill.[189] Although the spill covered vast amounts of ocean for over a month, there was only one clear day that coincided with a satellite overpass, and that was on April 7, 1989. Another disadvantage of satellite remote sensing is the difficulty in developing algorithms to highlight the oil slicks and the long time required to do so. For the *Exxon Valdez* spill, it took over two months before the first group managed to "see" the oil slick in the satellite imagery, although its location was precisely known. Recently, several workers have attempted to use MODIS visible data to detect oil spills.[190,191] To be successful, these techniques generally rely on ancillary data such as suspected position or other satellite data.

There is some information on slicks available from angular information. For example, Chust and Sagarminaga used the Multi-angle Imaging SpectroRadiometer (MISR) sensor aboard a satellite to detect oil spills on Lake Maracaibo, Venezuela.[192] This sensor uses nine push-broom cameras at fixed angles from nadir to 70.5° to examine particular surfaces. A comparison of this angular sensor shows that better contrast was obtained than a simple nadir camera on another satellite. Data analysis showed that oil spills appear in

greater contrast in those view angles affected by sun glitter because of the presence of oil.

Recently, IR data from satellite has been used to map the land oil pollution in Kuwait.[193] It was found that the old hydrocarbon-contaminated areas showed as much as 10°C difference from the surrounding land. Ground-truthing was used extensively in compiling the data. Casciello et al. also made an attempt to use IR imagery from the thermal IR region of the AVHRR satellite to locate known oil spills.[194]

Radar satellites, including ERS-1 and -2, Radarsat-1 and -2, and ENVISAT, are useful in detecting large offshore spills and in spotting anomalies.[195-198] Radarsat has been used for detecting oil seeps and smaller spills resulting from an oil barge.[199,200] The relative location of these smaller slicks was known before the detection. A novel application of Radarsat has been the study of oil lakes in the deserts of Kuwait.[201,202] A number of nations now use radar satellites routinely to provide imagery for larger spills and to give indications of ship discharges. ERS-1 and 2 have been used for mapping oil spills in the Caspian Sea.[202] Fortuny et al. describe the use of ERS-2 and ENVISAT to provide imagery during the *Prestige* incident off Spain.[203]

Torres Palenzuela and co workers used two ASAR (Advanced SAR) images from the Envisat satellite to study the Prestige spill off Spain.[204] Using several techniques that were readily-available, such as filtering and comparison to GIS data of the areas, several slicks were identified. These slicks were confirmed by recorded sightings from helicopters and ships.

Several countries have instituted satellite monitoring systems for oil pollution.[205,206] Many of these countries use processing methods as described above. Extensive programs are in place in the Baltic Sea, North Sea, and English Channel.[143] There are now beginning programs in the Black, Caspian, and Azov seas.[206,207] Canada has had a program in place for several years.[205] The Mediterranean Sea has had such a program for a long time.[141,142] A constellation of monitoring satellites is proposed for the Mediterranean sea.

In recent years, a number of new satellite-borne SAR sensors have been launched; see Table 6.2. While one of these sensors, Radarsat-2, operates in the traditional C—band, TerraSAR—X and Cosmos Skymed operate in the X—band, while the PALSAR sensor on ALOS operates in the L—band. As noted above, X—band is the preferred band for oil spill remote sensing in terms of Bragg scattering. All four of these new SAR satellites have polarimetric imaging modes (some are experimental vs. operational modes) and much higher spatial resolution (down to 3 m), which may have application for oil spill remote sensing. Radarsat-2, like its predecessor, is an operational commercial satellite that can be tasked to respond to emergency situations such as major oil spills. The time required to task Radarsat-2 in emergency mode is now 4 hours, which is a large improvement from the 12 hours required to task its predecessor. As noted above, VV polarization provides a superior clutter-to-noise ratio (CNR) over HH polarization for oil spill detection. Radarsat-2 is fully

TABLE 6.2 Current and Future Satellite-Borne SAR Sensors

Satellite	Launch Date	Owner/Operator	Band
ERS-2	1995	European Space Agency	C
RADARSAT-1	1995	Canadian Space Agency	C
RADARSAT-2	2007	Canadian Space Agency	C
ENVISAT (ASAR)	2002	European Space Agency	C
ALOS (PALSAR)	2006	Japan Aerospace Exploration Agency	L
TerraSAR-X	2007	German Aerospace Centre	X
Tandem -X	tbd	German Aerospace Centre	X
Cosmos Skymed-1/2	2007	Italian Space Agency	X
TecSAR	2008	Israel Aerospace Industries	X
Sentinel-1	2012	European Space Agency	C
RADARSAT-Constellation (3-satellites)	2014	Canadian Space Agency	C

polarimetric, and there is interest in investigating whether a dual polarization ScanSAR mode utilizing VV/VH polarizations will work for oil and ship detection, respectively, as part of the Integrated Satellite Tracking of Pollution (ISTOP) program.[208] The increased number of SAR satellites, as well as the plans to operate constellations of small satellites such as Cosmos (Constellation of Small Satellites for Mediterranean basin Observation), will provide increased temporal coverage with revisit times down to a few hours in some circumstances. The opportunity for increased frequency of image collection should prove useful to the oil spill response community. Figures 6.31 to 6.36 show the use of radar satellites and the look-alikes to oil that sometimes appear in the images.

6.10. OIL UNDER ICE DETECTION

The difficulties in detecting oil in or under ice are numerous. Ice is never a homogeneous material but rather incorporates air, sediment, salt, and water, many of which may present false oil-in-ice signals to the detection mechanisms. In addition, snow on top of the ice or even incorporated into the ice adds complications. During freeze-up and thaw in the spring, there may not be distinct layers of water and ice. There are many different types of ice and

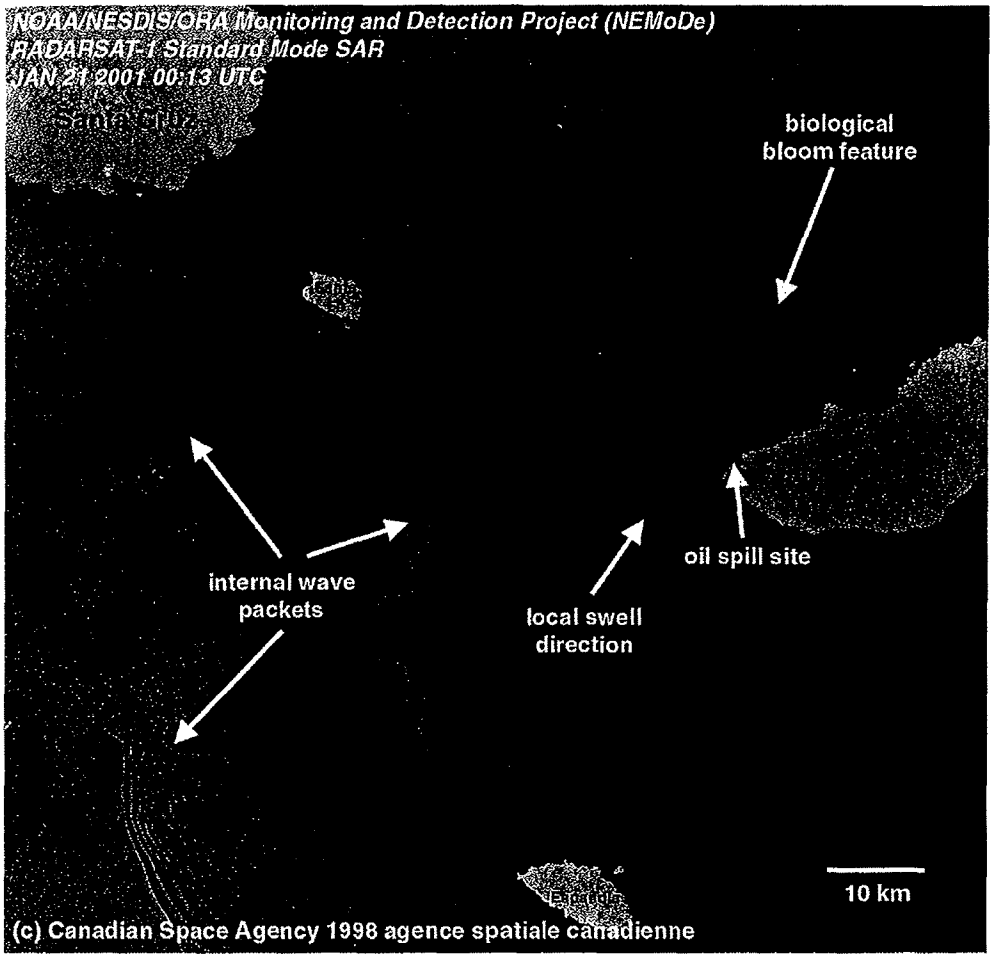

FIGURE 6.31 A satellite radar image of a known spill off the Galapagos Islands. Note that most of the image consists of slick look-alikes.

different ice crystalline orientations. A separate subsection in this book provides a review of oil in and under ice.

6.11. UNDERWATER DETECTION AND TRACKING

Many different techniques have been tried for underwater oil detection. First, the division should be made between oil in the water column or floating on a pycnocline, and oil on the bottom. Quite different physics and conditions can apply to these different situations.

Several parties have tried to use standard sonars to detect submerged oil on the bottom. Oil on the bottom can appear as a softer surface than ordinary bottom sediment.[209] The problem arises in that vegetation on the bottom also appears similar, and thus many false positives arise. In the water column, sonar can be useful as it can locate intermediate oil on pycnoclines; however, there is

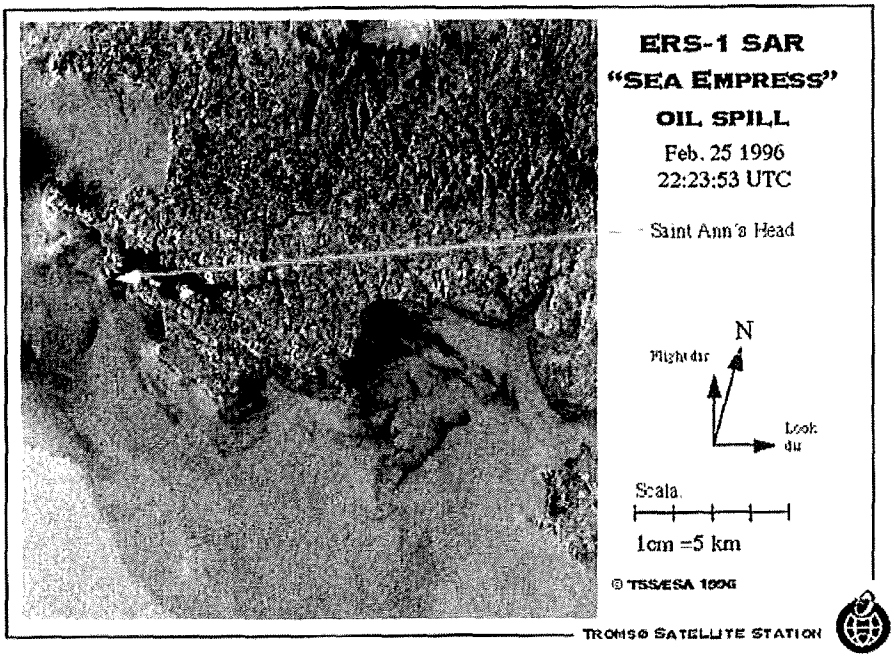

FIGURE 6.32 A satellite radar image of the large *Sea Empress* spill off the United Kingdom. The dark areas near the shore are calm areas. Note that the slick and these calm areas blend so that there is no delineation between them near the shoreline.

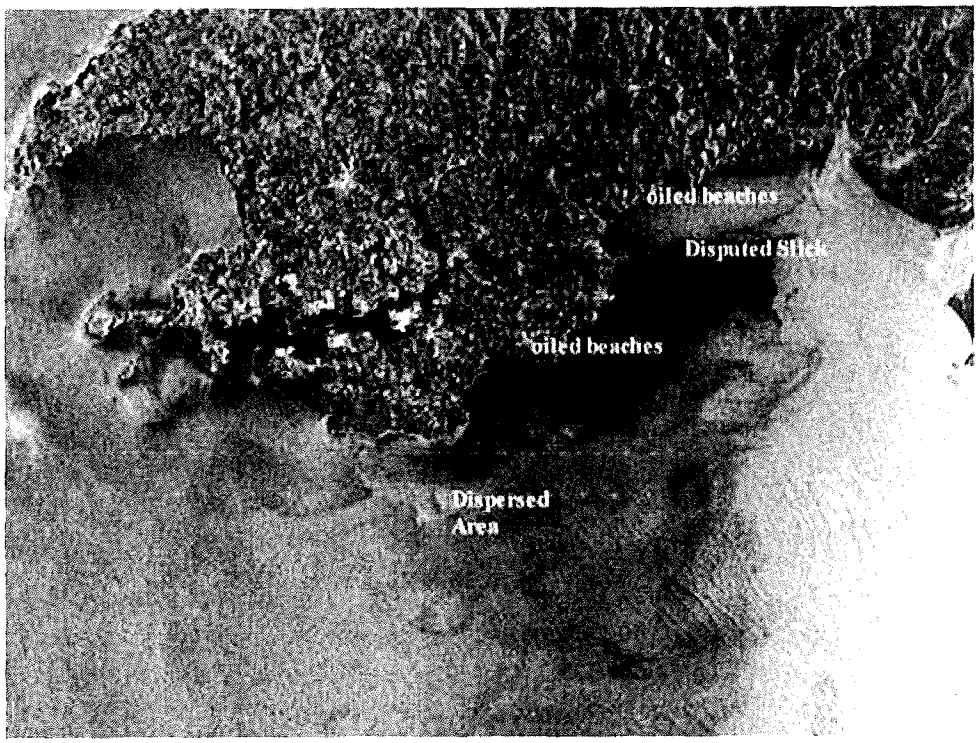

FIGURE 6.33 A Radarsat-1 image of the large *Sea Empress* spill off the United Kingdom. Similar features as in Figure 6.32 are noted.

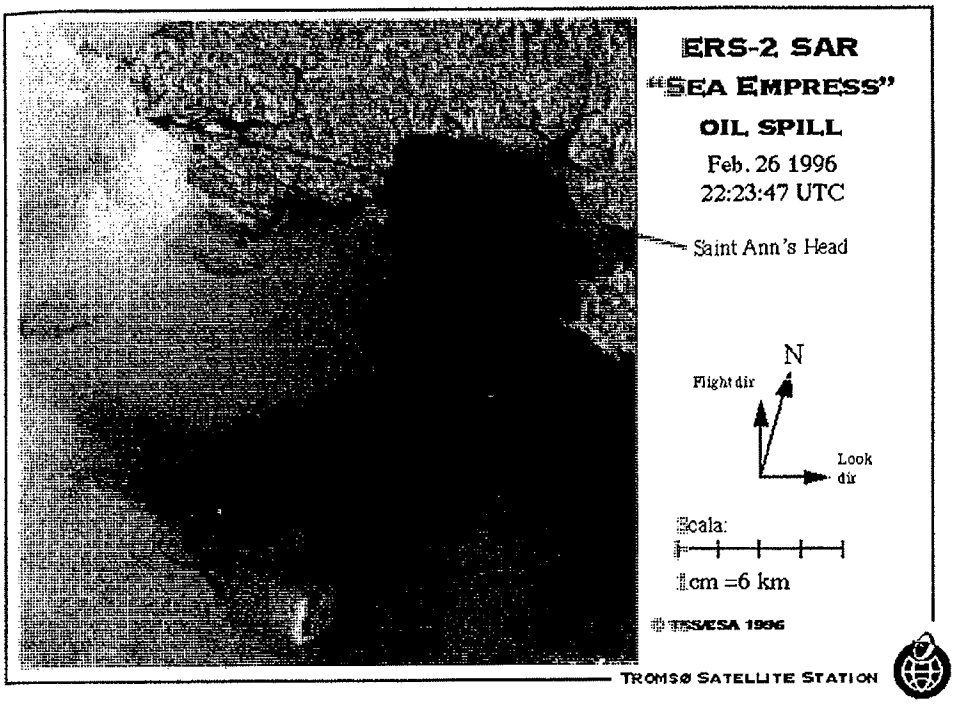

FIGURE 6.34 A third satellite radar image of the large *Sea Empress* spill off the United Kingdom. This image was taken a few days after the images in Figures 6.32 and 6.33. It appears that the oil slick has separated and some has moved to the bottom of the photograph and part toward the shore. This was never confirmed, and the "slick" at the bottom of the photograph may have indeed been oceanographic features.

no unique signature, and there are often weeds and other debris on pynoclines. Wendelboe et al. report on tests using a 200 and 400 kHz (dual-frequency) multibeam system.[210] The contributing signal is the lower acoustic reflectivity of the oil than typical bottom geological formation or the better reflection than weed beds. Wendelboe et al. used the backscatter signals from several tests to develop algorithms for oil detection. This was tested in a tank with a 90% success rate and a 23% false detection rate.

Oil on the bottom has successfully been mapped by underwater cameras, often mounted on sleds.[210-213] The problems with this technique are the bottom visibility— which is often insufficient to discriminate—and the difficulty in towing the camera vehicle as slow as 1 knot, the necessary speed. Pfeifer et al. were successful in employing mosaics of photographs to determine the aerial extent of oil on the seafloor.[212-213]

A low-technology approach had been historically employed. Heavy oil, oil such as would sink, often adheres to oil snares or pom-poms, which are polypropylene strips mounted much as a cheerleader's pom-pom. These can be mounted on a beam and towed over the bottom and then raised periodically to see if oil has adhered.[210] Alternatively, they can be mounted on an anchor with

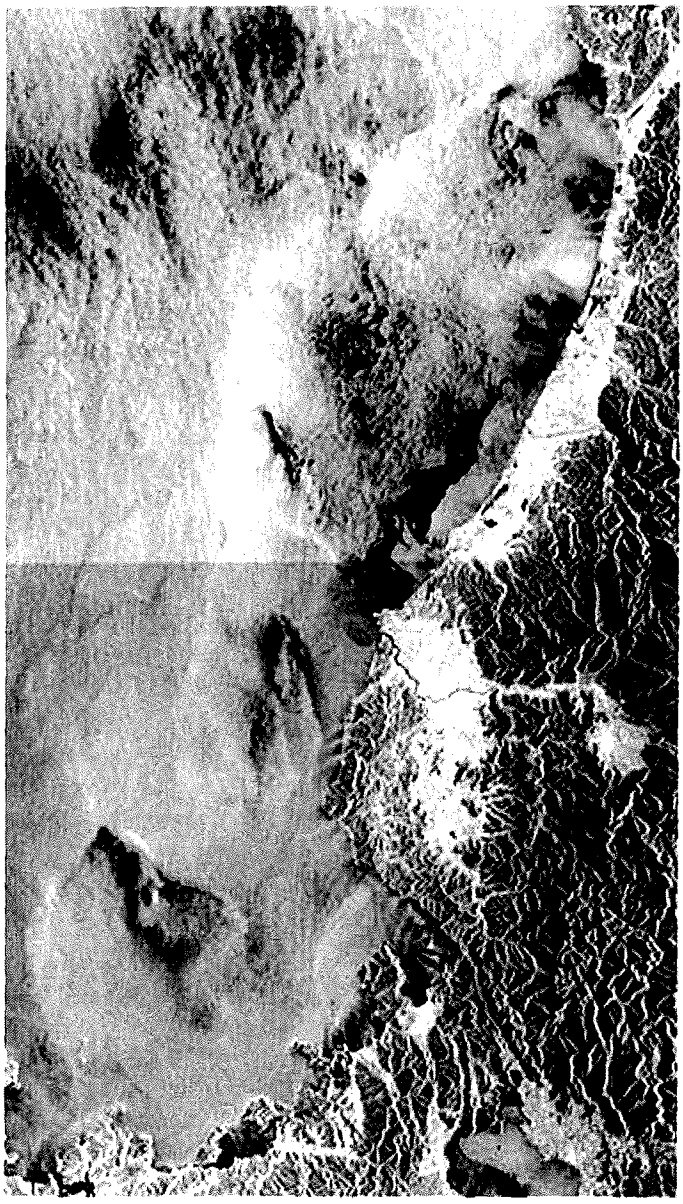

FIGURE 6.35 A radar image of the Nakhodka oil spill off the west coast of Japan (Radarsat-1). Only the black features on the lower half of the photograph and near the shoreline have been confirmed as oil. The remainder of the black areas are oceanographic features.

a marker buoy. These are then raised periodically to check whether the subsurface oil has contacted them.

Camilli et al. have successfully applied mass spectrometry to the detection of sunken heavy oil (Fuel Oil #6).[214] Using the small and enclosed mass spectrometer, TETHYS, the low-molecular-weight hydrocarbons coming from sunken oil masses are monitored. The mass spectrometer is mounted in a submersible that is driven over the seafloor. The exact position of the submersible is monitored closely using an acoustic positioning system on the surface. Signals then can be correlated closely to the position on the seafloor. Three ion peaks of m/z 43, 41, 27 are monitored to establish hydrocarbon

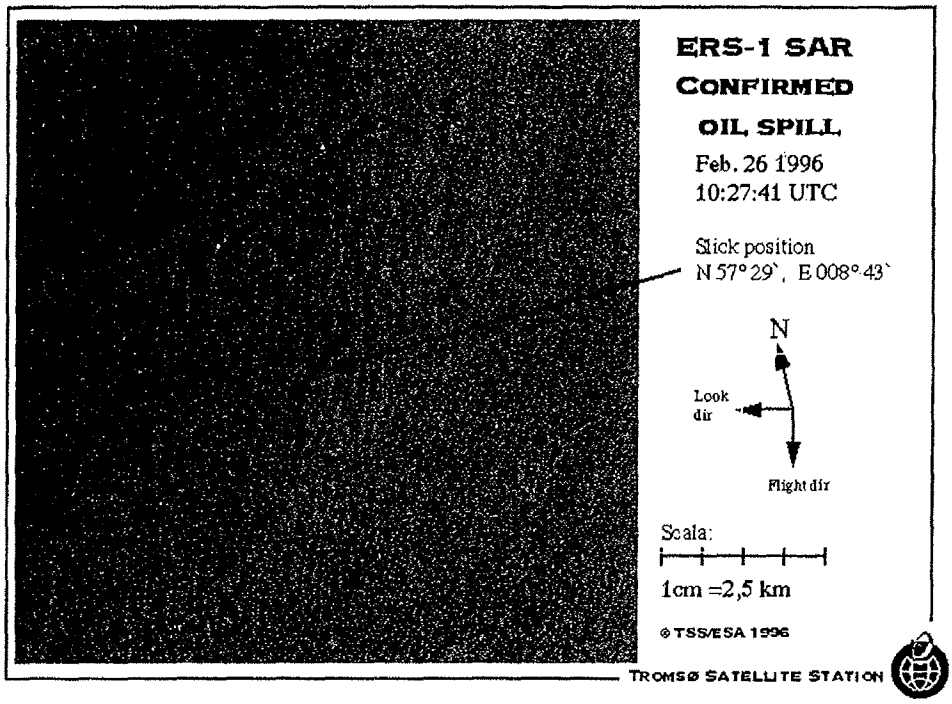

FIGURE 6.36 A satellite radar image of an oil slick in the North Sea. This slick was confirmed by aerial observation.

presence. Tests show that the ion peaks provide sensitivity as low as 0.4 ppb. This is fully sufficient to monitor sunken oil. Tests were conducted in a test tank and later over actual spills in the Gulf of Mexico. The technique was able to find concentrations of sunken oil and place the locations within 1 meter. The tests in the Gulf of Mexico were conducted at depths of 200 meters and confirmed by using cameras on the submersible.

6.12. SMALL REMOTE-CONTROLLED AIRCRAFT

Several parties have suggested using remote-controlled aircraft to provide more economical solutions for response personnel.[215,216] In fact, remote-controlled aircraft have been used by a number of parties for monitoring a variety of pollutants since the 1970s.[217]

Belgium employs an Unmanned Aerial Vehicle (UAV) of the B-Hunter class to routinely monitor its portion of the North Sea.[216] This is a large UAV that has visible and IR camera systems aboard. The unit has a 10-hour endurance over the targets.

A variety of commercial platforms are now available that can carry small sensors such as visible and IR cameras. Furthermore, automatic navigation technology has now made these units, especially helicopters, very much easier to fly than in previous years.

6.13. REAL-TIME DISPLAYS AND PRINTERS

A very important aspect of remote sensing is the production of data so that operations people can quickly and directly use it. Real-time displays are important, so that remote sensor operators can adjust instruments directly in flight and provide information quickly on the location or state of the spill. A major concern of the client is that data be rapidly available.[218] An additional concern is that the data from various sensors be available in a combined or fused form.[85] Furthermore, there is a need to correct this data for aircraft motion and to annotate the data with time and position. At this time, existing hardware and software must be adapted as commercial off-the-shelf equipment for directly outputting and printing sensor data is not yet available. The displays and operators of a remote sensing aircraft are shown in Figure 6.37.

6.14. ROUTINE SURVEILLANCE

One application of oil spill remote-sensing equipment is to detect and map slicks resulting from illegal discharges of oil from ships and offshore platforms. Historically, this task has always been performed using visual techniques, but in the past decade it has increasingly been turned over to aircraft with some

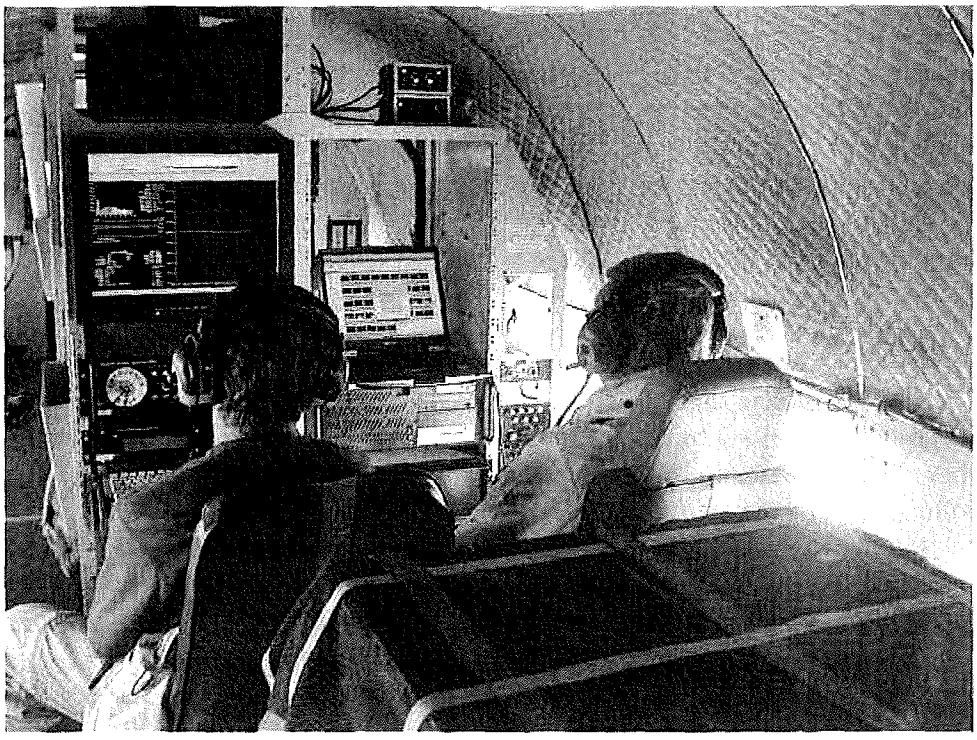

FIGURE 6.37 The interior of a remote sensing aircraft showing operators and displays. *Photography by Environment Canada.*

instrumentation. Typical instrumentation includes a SLAR, IR/UV scanner, and cameras. This sensor package is economical compared to more ideal packages and greatly improves capability beyond just visual observation. Limitations include limited ability to 'look into' ship wakes, limited night operations, and inability to positively identify oil slicks. Recent additions such as improved SLAR systems, better display systems, and nighttime cameras have added to the capability but do not overcome these limitations. Figure 6.38 shows pilots overflying the stern of a ship to ascertain whether it is discharging oil.

Many efforts have been made to perform surveillance of illegal discharges. Most existing operative remote systems are dedicated to this function. These are estimated to be around 35, most of these being around Europe.[219] There are intensive programs in some areas, for example, in the North Sea. Carpenter reports on the 18-year program of surveillance in the North Sea.[220] Some interesting statistics are noted. In 2004, 418 unidentified slicks were found, 65 slicks from oil rigs, and 57 slicks from ships. In 2004, 3,314 hours were flown in daylight and 594 in darkness. In the same year 91 slicks were found in the darkness and 449 in daylight.

Ferraro et al. describe a routine surveillance program using satellite and aircraft data for the Mediterranean Sea.[142] Future work in the Mediterranean Sea proposes a cluster of radar satellites to constantly monitor oil pollution.[221]

A word about aircraft is suitable here. A variety of aircraft are deployed as remote-sensing aircraft. Typically, different types are deployed for routine surveillance and for remote-sensing research. The latter requires flexibility in mounting sensors and in access to the outside of the aircraft. Figures 6.39 to 6.42 show some remote-sensing aircraft and highlight the modifications necessary.

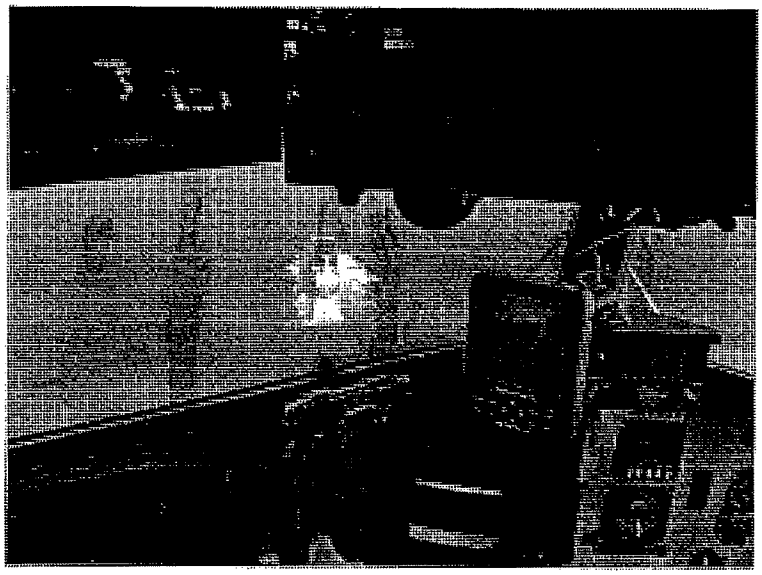

FIGURE 6.38 A ship viewed from the cockpit of a remote sensing airplane. The ship will be overflown to ascertain whether it is discharging oil. *Photography by Environment Canada.*

FIGURE 6.39 A view of a remote-sensing aircraft. The extensive airframe modifications are not visible in this photograph. The aircraft has extensive modifications in the interior to provide racks for equipment.

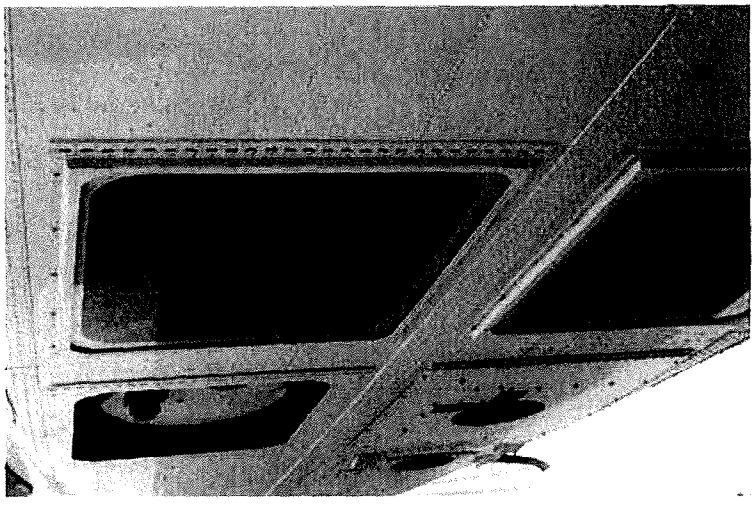

FIGURE 6.40 The bottom of the aircraft shown in Figure 6.39. This particular aircraft has 4 one-meter ports and one half-meter port. The direct opening in the one port is for a laser beam exit. *Photography by Environment Canada.*

FIGURE 6.41 A view of another remote-sensing aircraft. This aircraft carries experimental radars, and one of the radomes is visible under the aircraft. Such modification can cost millions of dollars and take two years to complete.

6.15. FUTURE TRENDS

Advances in sensor technology will continue to drive the use of remote sensors as operational oil spill response tools in the future. Cameras and thermal IR cameras that offer high sensitivity are cheap and plentiful. This improvement not only reduces the size and complexity of the sensor, but also the cost. In the next decade, advances in solid-state laser technology, in particular diode-pumped solid-state lasers, will greatly reduce the size and energy consumption of laser-based remote sensors. This will promote the use of these sensors in smaller, more economical aircraft within the budget of many more regulatory agencies and maritime countries. Rapidly improving computer capabilities will allow for true real-time processing. At the present time and for the foreseeable future, there is no single "Magic Bullet" sensor that will provide all the information required to detect, classify, and quantify oil in the marine and coastal environment. An example of the improvement in recent years is that of the night-vision camera. It is now possible to use this sensor to visualize oil at night. An illustration of this appears in Figure 6.43.

It will require the combined advances in sensor technologies and computer capabilities to gather, integrate, and merge several sources of data into a real-time format, usable by response crews in the field. If this type of information can be made available to response crews in a short enough timeframe following

FIGURE 6.42 A view of the other side of the aircraft shown in Figure 6.41. This shows a lateral radome on the side of the aircraft as well as the radome on the underside. This aircraft also has extensive modifications in the interior to provide racks for equipment and power to sensors. *Photography by Environment Canada.*

a spill incident, then it can be used to lessen the potentially disastrous effects of a major oil spill on the marine ecosystem.

As technology in remote-controlled systems evolve, it is possible to employ such technology in oil spill remote sensing. First efforts in the deployment of remote-controlled sensing aircraft have posted success and will, no doubt, be expanded in the future.[222]

6.16. RECOMMENDATIONS

Recommendations are based on the above considerations and include economy as a major factor. Table 6.3 shows the considerations related to the development state, cost, and use of the sensor, and Table 6.4 shows the applicability of the sensor to various functions. The laser fluorosensor offers the only potential for discriminating between oiled and unoiled weeds or shoreline, and for positively identifying oil pollution on ice, among ice, and in a variety of other situations. This instrument, however, is large and expensive. A cheap sensor recommended for oil spill work is an IR camera. This is the cheapest undiscriminating device. This is the only piece of equipment that can be purchased off-the-shelf.

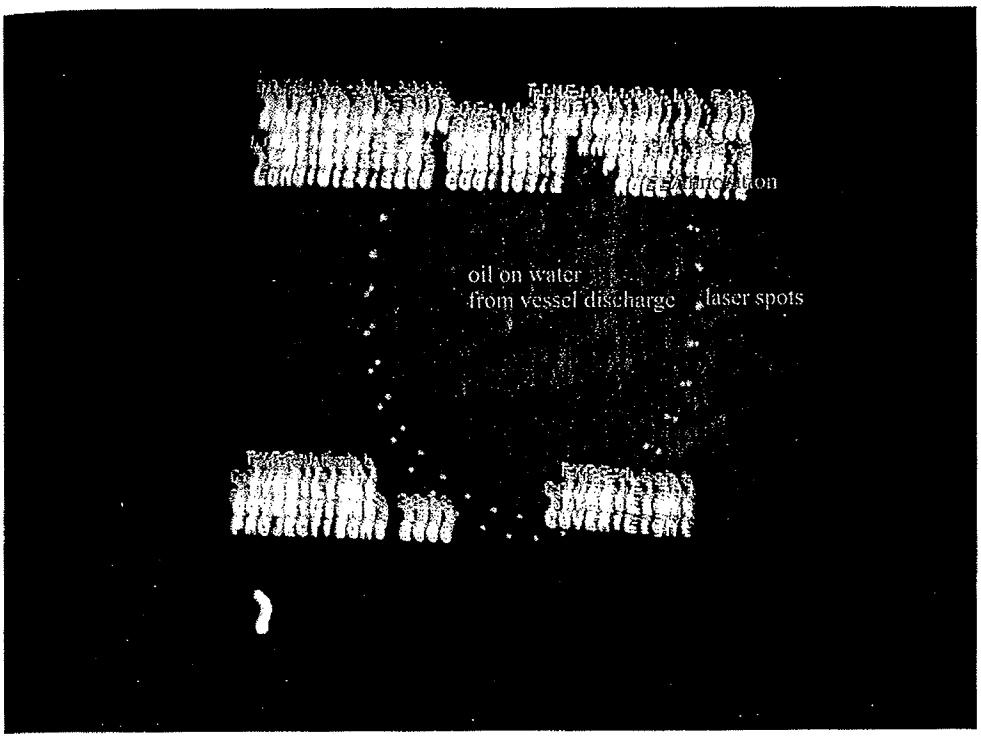

FIGURE 6.43 A night-vision display. The annotation shows the various features of the image. *Photography by Environment Canada.*

All other sensors require special order and, often, development. Radar, though low in priority for purchase, offers the only potential for large area searches and foul weather remote sensing. Most other sensors are experimental or do not offer good potential for oil detection or mapping. Any sensor package should include a real-time printer and display, and a downlink.

In order to respond effectively to major marine oil spills, a combination of airborne and satellite-borne sensor systems is recommended. Improvements in the resolution of satellite-based systems, particularly SAR systems combined with the increased number of such systems and the ability to steer them to image the area of the oil spill, will lead to their increased use in a tactical role. Being capable of imaging vast areas of the open ocean will ensure that satellite-borne sensors will also continue to be used in a strategic manner. There are a number of commercially available airborne sensor systems that provide near real-time information on oil slick location and indications of thicker areas of the pollution in an easily interpretable graphical manner. These airborne sensor systems are currently being employed by a large number of maritime nations in conjunction with satellite-based sensor systems.

Historically, satellite sensors suffered from problems of low resolution and the low frequency of scene observation. These inadequacies are now being addressed by higher resolution systems with multiple imaging modes and the

TABLE 6.3 Attributes for Airborne Sensor Selection

Sensor	State of Development	Amount of Experience in Use	Specific to Oil	Immunity to False Targets	Typical Coverage (km)	Acquisition Cost Range k$	Aircraft Physical Requirements
Still Camera	High	High	Poor	Poor	0.25 to 2	1 to 5	no
Video	High	High	Poor	Poor	0.25 to 5	1 to 10	no
Night Time Vision Camera	Medium	Medium	Poor	Poor	0.25 to 2	5 to 20	no
IR Camera (8–14 μm)	High	Medium	Medium	Medium	0.25 to 2	20 to 50	no
UV Camera	Medium	Medium	Poor	Poor	0.25 to 2	4 to 20	no
Multi-Spectral Scanner	Medium	Medium	Poor	Poor	0.25 to 2	100 to 200	some
Radar	High	High	Medium	Poor	5 to 50	1200 to 8000	yes-Dedicated
Microwave Radiometer	Medium	Medium	Medium	Medium	1 to 5	400 to 1000	yes-Dedicated
Laser Fluorosensor	Medium	Limited	Good	Good	0.01 to 0.1	300 to 1000	yes-Dedicated

TABLE 6.4 Sensor Suitability for Various Missions

Sensor	Support for Cleanup	Night & Fog Operation	Detection of Oil with Debris	Oiled Shoreline Survey	Spill Mapping	Ship Discharge Surveillance	Enforcement and Prosecution
Still Camera	2	n/a	1	2	2	2	2
Video	2	n/a	1	2	2	2	2
Night Time Vision Camera	3	4	1	n/a	2	2	2
IR Camera (8–14 μm)	4	2	1	n/a	3	3	3
UV Camera	2	n/a	n/a	n/a	3	2	1
UV/IR Scanner	4	2	1	n/a	4	3	3
Multi-Spectral Scanner	1	n/a	n/a	1	2	1	1
Radar	n/a	4	n/a	n/a	4	3	2
Microwave Radiometer	1	3	n/a	n/a	2	2	1
Laser Fluorosensor	4	3	5	5	1	5	5

Key: n/a = not applicable; numerical values represent a scale from 1 = poorly suited to 5 = ideally suited

ability to steer the sensor to look in the direction of the target of interest. There are an increasing number of satellite-borne SAR and optical sensors, some of which currently or soon will operate in constellations to provide increased coverage of the Earth's surface. These enhanced capabilities will allow for the possible use of these sensors in a tactical mode of operation. In spite of these increased capabilities, there remains an essential role for airborne oil spill remote-sensing platforms. The ability to collect and deliver real-time oil slick location information will ensure the continued use of airborne systems in spite of their high operational costs.

If this type of real-time oil spill remote-sensing information can be made available to response crews in a short enough timeframe following a spill incident, the information can be used to mitigate the potentially disastrous effects of a major oil spill on the marine ecosystem.

ACKNOWLEDGMENTS

The authors acknowledge the many parties who contributed to this chapter, including the Canada Centre for Remote Sensing, and the Canadian Space Agency. In particular, they acknowledge Environment Canada for the many photographs in this chapter.

REFERENCES

1. Serra-Sogas N, O'Hara PD, Canessa R, Keller P, Pelot R. Visualization of Spatial Patterns and Temporal Trends for Aerial Surveillance of Illegal Oil Discharges in Western Canadian Marine Waters. *Mar Pollut Bull* 2008;**815**.
2. Brown CE, Fingas MF. The Latest Developments in Remote Sensing Technology for Oil Spill Detection. *Interspill* 2009.
3. Fingas MF, Brown CE. Review of Oil Spill Remote Sensing, *Proceedings of SPILLCON 2000*, Australian Marine Safety Authority, Sydney, www.meetingplanners.com.au/spillcon, 2000.
4. Fingas MF, Brown CE. Review of Oil Spill Remote Sensors, *Proceedings of the Seventh International Conference on Remote Sensing for Marine and Coastal Environments*. Ann Arbor, MI: Veridien; 2002.
5. Fingas M, Brown CE, Review of Oil Spill Remote Sensing, *Proceedings of the 8th International Conference on Remote Sensing for Marine and Coastal Environments*. Ann Arbor, MI: Altarum; 2005.
6. Hengstermann T, Robbe N. Airborne Oil Spill Remote Sensing. *Hydro International* 2008;**10**.
7. Jha MN, Levy J, Gao Y. Advances in Remote Sensing for Oil Spill Disaster Management: State-of-the-Art Sensors Technology for Oil Spill Surveillance. *Sensors* 2008;**236**.
8. Fingas MF, Brown CE, Gamble L. The Visibility and Detectability of Oil Slicks and Oil Discharges on Water. *AMOP* 1999;**865**.
9. Taft DG, Egging DE, Kuhn HA. Sheen Surveillance: An Environmental Monitoring Program Subsequent to the 1989 *Exxon Valez* Shoreline Cleanup, *Exxon Valdez* Oil Spill: Fate and Effects in Alaskan Waters. *ASTM STP* 1995;**215**:1219.

10. Lehr WJ. Oil Spill Monitoring Using a Field Microcomputer-GPS Receiver Combination, *Proceedings of the Second Thematic Conference on Remote Sensing for Marine and Coastal Environments: Needs, Solutions and Applications*, ERIM, 1994;**I-435**.
11. O'Neil RA, Neville RA, Thompson V. *The Arctic Marine Oilspill Program (AMOP) Remote Sensing Study*, Environment Canada Report EPS 4-EC-83–3, 1983.
12. Brown HM, Bittner JP, Goodman RH. *The Limits of Visibility of Spilled Oil Sheens*, Proceedings of the Second Thematic International Airborne Remote Sensing Conference and Exhibition, ERIM, 1996;**III 327**.
13. Taylor S. *0.45 to 1.1 μm Spectra of Prudhoe Crude Oil and of Beach Materials in Prince William Sound*, Alaska, CRREL Special Report No. 92–5, 1992.
14. Huang M, Yu Y, Zhang Y, Shen J, Qi X. Analysis of Water Spectral Features of Petroleum Pollution and Estimate Models from Remote Sensing Data. *SPIE* 2008;**712312**.
15. Ahmed S, Gilerson A, Oo M, Zhou J, Chowhardy J, et al. The Polarization Properties of Reflectance from Coastal Waters and the Ocean-Atmosphere System. *SPIE* 2006; **636003**.
16. Carnesecchi F, Byfield V, Cipollini P, Corsini G, Diani M. An Optical Model for the Interpretation of Remotely Sensed Multispectral Images of oil. *SPIE* 2008;**710504**.
17. Bianchi R, Cavalli RM, Marino CM, Pignatti S, Poscolieri M. Use of Airborne Hyperspectral Images to Assess the Spatial Distribution of Oil Spilled During the Trecate Blow-Out (Northern Italy). *SPIE* 1995;**352**.
18. Bagheri S, Stein M, Zetlin C. Utility of Airborne Videography as an Oil Spill-Response Monitoring System. In: *Encyclopedia of Environmental Control Technology*, **367**. Gulf Publishing Company; 1995.
19. Brown CE, Fingas MF, Marois R. Oil Spill Remote Sensing: Laser Fluorosensor Demonstration Flights off the East Coast of Canada. *AMOP* 2004;**317**.
20. Brown CE, Fingas MF, Marois R. Oil Spill Remote Sensing Flights in the Coastal Waters Around Newfoundland, *Proceedings of the Eighth International Conference on Remote Sensing for Marine and Coastal Environments*. Altarum; 2005.
21. Palmer D, Borstad GA, Boxall SR. Airborne Multi Spectral Remote Sensing of the January 1993 Shetlands Oil Spill, *Proceedings of the Second Thematic Conference on Remote Sensing for Marine and Coastal Environments: Needs, Solutions and Applications*, ERIM, 1994;**I-546**.
22. Wadsworth A, Looyen WJ, Reuter R, Petit M. Aircraft Experiments with Visible and Infrared Sensors. *Int J Remote Sens* 1992;**1175**.
23. Locke C, White M, Michel J, Henry C, Sellars JD, Aslaksen ML. Use of Vertical Digital Photography at the Bayou Perot, LA, Spill for Oil Mapping and Volume Estimation. *IOSC* 2008;**127**.
24. Stelmaszewski A, Krol T, Toczek H. Light Scattering in Baltic Crude Oil – Seawater Emulsion. *Oceanologia* 2009;**405**.
25. Hurford N. Review of Remote Sensing Technology. In: Lodge AE, editor. *The Remote Sensing of Oil Slicks*, **7**. John Wiley and Sons; 1989.
26. Goodman RH. Application of the Technology in North America. In: Lodge AE, editor. *The Remote Sensing of Oil Slicks*, **39**. John Wiley and Sons; 1989.
27. Belore RC. A Device for Measuring Oil Slick Thickness. *Spill Tech News* 1982;**44**.
28. Neville RA, Thompson V, Dagg K, O'Neil RA. An Analysis of Multispectral Line Scanner Imagery from Two Test Spills, *Proceedings of First Workshop Sponsored by Working Group I of the Pilot Study on the Use of Remote Sensing for the Control of Marine Pollution, NATO Challenges of Modern Society*, **201**, 1979.

29. Bolus RL. Airborne Testing of a Suite of Remote Sensors for Oil Spill Detecting on Water, *Proceedings of the Second Thematic International Airborne Remote Sensing Conference and Exhibition*, ERIM, 1996;**III 743**.
30. Goodman RH. *Simple Remote Sensing System for the Detection of Oil on Water*, Environmental Studies Research Fund Report Number 98, 1988.
31. Seakem Oceanography, *Remote Sensing Chronic Oil Discharges*, Environment Canada Report EE-108, 1988.
32. Kennicutt MC, MacDonald IR, Rogne T, Giammona C, Englehardt R. The *Tenyo Maru* Oil Spill: A Multi-Spectral and Sea Truth Experiment. *AMOP* 1992;**349**.
33. Rogne T, Macdonald I, Smith A, Kennicutt MC, Giammona C. Multi-Spectral Remote Sensing and Truth Data from the *Tenyo Maru* Oil Spill, *Proceedings of the First Thematic Conference on Remote Sensing for Marine and Coastal Environments*, ERIM 37 [also published in *Photogramm Eng Rem Sens*, 1993, 1992;**391**.
34. Rogne TJ, Smith AM. *Tenyo Maru Oil Spill Remote Sensing Data Analysis*. Washington, D.C: Marine Spill Response Corporation; 1992. MSRC Technical Report Series 92-003.
35. Salisbury JW, D'Aria DM, Sabins FF. Thermal Infrared Remote Sensing of Crude Oil Slicks. *Remote Sens Environ* 1993;**225**.
36. Hover GL. Testing of Infrared Sensors for U.S. Coast Guard Oil Spill Response Applications, *Proceedings of the Second Thematic Conference on Remote Sensing for Marine and Coastal Environments: Needs, Solutions and Applications*, ERIM 1994;**I-47**.
37. Grierson IT. Use of Airborne Thermal Imagery to Detect and Monitor Inshore Oil Spill Residues During Darkness Hours. *Environ Manage* 1998;**905**.
38. Shih W-C, Andrews AB. Infrared Contrast of Crude-Oil-Covered Water Surfaces. *Opt Lett* 2008;**3019**.
39. Brown HM, Baschuk JJ, Goodman RH. The Limits of Visibility of Spilled Oil Sheens. *AMOP* 1998;**805**.
40. Brown CE, Fingas MF. Review of the Development of Laser Fluorosensors for Oil Spill Application. *Mar Pollut Bull* 2003;**477**.
41. Brown CE, Fruhwirth M, Wang Z, Lambert P, Fingas M. Airborne Oil Spill Sensor Test Program, *Proceedings of the Second Thematic Conference on Remote Sensing for Marine and Coastal Environments: Needs, Solutions and Applications*, ERIM, 1994;**I-19**.
42. Brown CE, Fingas MF, An J. Laser Fluorosensors: A Survey of Applications and Developments of a Versatile Sensor. *AMOP* 2001;**485**.
43. Brown CE, Nelson R, Fingas MF, Mullin JV. Airborne Laser Fluorosensing: Overflights During Lift Operations of a Sunken Oil Barge, *Proceedings of the Fourth Thematic Conference on Remote Sensing for Marine and Coastal Environments*, ERIM 1997;**I 23**.
44. Brown CE, Marois R, Fingas MF, Choquet M, Monchalin J-P, Mullin J, et al. Airborne Oil Spill Sensor Testing: Progress and Recent Developments. *IOSC* 2001;**917**.
45. Brown CE, Fingas MF. Review of the Development of Laser Fluorosensors for Oil Spill Application. *Mar Pollut Bull* 2003;**477**.
46. Hengstermann T, Reuter R. Lidar Fluorosensing of Mineral Oil Spills on the Sea Surface. *Appl Optics* 1990;**3218**.
47. Balick L, DiBenedetto JA, Lutz SS. Fluorescence Emission Spectral Measurements for the Detection of Oil on Shore, *Proceedings of the Fourth Thematic Conference on Remote Sensing for Marine and Coastal Environments*, ERIM 1997;**I 13**.
48. Sarma AK, Ryder AG. Comparison of the Fluoresence Behaviour of a Biocrude Oil and Crude Petroleum Oils. *Energy & Fuels* 2006;**783**.

49. Samberg A. The State-of-the-Art of Airborne Laser Systems for Oil Mapping. *Can J Rem Sens* 2007;**143**.
50. Jha MN, Gao Y. Oil Spill Contingency Planning Using Laser Fluorosensors and Web-Based GIS. *Proceedings Oceans Marine Technology Society*; 2008.
51. Diebel D, Hengstermann T, Reuter R, Willkomm R. Laser Fluorosensing of Mineral Oil Spirits. In: Lodge AE, editor. *The Remote Sensing of Oil Slicks*, **127**. John Wiley; 1989.
52. Geraci AL, Landolina F, Pantani L, Cecchi G. Laser and Infrared Techniques for Water Pollution Control. *IOSC* 1993;**525**.
53. Pantani L, Cecchi G, Bazzani M. Remote Sensing of Marine Environments with the High Spectral Resolution Fluorosensor, FLIDAR 3. *SPIE* 1995;**56**.
54. Campbell I, McStay D. A Ship borne System for the Detection of Surface Oil. In: *Advanced Technologies for Environmental Monitoring and Remediation*, **214**. International Society for Optical Engineering; 1995.
55. Hoge FE, Swift RN. Oil Film Thickness Measurement Using Airborne Laser-Induced Water Raman Backscatter. *Appl Optics* 1980;**3269**.
56. Piskozub J, Drozdowska V, Varlamov V. A Lidar System for Remote Measurement of Oil Film Thickness on Sea Surface, *Proceedings of the Fourth Thematic Conference on Remote Sensing for Marine and Coastal Environments*, ERIM 1997;**I386**.
57. Goodman R, Brown CE. Oil Detection Limits for a Number of Remote Sensing Systems, *Proceedings of the Eighth International Conference on Remote Sensing for Marine and Coastal Environments*. Alterum Conferences; 2005.
58. Fingas MF. A Simple Night Time Oil Slick Detector. *Spill Tech News* 1982;**137**.
59. Dick R, Fruhwirth M, Brown C. Laser Fluorosensor Work in Canada, *Proceedings of the First Thematic Conference on Remote Sensing for Marine and Coastal Environments*, ERIM, 1992;**223**.
60. James RTB, Dick R. Design of Algorithms for the Real-Time Airborne Detection of Littoral Oil-Spills by Laser-Induced Flourescence. *AMOP* 1996;**1599**.
61. Brown CE, Fingas MF, Gamble RL, Myslicki GE. The Remote Detection of Submerged Oil, *Proceedings of the Third R&D Forum on High-Density Oil Spill Response*, IMO, 2002;**46-54**.
62. Brown CE, Marois R, Myslicki G, Fingas MF. Initial Studies on the Remote Detection of Submerged Orimulsion with a Range-Gated Laser Fluorosensor, *AMOP*, 2002;**773**.
63. Brown CE, Marois R, Myslicki G, Fingas MF, MacKay R. Remote Detection of Submerged Orimulsion with a Range-Gated Laser Fluorosensor. *IOSC* 2003;**779**.
64. Brown CE, Marois R, Gamble RL, Fingas MF. Further Studies on the Remote Detection of Submerged Orimulsion with a Range-Gated Laser Fluorosensor. *AMOP* 2003;**279**.
65. Brown CE, Fingas M, Marois R, Fieldhouse B, Gamble RL. Remote Sensing of Water-in-Oil Emulsions: Initial Laser Fluorosensor Studies. *AMOP* 2004;**295**.
66. Ulaby FT, Moore RK, Fung AK. Microwave Remote Sensing: Active and Passive. *Artech House* 1989;**1466**.
67. Goodman RH. Remote Sensing Resolution and Oil Slick Inhomogeneities, *Proceedings of the Second Thematic Conference on Remote Sensing for Marine and Coastal Environments: Needs, Solutions and Applications*, ERIM, 1994;**I 1-17**.
68. Fäst O. Remote Sensing of Oil on Water—Air and Space-Borne Systems. *Proceedings of the DOOS Seminar* 1986.
69. Skou N, Sorensen BM, Poulson A. A New Airborne Dual Frequency Microwave Radiometer for Mapping and Quantifying Mineral Oil on the Sea Surface, *Proceedings of the Second*

Thematic Conference on Remote Sensing for Marine and Coastal Environments, ERIM, 1994;**559**.

70. Mussetto MS, Yujiri L, Dixon DP, Hauss BI, Eberhard CD. Passive Millimeter Wave Radiometric Sensing of Oil Spills, *Proceedings of the Second Thematic Conference on Remote Sensing for Marine and Coastal Environments: Needs, Solutions and Applications*, ERIM, 1994;**I 35**.
71. Zhifu S, Wiesbeck W. A Study of Passive Microwave Remote Sensing, *Proceedings of the 1988 International Geoscience and Remote Sensing Symposium*, 1988;**1091**.
72. Süss H, Grüner K, Wilson WJ. Passive Millimeter Wave Imaging: A Tool for Remote Sensing. *Alta Frequenza* 1989;**457**.
73. Pelyushenko SA. The Use of Microwave Radiometer Scanning System for Detecting and Identification of Oil Spills, *Proceedings of the Fourth Thematic Conference on Remote Sensing for Marine and Coastal Environments*, ERIM, 1997;**I 381**.
74. McMahon OB, Brown ER, Daniels GD, Murphy TJ, Hover GL. Oil Thickness Detection Using Wideband Radiometry. *IOSC* 1995;**15**.
75. McMahon OB, Murphy TJ, Brown ER. Remote Measurement of Oil Spill Thickness, *Proceedings of the Fourth Thematic Conference on Remote Sensing for Marine and Coastal Environments*, ERIM, 1997;**I-353**.
76. Nunziata F, Migliaccio M, Sobieski P. A BPM Two-Scale Contrast Model. *IGARSS* 2008; **IV-593**.
77. Frysinger GS, Asher WE, Korenowski GM, Barger WR, Klusty MA, Frew NM, et al. Study of Ocean Slicks by Nonlinear Laser Processes in Second-Harmonic Generation. *J Geophys Res* 1992;**5253**.
78. Alpers W, Hühnerfuss H. Radar Signatures of Oil Films Floating on the Sea Surface. *IGARSS* 1987;**741**.
79. Poitevin J, Khaif C. A Numerical Study of the Backscattered Radar Power in Presence of Oil Slicks on the Sea Surface, *Proceedings of the First Thematic Conference on Remote Sensing for Marine and Coastal Environments*, ERIM, 1992;**171**.
80. Hühnerfuss H, Alpers W, Witte F. Layers of Different Thicknesses in Mineral Oil Spills Detected by Grey Level Textures of Real Aperture Radar Images. *I.J Rem Sens* 1989;**1093**.
81. Gens R. Oceanographic Applications of SAR Remote Sensing. *GIScience and Rem Sens* 2008;**275**.
82. Bartsch N, Grüner K, Keydel W, Witte F. Contribution to Oil Spill Detection and Analysis with Radar and Microwave Radiometer: Results of the Archimedes II Campaign. *IEEE Trans Geosci Remote* 1987;**677**.
83. Mastin GA, Mason JJ, Bradley JD, Axline RM, Hover GL. A Comparative Evaluation of SAR and SLAR, *Proceedings of the Second Thematic Conference on Remote Sensing for Marine and Coastal Environments: Needs, Solutions and Applications*, ERIM, 1994;**I-7**.
84. Brown CE, Fingas MF. Synthetic Aperture Radar Sensors: Viable for Marine Oil Spill Response? *AMOP* 2003;**299**.
85. Zielinski O, Robbe N. Past and Future of Airborne Pollution Control. *Interspill* 2004.
86. Dyring A, Fäst O. MSS Puts the Aircraft in the Oil Spill Tracking Network. *Interspill* 2004.
87. Intera Technologies, *Radar Surveillance in Support of the 1983 COATTF Oil Spill Trials*, Environment Canada Report EE-51, 1984.
88. C-CORE (Centre for Cold Ocean Resources Engineering), *Microwave Systems for Detecting Oil Slicks in Ice-Infested Waters: Phase I - Literature Review and Feasibility Study*, Environment Canada Report EPS 3-EC, 1981;**81-3**.

89. Macklin JT. The Imaging of Oil Slicks by Synthetic Aperture Radar. *GEC Journal of Research* 1992;**19**.
90. Kozu T, Umehara T, Ojima T, Suitsu T, Masuyko H, Inomata H. Observation of Oil Slicks on the Ocean by X-Band SLAR. *IGARSS* 1987;**735**.
91. Madsen S, Skou N, Sorensen BM. Comparison of VV and HH Polarized SLAR for Detection of Oil on the Sea Surface, *Proceedings of the Second Thematic Conference on Remote Sensing for Marine and Coastal Environments: Needs, Solutions and Applications*, ERIM, 1994;**I-498**.
92. Hühnerfuss H, Alpers W, Dannhauer H, Gade M, Lange PA, Neumann V, et al. Natural and Man-Made Sea Slicks in the North Sea Investigated by a Helicopter-Borne 5-Frequency Radar Scatterometer. *Int J Rem Sens* 1996;**1567**.
93. Hielm JH. NIFO Comparative Trials. In: Lodge AE, editor. *The Remote Sensing of Oil Slicks*, **67**. John Wiley and Sons; 1989.
94. Marghany M, Cracknell AP, Hasim M. Modification of Fractal Algorithm for Oil Spill Detection from Radarsat-1 SAR Data. *Int J Appl Earth Observ Geoinform* 2009;**96**.
95. Gade M, Alpers W, Huehnerfuss H, Wismann V. Radar Signatures of Different Oceanic Surface Films Measured During the SIR-C-X-SAR Missions. In: *Remote Sensing* 1996; **96**:233.
96. Okamoto K, Kobayashi T, Masuko H, Ochiai S, Horie H, Kumagai H, et al. Results of Experiments Using Synthetic Aperture Radar Onboard the European Remote Sensing Satellite 1-4. Artificial Oil Pollution Detection. *J Commun Res Lab* 1996;**327**.
97. Migliaccio M, Gambardella A, Tranfaglia A. SAR Polarimetry to Observe Oil Spills. *IEEE T Geosci Remote* 2007;**506**.
98. Migliaccio M, Nunziata F, Gambardella A. On the Co-Polarized Phase Difference for Oil Spill Observation. *Int J Rem Sens* 2009;**1587**.
99. Gambardella A, Migliaccio M, De Grandi G. Wavelet Polarimetric SAR Signature Analysis of Sea Oil Spills and Look-Alike Features. *IGARSS* 2007;**983**.
100. Nunziata F, Gambardella A, Migliaccio M. On the Use of Dual-Polarized SAR Data for Oil Spill Observation. *IGARSS* 2008;**II-225**.
101. Forget P, Brochu P. Slicks. Waves and Fronts Observed in Sea Coastal Area by an X-Band Airborne Synthetic Aperture Radar. In: *Remote Sensing of the Environment* 1996;**1**.
102. Marmorino GO, Thompson DR, Graber HC, Trump CL. Correlation of Oceanographic Signatures Appearing in Synthetic Aperature Radar and Interferometric Synthetic Aperture Radar Imagery with In-Situ Measurements. *J Geophys Res* 1997;**723**:18.
103. Tennyson EJ. Shipborne Radar as an Oil Spill Tracking Tool. *AMOP* 1985;**385**.
104. Nøst E, Egset CN. Oil Spill Detection System—Results from Field Trials. *Proceedings Oceans Marine Technology Society* 2006.
105. Gangeskar R. Automatic Oil-Spill Detection by Marine X-Band Radars. *Sea Technology* August 2004;**40-45**.
106. Topouzelis K, Karanthanassi V, Pavlakis P, Rokos D. Potentiality of Feed-Forward Neural Networks for Classifying Dark Formation to Oil Spills and Look-Alikes. *Geocarto International* 2009;**179**.
107. Solberg R, Theophilopoulos N. ENVISYS—A Solution for Automatic Oil Spill Detection in the Mediterranean, *Proceedings of the Fourth Thematic Conference on Remote Sensing for Marine and Coastal Environments*, ERIM, 1997;**I-3**.
108. Wahl T, Eldhuset K, Skøelv Å. Ship Traffic Monitoring and Oil Spill Detection Using ERS-1, In: *Proceedings of the International Symposium "Operationalization of Remote Sensing"* ITC; 1993;**97**.

109. Bern T-I, Wahl T, Anderssen T, Olsen R. Oil Spill Detection Using Satellite Based SAR: Experience from a Field Experiment. *Photogramm Eng Rem S* 1993;**423**.
110. Yan X-H, Clemente-Colon P. The Maximum Similarity Share Matching (MSSM) Method Applied to Oil Spill Feature Tracking Observed in SAR Imagery. In: *Proceedings of the Fourth Thematic Conference on Remote Sensing for Marine and Coastal Environments.* ERIM, 1997;**I-43**.
111. Bentz CM, Politano AT, Ebecken NFF. Automatic Recognition of Coastal and Oceanic Environmental Events with Orbital Radars. *IGARSS* 2007;**914**.
112. Trivero P, Biamino W, Nirchio F. High Resolution COSMO-SkyMed SAR Images for Oil Spills Automatic Detection. *IGARSS* 2007;**2**.
113. Tian W, Shao Y, Wang S. A System for Automatic Identification of Oil Spill in ENVISAT ASAR. *IGARSS* 2008;**III-1394**.
114. Shao Y, Tian W, Wang S, Zhang F. Oil Spill Monitoring Using Multi-Temporal SAR and Microwave Scatterometer Data. *IGARSS* 2008;**III-1378**.
115. Rodriguez MH, Bannerman K, Caceres RG, Pellon de Miranda F, Pedroso EC. Cantarell Natural Seep Modelling Using SAR Derived Ocean Surface Wind and Meteo-Oceanographic Buoy Data. *IGARSS* 2007;**3257**.
116. Robson M, Secker J, Vachon PW. Evaluation of eCognition for Assisted Target Detection and Recognition in SAR Imagery. *IGARSS* 2006;**145**.
117. Garcia-Pineda OI, MacDonald, Zimmer B. Synthetic Aperture Radar Image Processing Using the Supervised Textural-Neural Network Classification Algorithms. *IGARSS* 2008; **IV-1265**.
118. Morales DJ, Moctezuma M, Parmiggiani F. Detection of Oil Slicks in SAR Images Using Hierarchial MRF. *IGARSS* 2008;**III-1390**.
119. Bertacca M. A FEXP Model Short Range Dependence Analysis for Improving Oil Slicks and Low-Wind Areas Discrimination in SAR Imagery. *IGARSS* 2006;**959**.
120. Topouzelis KN. Oil Spill Detection by SAR Images: Dark Formation Detection, Feature Extraction, and Classification Algorithms. *Sensors* 2008;**6642**.
121. Topouzelis K, Karanthanassi V, Pavlakis P, Rokos D. Dark Formation Detection Using Neural Networks. *Int J Remote Sens* 2008;**4705**.
122. Topouzelis K, Stathakis D, Karanthanassi V. Investigation of Genetic Contribution to Feature Selection for Oil Spill Detection. *Int J Remote Sens* 2009;**179**.
123. Karathanassi K, Topouzelis P, Pavlakis, Rokos D. An Object-Oriented Methodology to Detect Oil Spills. *Int J Remote Sens* 2006;**5235**.
124. Topouzelis K, Karanthanassi V, Pavlakis P, Rokos D. Detection and Discrimination Between Oil Spills and Look-Alike Phenomena Through Neural Networks. *ISPRS Journal of Photogrammetry & Remote Sensing* 2007;**264**.
125. Karantzalos K, Argialas D. Automatic Detection and Tracking of Oil Spills in SAR Imagery with Level Set Segmentation 2008;**6281**.
126. Tahvonen K, Pyhaelahti T. The Use of Environmental Data in Reliability: Assessment of Oil Spill Detection by SAR Imagery. *IGARSS* 2006;**3671**.
127. Karvonen J, Heiler I, Similae M, Tahvonen K. Oil Spill Detection with Radarsat-1 in the Baltic Sea. *IGARSS* 2006;**4075**.
128. Shi L, Ivanov AY, He M, Zhao C. Oil Spill Mapping in the Western Part of the East China Sea Using Synthetic Aperture Radar Imagery. *International Journal of Remote Sensing* 2008;**6315**.
129. Muellenhoff O, Bulgarelli B, Ferraro G, Topouzelis K. The Use of Ancillary Metocean Data for the Oil Spill Probability Assessment in SAR Images. *Fresenius Environ Bull* 2008;**1382**.

130. Muellenhoff O, Bulgarelli B, Ferraro G, Perkovic M, Topouzelis K, Sammarini V. Geospatial Modelling of Metocean and Environmental Ancillary Data for the Oil Probability Assessment in SAR Images. *SPIE* 2008;**71100R**.
131. Assilzadeh H, Gao Y. Oil Spill Emergency Response Mapping for Coastal Area Using SAR Imagery and GIS. *Proceedings Oceans Marine Technology Society* 2008.
132. Migliaccio M. A Physical Approach for the Observation of Oil Spills in SAR Images. *IEEE J Oceanic Eng* 2005;**496**.
133. Migliaccio M, Ferrara G, Gambardella A, Nunziata F, Sorrentino A. A Physically Consistent Stochastic Model to Observe Oil Spills and Strong Scatterers on SLC SAR Images. *IGARSS* 2007;**1322**.
134. Gambardella A, Giacinto G, Migliaccio M. On the Mathematical Formulation of the SAR Oil-Spill Observation Problem. *IGARSS* 2008;**III-1382**.
135. Marghany M, Cracknell AP, Hasim M. Comparison Between Radarsat-1 SAR Different Data Modes for Oil Spill Detection by a Fractal Box Counting Algorithm. *Intern J Dig Earth* 2009;**237**.
136. Marghany M, Cracknell AP, Hasim M. Modification of Fractal Algorithm for Oil Spill Detection from Radarsat-1 SAR Data. *Intern J Applied Earth Observ Geoinform* 2009;**96**.
137. Danisi A, Di Martino G, Iodice A, Riccio D, Ruello G, et al. SAR Simulation of Ocean Scenes Covered by Oil Slicks with Arbitrary Shapes. *IGARSS* 2007;**1314**.
138. Zhang F, Shao Y, Tian W, Wang S. Oil Spill Identification Based on Textural Information of SAR Image. *IGARSS* 2008;**IV-1308**.
139. Tello M, Bonastre R, Lopez-Martinez C, Mallorqui JJ, Danisi A. Characterization of Local Regularity in SAR Imagery by Means of Multiscale Techniques: Application to Oil Spill Detection. *IGARSS* 2007;**5228**.
140. Lounis BG, Mercier, Belhadj-Aissa A. Statistical Similarity Measure for Oil Slick Detection in SAR Image. *IGARSS* 2008;**I-233**.
141. Pelizzari S, Bioucas-Dias J. Oil Spill Segmentation of SAR Images via Graph Cuts. *IGARSS* 2007;**1318**.
142. Ferraro G, Bernardini A, David M, Meyer-Roux S, Muellenhoff O, et al. Towards an Operational Use of Space Imagery for Oil Pollution Monitoring in the Mediterranean Basin: A Demonstration in the Adriatic Sea. *Mar Pollut Bull* 2007;**403**.
143. Ferraro G, Meyer-Roux S, Muellenhoff O, Pavilha M, Svetak J, Tarchi D, et al. Long-term Monitoring of Oil Spills in European Seas. *Int J Rem Sens* 2009;**627**.
144. Ferraro G, Baschek B, De Monpellier G, Njoten O, Perkovic M. On the SAR Derived Alert in the Detection of Oil Spills According to the Analysis of the EGEMP. *Mar Pollut Bull* 2010:91.
145. Adamo M, De Carolis G, De Pasquale V, Pasquariello G. On the Combined Use of Sun Glint MODIS and MERIS Signatures and SAR Data to Detect Oil Slicks. *SPIE* 2006;**63600G**.
146. Sipelgas L, Uiboupin R. Elimination of Oil Spill Like Structures from Radar Image Using MODIS Data. *IGARSS* 2007;**429**.
147. Vesecky, Laws JFK, Paduan JD. Monitoring of Coastal Vessels Using Surface Wave HF Radars: Multiple Frequency, Multiple Site, and Multiple Antenna Considerations. *IGARSS* 2008;**I405**.
148. Pinel N, Bourlier C. Forward Propagation of Thick Oil Spills on Sea Surface for a Coastal Coherent Radar. *IGARSS* 2008;**IV-1125**.
149. Demarty Y, Gobin V, Thirion L, Guinvarc'h R, Lesturgie M. Exact Electromagnetic Modeling of the Scattering of Realistic Sea Surfaces for HFSWR Applications. *IGARSS* 2007;**1004**.

150. Schultz-Stellenfleth J, Lehner S, Koenig T, Reppucci A, Brusch S. Use of Tandem Pairs of ERS-2 and ENVIRSAT SAR Data for the Analysis of Oceanographic and Atmospheric Processes. *IGARSS* 2007;**3265**.
151. Goodman RH, Fingas MF. The Use of Remote Sensing for the Determination of Dispersant Effectiveness. *AMOP* 1988;**377**.
152. Jensen HV, Andersen JHS, Daling PS, Noest E. Recent Experience from Multiple Remote Sensing and Monitoring to Improve Oil Spill Response Operations. *IOSC* 2008;**407**.
153. Hollinger JP, Mennella RA. Oil Spills: Measurements of Their Distributions and Volumes by Multifrequency Microwave Radiometry. *Science* 1973;**54**.
154. Parker HD, Cormack D. *Evaluation of Infrared Line Scan (IRLS) and Side-looking Airborne Radar (SLAR) over Controlled Oil Spills in the North Sea*. Warren Spring Laboratory Report; 1979.
155. Hurford N, Martinelli FN. *Use of an Infrared Line Scanner and a Side-Looking Airborne Radar to Detect Oil Discharges from Ships*. Stevenage, UK: Warren Spring Laboratory Report; 1982.
156. Hurford N, Martinelli FN. Use of an Infrared Line Scanner and a Side-Looking Airborne Radar to Detect Oil Discharges from Ships. In: Massin JM, editor. *Remote Sensing for the Control of Marine Pollution*, **405**. Plenum Press; 1984.
157. MacDonald IR, Guinasso Jr NL, Ackleson SG, Amos JF, Duckworth R, Sassen R, et al. Natural Oil Slicks in the Gulf of Mexico Visible from Space. *J Geophys Res* 1993;**351**:16.
158. Brown HM, Bittner JP, Goodman RH. *Visibility Limits of Spilled Oil Sheens*. Calgary, Alberta: Imperial Oil Internal Report; 1995.
159. Brown HM, Goodman RH. In-Situ Burning of Oil in Ice Leads. *AMOP* 1986;**245**.
160. Brown CE, Fingas MF, Monchalin J-P, Neron C, Padioleau C. Airborne Measurement of Oil Slick Thickness. *AMOP* 2006;**911**.
161. Reimer ER, Rossiter JR. *Measurement of Oil Thickness on Water from Aircraft; A. Active Microwave Spectroscopy; B: Electromagnetic Thermoelastic Emission*. Environmental Studies Revolving Fund Report Number 078; 1987.
162. Goodman R, Brown H, Bittner J. The Measurement of Thickness of Oil on Water, in *Proceedings of the Fourth Thematic Conference on Remote Sensing for Marine and Coastal Environments*, ERIM, 1997;**I-31**.
163. Aussel JD, Monchalin J-P. *Laser-Ultrasonic Measurement of Oil Thickness on Water from Aircraft, Feasibility Study*. Québec: Industrial Materials Research Institute Report; 1989.
164. Krapez JC, Cielo P. Optothermal Evaluation of Oil Film Thickness. *J Appl Phys* 1992;**1255**.
165. Choquet M, Héon R, Vaudreuil G, Monchalin J-P, Padioleau C, Goodman RH. Remote Thickness Measurement of Oil Slicks on Water by Laser Ultrasonics. *IOSC* 1993.
166. Brown CE, Fingas MF, Choquet M, Blouin A, Drolet D, Monchalin J-P, et al. The LURSOT sensor: Providing Absolute Measurements of Oil Slick Thickness, *Proceedings of the Fourth Thematic Conference on Remote Sensing for Marine and Coastal Environments*. ERIM, 1997;**I-393**.
167. Brown CE, Fingas MF. Development of Airborne Oil Thickness Measurements. *Mar Pollut Bull* 2003;**485**.
168. Brown CE, Fingas MF, Monchalin J-P, Neron C, Padioleau C. Airborne Oil Slick Thickness Measurements: Realization of a Dream. Altarum: *Proceedings of the Eighth International Conference on Remote Sensing for Marine and Coastal Environments* 2005.
169. Monchalin JP. Optical Detection of Ultrasound. *IEEE T Ultrason, Ferroelectr Freq Con* 1986;**485**.

170. Svejkovsky J, Muskat J, Mullin J. Mapping Oil Spill Thickness with a Portable Multispectral Aerial Imager. *IOSC* 2008;**131.**
171. Pogorzelski SJ. Ultrasound Scattering for Characterization of Marine Crude Oil Spills. In: *Encyclopedia of Environmental Control Technology*, **485**. Gulf Publishing; 1995.
172. Optimare, http://www.optimare.de/cms/en/divisions/fek.html, site accessed April 2009.
173. Swedish Space Corporation, http://www.ssc.se/?id=5772, site accessed April 2009.
174. Armstrong L, Fäst O, Schneider HA, Abrahamsson AH. Integration of Airborne AIS Brings a New Dimension to the Detection of Illegal Discharge of Oil Spills. *IOSC* 2008;**179.**
175. Brown CE, Fingas MF. A Review of Current Global Oil Spill Surveillance, Monitoring and Remote Sensing Capabilities. *AMOP* 2005;**789.**
176. Dean KG, Stringer WJ, Groves JE, Ahlinas K, Royer TC. The *Exxon Valdez* Oil Spill: Satellite Analyses. In: Spaulding ML, Reed M, editors. *Oil Spills: Management and Legislative Implications*, **492**. ASCE; 1990.
177. Dawe BR, Parashar SK, Ryan TP, Worsfold RO. *The Use of Satellite Imagery for Tracking the KURDISTAN Oil Spill.* Environment Canada Report EPS 4-EC-81–6 1981.
178. Alfoldi TT, Prout NA. *The Use of Satellite Data for Monitoring Oil Spills in Canada.* Environment Canada Report EPS 3-EC-82–5 1982.
179. Cross A. Monitoring Marine Oil Pollution Using AVHRR Data: Observations off the Coast of Kuwait and Saudi Arabia during January 1991. *Int J Rem Sens* 1992;**781.**
180. Rand RS, Davis DA, Satterwhite MB, Anderson JE. *Methods of Monitoring the Persian Gulf Oil Spill Using Digital and Hardcopy Multiband Data.* U.S. Army Corps of Engineers Report, TEC-0014, 1992.
181. Al-Ghunaim I, Abuzar M, Al-Qurnas FS. Delineation and Monitoring of Oil Spill in the Arabian Gulf Using Landsat Thematic Mapper (TM) Data. In: *Proceedings of the First Thematic Conference on Remote Sensing for Marine and Coastal Environments.* ERIM 1992;**1151.**
182. Al-Hinai KG, Khan MA, Dabbagh AE, Bader TA. Analysis of Landsat Thematic Mapper Data for Mapping Oil Slick Concentrations—Arabian Gulf Oil Spill 1991. *Arabian J Sci Eng* 1993;**85.**
183. Cecamore P, Ciappa A, Perusini V. Monitoring the Oil Spill Following the Wreck of the Tanker HAVEN in the Gulf of Genoa through Satellite Remote Sensing Techniques, In: *Proceedings of the First Thematic Conference on Remote Sensing for Marine and Coastal Environments.* ERIM 1992;**183.**
184. Voloshina IP, Sochnev OY. "Observations of Surface Contamination of the Region of the Kol'shii Gulf from IR Measurements. *Soviet J Rem Sens* 1992;**996.**
185. Li Y, Yu S, Ma L, Liu M, Li Q. Satellite Image Processing and Analyzing for Marine Oil Spills. *SPIE* 2008;**712311.**
186. Alawadi FC, Amos V, Byfield, Petrov P. The Application of Hyperspectral Image Techniques on Modis Data for the Detection of Oil Spills in the RSA. *SPIE* 2008;**71100Q.**
187. Lotliker A, Mupparthy R, Kumer S, Nayak S. Evaluation of Hi-Resolution MODIS-Aqua Data for Oil Spill Monitoring. *SPIE* 2008;**71500S.**
188. Clark CD. Satellite Remote Sensing for Marine Pollution Investigations. *Mar Pollut Bull* 1989;**92.**
189. Noerager JA, Goodman RH. Oil Tracking, Containment and Recovery During the *Exxon Valdez* Response. *IOSC* 1991;**193.**
190. Li Y, Liu Y, Ma L, Li X. Oil Spill Monitoring Using MODIS Data. *SPIE* 2007;**67955G.**
191. Li Y, Ma L, Yu S, Li C, Li Q. Remote Sensing of Marine Oil Spills and its Applications. *SPIE* 2008;**71450C.**

192. Chust G, Sagarminaga Y. The Multi-angle View of MISR Detects Oil Slicks under Sun Glitter Conditions. *Remote Sensing of the Environment* 2007;**232**.
193. ud din S, Al Dousari A, Literathy P. Evidence of Hydrocarbon Contamination from the Burgan Oil Field, Kuwait—Interpretations from Thermal Remote Sensing Data. *J Environ Manage* 2008;**605**.
194. Casciello D, Lacava T, Pergola N, Tramutoli V. Robust Satellite Techniques (RST) for Oil Spill Detection and Monitoring, In: *Proceedings of MultiTemp 2007—2007 International Workshop on the Analysis of Multi—Temporal Remote Sensing Images* 2007.
195. Brown CE, Fingas MF. New Space-Borne Sensors for Oil Spill Response. *IOSC* 2001;**911**.
196. Brown CE, Fingas MF. Upcoming Satellites: Potential Applicability to Oil Spill Remote Sensing. *AMOP* 2001;**495**.
197. Brown CE, Fingas MF, Lukowski TJ. Airborne and Space-Borne Synergies: The Old Dog Teaches Tricks to a New Bird, In: *Proceedings of the Fifth International Airborne Remote Sensing Conference and Exhibition*. Veridien, 2002.
198. Brown CE, Fingas MF. Synthetic Aperture Radar Sensors: Viable for Marine Oil Spill Response? *AMOP* 2003;**299**.
199. Biegert EK, Baker RN, Berry JL, Mott S, Scantland S. Gulf Offshore Satellite Applications Project Detects Oil Slicks Using Radarsat. *International Symposium: Geomatics in the Era of Radarsat* 1997.
200. Werle D, Tittley B, Theriault E, Whitehouse B. Using Radarsat-1 SAR Imagery to Monitor the Recovery of the Irving Whale Oil Barge, In: *Proceedings of International Symposium: Geomatics in the Era of Radarsat* 1997.
201. Kwarteng A, Singhroy V, Saint-Jean R, Al-Ajmi D. Radarsat SAR Data Assessment of the Oil Lakes in the Greater Burgan Oil Field, Kuwait, In: *Proceedings of International Symposium: Geomatics in the Era of Radarsat* 1997.
202. Ivanov AY, Ermoshkin IS. Mapping of Oil Spills in the Caspian Sea Using the ERS-1.ERS-2 SAR Image Quick-Looks and GIS. *Interspill* 2004.
203. Fortuny J, Tarchi D, Ferraro G, Sieber A. The use of Satellite Radar Imagery in the Prestige Accident. *Interspill* 2004.
204. Torres Palenzuela JM, Vilas LG, Cuadrado MS. *Use of ASAR Images to Study the Evolution of the Prestige Oil Spill off the Galician Coast.* 2006;**1931**.
205. Gauthier M-F, Weir L, Ou Z, Arkett M, De Abreu R. Integrated Satellite Tracking of Pollution: A New Operational Program. *IGARSS* 2007;**967**.
206. Olga LM, Marina B, Tatiana K, Andrey, Vladimir K. Multisensor Approach to Operational Oil Pollution Monitoring in Coastal Zones. *IGARSS* 2008;**III-1386**.
207. Kostianoy A, Lavrova O, Mityagina M, Bocharova T, Litovchenko K, et al. Complex Monitoring of Oil Pollution in the Baltic, Black and Caspian Seas. *Proceedings Envisat Symposium* 2007;**23**.
208. DeAbreu R, Gauthier M-F, Van Wychen W. SAR-Based Oil Pollution Surveillance in Canada: Operational Implementation and Research Priorities, In: *Proceedings OceanSAR 2006—Third Workshop on Coastal and Marine Applications of SAR* 2006.
209. Redman R, Pfeifer C, Brzozowski E, Markian R. A Comparison of Methods for Locating, Tracking and Quantifying Submerged Oil Used During the T/B DBL 152 Incident. *IOSC* 2008;**255**.
210. Wendelboe G, Fonseca L, Ericksen M, Hvidbak F, Mutschler M. Detection of Heavy Oil on the Seabed by Application of a 400 kHz Multibeam Echo Sounder. *AMOP* 2009;**791**.
211. Michel J. Spills of Nonfloating Oil: Evaluation of Response Technologies. *IOSC* 2008;**261**.

212. Pfeifer CE, Brzozowski R, Markian, Redman R. Quantifying Percent Cover of Submerged Oil Using Underwater Video Imagery. *IOSC* 2008;**269**.
213. Pfeifer CE, Brzozowski R, Markian, Redman R. Long-Term Monitoring of Submerged Oil in the Gulf of Mexico Following the T/B DBL 152 Incident. *IOSC* 2008;**275**.
214. Camilli R, Bingham B, Reddy CM, Nelson RK, Duryea AN. Method for Rapid Localization of Seafloor Petroleum Contamination Using Concurrent Mass Spectrometry and Acoustic Positioning. *Mar Pollut Bull* 2009;**1505**.
215. Lehr WJ. The Potential Use of Small UAS in Spill Response. *IOSC* 2008;**431**.
216. Donnay E. Use of Unmanned Aerial Vehicle (UAV) for the Detection and Surveillance of Marine Oil Spills in the Belgian Part of the North Sea. *AMOP* 2009;**771**.
217. Li K, Fingas MF, Paré JRP, Boileau P, Beaudry P, Dainty E. The Use of Remote-Controlled Helicopters for Air Sampling in an Emergency Response Situation, in. *AMOP* 1994;**139**.
218. Goodman RH. Overview and Future Trends in Oil Spill Remote Sensing. *Spill Sci Techn* 1994;**11**.
219. Huisman J. Use of Surveillance Technology to Support Response Decision Making and Impact Assessment. *Interspill* 2006.
220. Carpenter A. The Bonn Agreement Aerial Surveillance Programme: Trends in North Sea Oil Pollution: 1986–2004. *Marine Pollution Bulletin* 2007;**149**.
221. De Dominicis M, Pinardi N, Coppini G, Tonani M, Guarnieri A, et al. *Interspill* 2009.
222. Allen J, Walsh B. Enhanced Oil Spill Surveillance, Detection and Monitoring through the Applied Technology of Unmanned Air Systems. *IOSC* 2008;**113**.

Chapter 11

Oil Spill Trajectory Forecasting Uncertainty and Emergency Response

Debra Simecek-Beatty

Chapter Outline

11.1. INTRODUCTION: THE IMPORTANCE OF FORECAST UNCERTAINTY

Winds and currents play an important role in oil spill transport; and, occasionally, oil moves in a direction that results in unexpected outcomes. One of the most dramatic examples of the latter phenomenon occurred during the 1984 explosion and subsequent breakup of the T/V *Puerto Rican*. The accident resulted in more than 5,678,000 liters of oil spilling into the Gulf of the Farallones in California. Initially, the oil slick moved southerly as forecasted, thereby avoiding the large seabird and mammal colonies at the Farallone Islands. Oil protection and recovery equipment were deployed to the south, leaving the Farallone Islands and the northern California shoreline unprotected and exposed. On day 5 of the spill, the slick made a sudden and remarkable reversal, and overnight, the oil moved northward approximately 50 km from its location on the previous day. The trajectory forecast completely missed the reversal. Oiled birds and shoreline oiling were reported on the Farallone Islands.[1] By day 10, the spill made landfall along the northern California coast

Oil Spill Science and Technology. DOI: 10.1016/B978-1-85617-943-0.10011-5

at Point Reyes.[2] Oil observations and trajectory forecasts were a critical factor in forming daily operational oil recovery and protection decisions. In this instance, the consequences of an inaccurate trajectory forecast were devastating.

An in-depth analysis of the meteorological and oceanographic data collected during the T/V *Puerto Rican* incident suggested that a reversal in the outer continental shelf current transported the oil rapidly to the north. This "dramatic" reversal was likely related to the onset of the Davidson Current or other larger-scale phenomena, which was not predictable with the available oceanographic measurement data.[3] Given these sparse real-time environmental data, today's models would still have difficulty accurately forecasting the current reversal, particularly in the short period required during an emergency response. The difference, however, is that current-day modelers now include uncertainty as part of the trajectory forecast. Today, emergency responders are briefed with both the estimate of the oil movement and alternative possibilities that could present a significant threat to valuable resources.

Most decision makers understand that forecasting is imperfect. The physical processes acting on the oil spill are chaotic and complex, and trajectory forecast uncertainty is inevitable. As shown in the T/V *Puerto Rican* incident and countless other oil spills, there are good practical reasons for disseminating trajectory uncertainty and ensuring that the response community understands the consequences of uncertainty.

Figure 11.1 shows a rough representation of the actual and predicted oil movement for the T/V *Puerto Rican* incident on the fifth day of the spill. The circle is a hypothetical boundary and introduced here for demonstration. The circle represents the possible errors in the model input data and plausible variations in the transport processes. This includes a possible scenario of surface current reversal. In this instance, the area is especially complex and difficult to model so that the level of forecast uncertainty is high.

The large bounded area provides a visual cue to the response community about the limitation of the spill model(s). If a high-value resource is within the uncertainty but not within the "best estimate," responders should seriously consider protecting the resource from oil impact. This example demonstrates that communicating uncertainty information can avoid misrepresenting the capability of oil spill modeling, better convey "what we do know" and "what we don't know," and help responders make more informed decisions and avoid problems.[4] This is "a minimum regret" approach to protecting high-value resources.

11.2. THE BASICS OF OIL SPILL MODELING

Responders, particularly those interested in the operational aspects of a spill, are often in need of a quick, "back-of-the-envelope" estimate of the spill's trajectory. They have a general idea about oil behavior and understand that wind and current are important factors in a trajectory forecast. The technique

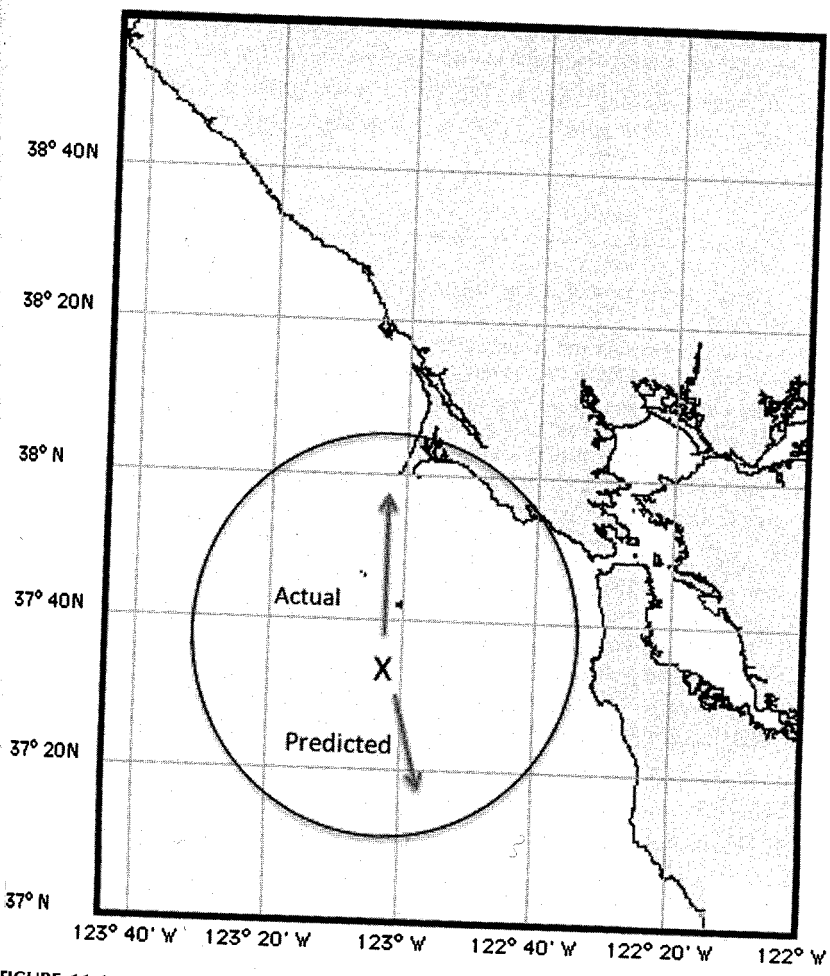

FIGURE 11.1 Actual and predicted oil movement for the T/V *Puerto Rican* spill on day 5. Bounding circle represents uncertainty.[6]

depicted below is a learning tool. It can be very difficult to get a feel for oil spill modeling due to the complicated interactions of the various processes. The main characteristic of a "back-of-the-envelope" trajectory is the use of simplified assumptions for computational simplicity. In this type of estimate, there is no oil weathering, oil spreading, or mixing, and the current is assumed steady and persistent over time. Before using this type of approach, be mindful of these assumptions and recognize that this "best estimate" of the slick movement can have significant errors when extrapolating too far out in time.

The calculation is explained in Figure 11.2 and involves plotting the wind drift and surface vectors on a nautical chart. The sum of the two vectors, the

resultant vector, is the distance traveled by the spill (Figure 11.3). Oil drifts with the surface current at 100% of the current speed, but only at a fraction of the wind speed. Perhaps one of the best known rules of thumb in oil spill modeling is the "3% rule."[6,7] This rule has some theoretical basis and has

1. Plot the last known location of the spill on a nautical chart. Note the time of the observation.
2. Determine the direction and velocity of the surface current. Using oceanographic convention, the surface current is reported as the direction 'to'.
3. Calculate the length of the surface current vector by multiplying the velocity by hours of drift. The hours of drift will be the total duration of the trajectory forecast period. For example, if the surface current velocity is 5 cm/s and the forecast period (hours of drift) is 3 hours, then the length of the surface current vector 0.6 km.
4. Draw a line on the chart extending from the last known location of the spill in the direction of the surface current. Use the compass rose on the chart to orient the line. The length of the line is the length of the surface current vector. In the example, the length of the line would be 0.3 nautical miles. To properly scale the line, use either the scale on the chart or use the latitude as a scale (1degree of latitude equals approximately 111 km).
5. Using the following table, collect the wind data.

Time	Wind Period	No. of Hours	Wind Direction	Wind Velocity	*Leeway (0.03)	Vector Contribution
						km
						km
						km
						km

The time field is time of the observation (or forecast); wind period is start and end time for wind speed and direction; number of hours is duration in hours; wind direction is direction the wind is coming from; wind velocity is wind speed in miles per hour. For these calculations, 3% of the wind speed (0.03) is the leeway or wind drift factor for an oil spill. Multiply wind velocity by 0.03 and enter the value in *leeway field. The vector contribution is the length of the wind vector. It is calculated by multiplying *leeway by number of hours (similar to step 3).

6. Returning to the nautical chart, draw a line extending from the end of the surface current vector (from step 4) in the direction and distance of the first entry in the vector contribution field. At the end of this vector, draw a line in the direction and distance of the second entry in the vector contribution field. Continue this process until all wind vectors are plotted on the chart.
7. The predicted location of the slick is at the end of the last vector plotted. The time for the predicted location is the sum of the number of hours added to the time of the last reported location of the slick. Remember, the surface current is assumed constant for this time period

FIGURE 11.2 A simple prediction of the oil slick movement using vector addition of the components due to wind and current. *Modified from USCG.*[16]

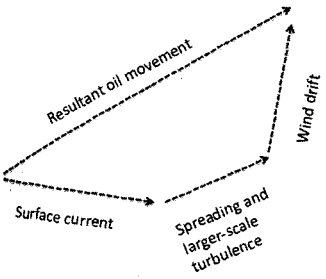

FIGURE 11.3 The sum of the surface current and wind drift vectors are the resultant oil movement.

been verified in the field and laboratory experiments.[8,9] The 3% rule has been successfully used as wind drift factor or leeway for most fresh oil spills.

Uncertainty can be calculated by considering other possible factors. For instance, suppose the spilled oil is a viscous residual fuel oil. The 3% rule represents average conditions, but the actual factor ranges from 1 to 6%.[10] Viscous oils are often subject to overwash by waves. While submerged, viscous oils will only drift at the speed of the water current and, hence, will have a net lower drift speed than that given by the 3% rule. On the other hand, oil caught in the convergences in windrows will move faster than the average 3%.[11] To use uncertainty in the rough estimate, do the calculation with 1% and then 6% of the wind speed. For a 6-hour forecast at a constant 7.7 m/s wind speed, the oil will travel between 1.6 km at 1% and 10 km at 6%. The resulting forecast will be a best guess of a 5 km (3%) displacement with an uncertainty spanning 1.6 km, 1%, to 10 km, 6%. Similar calculations could be employed for uncertainty in the location and direction and speed of the current and wind. Rather quickly, rough calculations using simple vector addition become unwieldy. At this point, serious consideration should be given to applying a more sophisticated approach to the problem.

But what oil spill model(s) should be used? Without a grasp of the underlying principles and assumptions, the mere use of a model does not necessarily lead to a good or better answer. Depending on the spill incident, more than one model may be used because a particular model may perform better in certain situations. Performance varies because models assume different things, represent the physics in different ways, have different resolutions, are initialized differently, and often solve the equations in different ways. Therefore, one model's simulation of a particular aspect of the spill fate and behavior may be rigorous, but it is likely to be weaker in other aspects. A key point to remember is that a model's uncertainty will vary over time as environmental conditions change, and also spatially due to resolution and boundary limitations. Discussions of the strengths and weaknesses of oil spill models can be found in the literature.[12-15]

In general, oil spill models use a combination of Eulerian and Lagrangian methods to simulate oil behavior. The velocity field for winds and currents are derived using Eulerian techniques and are represented as individual velocity

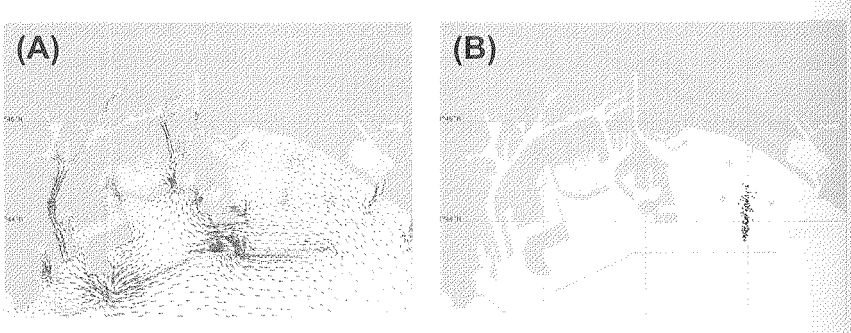

FIGURE 11.4 Examples of current velocity field (A) and particles (B).

vectors at fixed points in the model domain (Figure 11.4A). Oil patches are represented as individual particles that may be referred to as Lagrangian elements (Le's), spillets, or splots.[17,18] The paths of the particles are tracked as they move along the map (Figure 11.4B). Algorithms may vary but most models will need to account for winds, currents, turbulence, and spill details as input data to initialize and move the particles. In most instances, these processes are parameterized from other models or submodels, and they all come with their own uncertainty.

11.3. TRAJECTORY MODEL UNCERTAINTIES

Oil spill models are very sensitive to errors in the initial input data, such as the details of the release and the wind and current forecasts. Furthermore, the mathematical calculations used to simulate oil movement are likely based on empirical approximations and assumptions and are subject to time step and grid limitations. Trajectory model uncertainty refers to changes in the forecast as a result of these errors. Unfortunately, quantitative assessment of the errors in trajectory modeling is difficult and limited. In addition, oil spills are notorious for occurring in areas where the environmental data are temporally and spatially incomplete. This leads to a forecast process that often relies on the forecaster's subjective judgment and approximated input. The ranking of uncertainty as low, medium, and high for trajectory forecasts and the model inputs presented here are subjective. But the forecaster's subjective judgment can be an invaluable resource, and, at least as anecdotal data suggest, it may be better than a model alone at estimating errors.

The fact that the initial estimates are inaccurate and the model itself has inadequacies leads to forecast errors that grow over time. For this reason short-range forecasts usually have less error than long-range forecasts (Table 11.1).

For larger spill events, the model input data should contain fewer errors due to better field observations, such as remote sensing and visual overflights of the spill. The result is that the multiple forecasts produced daily should actually

TABLE 11.1 Uncertainty for Trajectory Forecasts

Oil Spill Trajectory Forecast	Uncertainty
24-hrs	Low – Medium
24 to 48-hrs	Medium
48 to 72-hrs	Medium – High
72+ hrs	High

improve over time. On the first day of a big spill, the uncertainty for the initial forecast will likely range from low to high. On the second day, with more on-scene observations, the uncertainty typically ranges from low to medium. By the third day, the uncertainty should be lower.

A sophisticated model with extensive data input requirements does not necessarily produce a better forecast. There are an optimal number of input parameters that will determine the total model uncertainty. The model output is only as good as the largest error input. This is the reason that the performances of complex models are often no better, and sometimes worse, than the predictions of the simpler models. The back-of-the-envelope calculation in Section 2 used only a one-time surface current measurement with a constant speed and direction lasting for a few hours. This approach has serious limitations in regard to time and spatially varying currents. The advantage is that the results can be quickly passed on to the decision maker. In contrast, an oil spill model that uses forecast currents from a hydrodynamic model with extensive input data requirements (e.g., real-time salinity and temperature data at various depths) may not yield a successful result or be as useful because, for most emergency spill incidents, the input data to initiate a three-dimensional hydrodynamic model is not available in a timely manner. In fact, the three-dimensional model may have to rely on historical data rather than input conditions specific to the spill event. Complex models work well only when the extensive data requirements are satisfied, which rarely can be fulfilled at an oil spill response.

11.3.1. Release Details

In 1987, the barge *Hana* encountered rough seas while transporting Bunker C fuel oil to the Maui power plant in Hawaii. On the southwest side of Molokai Island, the barge reported spilling approximately 11,360 liters of oil. At the time of the incident, the wind forecast was northeast at 13 to 15 m/s for the next 24 hours. Using this information, the trajectory forecast did not indicate any beaching of the oil and indicated the slick would move to the southwest and out to sea. The next day, "a lot of oil" came ashore on Oahu. How could the

TABLE 11.2 Uncertainties for Oil Spill Release Details

Release Details	Uncertainty
Location	Low – Medium
Time	Low – Medium
Day	Low
Night	Low – Medium
Oil Properties	Medium – High
Potential Spill Volume	Low – Medium
Actual Spill Volume	High
Leak Rate	High

trajectory be so wrong? First, the trajectory forecaster was given incorrect information about the release. In fact, the location of the actual release site was off by 18.5 km. Second, the spill volume was later determined to be over 227,000 liters of oil and not 11,360 liters as initially reported. The larger spill volume affected the trajectory as more oil was spread out over a larger area. Third, the overnight winds were actually from the east and not the northeast as initially forecasted.

Unfortunately, there is no reliable way to quantify the errors related to the details of a release. Table 11.2 provides uncertainty for oil spill releases based on decades of experience. If the spill occurs during daylight and there is an experienced overflight observer who can provide coordinates for the spill with a description of the slick, confirmation about the likely spill volume, and a source, then the uncertainty is relatively low. Conversely, release details for a spill occurring at night during a storm or in fog without confirmation from an experienced observer will likely carry a high uncertainty.

11.3.2. Wind

Discussions with the local meteorologist can provide valuable insight about the availability of atmospheric models for a specific area and the model limitations. Ideally, time-dependent and spatially varying wind field from an atmospheric model is imported directly into the oil spill model. However, careful consideration is needed before bringing in the wind forecast. Localized phenomena, which are at a smaller scale than the resolution of the atmospheric model, may have a great influence on the oil spill trajectory. Oil spills spread out quickly, but, even for the larger spills, the slick dimensions are frequently smaller than

the resolution of many atmospheric models. This means, for instance, that the wind at the source of the spill could be different from the wind at the leading edge of the slick. A coarse-resolution atmospheric model may have only one wind vector to represent the entire spill area, much like the back-of-the-envelope calculation in Section 2. Table 11.3 provides examples of typical atmospheric model resolutions. Nested grid systems use a low-resolution, global weather model to provide boundary conditions for high-resolution, regional models. A review of a specific atmospheric model will likely reveal qualitative errors. The other challenge is the time resolution of models. The oil trajectory model may have time steps of 15 minutes, but the wind model may be resolving winds at every hour.

For most spills in estuaries, the regional models are suited for oil spill trajectory modeling. But even with regional models, local effects, such as the land–sea breeze, may not be sufficiently resolved. This can wreak havoc with a trajectory forecast. Shoreline oiling is enhanced with an onshore wind and a falling tide (Figure 11.5A); accurately forecasting the onshore wind is important to getting the trajectory forecast correct. As the tide ebbs, the intertidal areas are exposed, and, if the wind is blowing onshore, the oil adheres and smears down the beach face (Figure 11.5B).

An example of the land–sea breeze phenomenon and the difficulty forecasting the timing of shoreline oiling occurred during the 1990 T/V *American Trader* incident. The vessel ran over its anchor, punctured the hull, and spilled over 1.5 million liters of North Slope crude oil. The spill occurred about 1.5 km off Huntington Beach, California. The net oil slick drift was small due to light winds and a weak surface current. The trajectory forecast repeatedly missed the timing of the shoreline oiling due to the interaction of the land–sea breeze and tide. For a few days, the tides and winds were synchronized such that the falling tide coincided with an offshore wind due to the sea breeze. The oil floated up the beach face with the rising tide, but the oil did not adhere as an offshore wind (land breeze) pushed the oil out to sea. This pattern continued for several days

TABLE 11.3 Grid Resolutions of Atmospheric Models (Modified from Kalnay[19])

Atmospheric Models	Grid Resolution
Climate	Several hundred kilometers
Global weather	50–100 km
Regional meso-scale	10–50 km
Storm scale	1–10 km

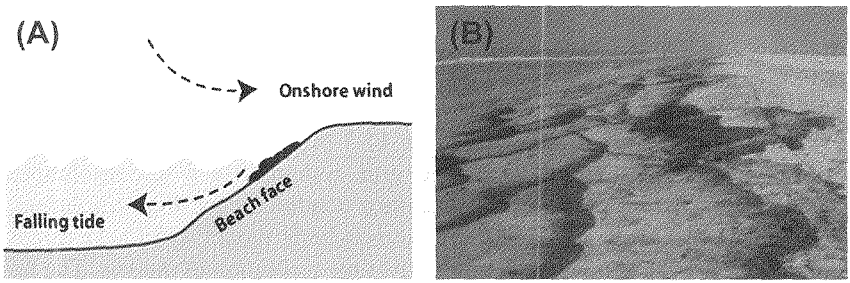

FIGURE 11.5 Falling tide and onshore wind (A), and shoreline oiling due to falling tide and onshore wind (B).

until the tides and land breeze were no longer synchronized, and then the oil stranded on the beach. When local details are important, a higher spatial resolution model should be used and the uncertainty should be carefully conveyed.

If a suitable atmospheric model is unavailable, the marine forecaster can provide details about the wind forecast and its likely error bounds. This requires a good verbal briefing by the meteorologist. The meteorologist can provide information about wind shift timing, the strength of the pressure gradient, location of high/low fronts, and local effects. The result can be a wind data file containing the meteorologist's best estimate and error estimate, which can then be fed directly into the model. As an example, the wind forecast may indicate wind from the south at 7.7 m/s for 12 hours, becoming southwest at 5 m/s. This data is used to compute the best estimate of the wind and is entered into the spill model. If the meteorologist indicates that the forecast wind shift could be off by 3 hours, the wind direction off by 20 degrees, and the speeds by 2.5 m/s, the original wind file is modified or an additional file is created with this data. This represents uncertainty in the wind forecast.

The accuracy of the forecast depends, among other things, on special weather features, length of the forecast period, and ability of the forecasters to localize their prediction to the spill site (Table 11.4). Optimum wind forecast periods are usually between 6 and 24 hours. For a wind forecast beyond five days, serious consideration should be given to using climatological winds and generating a probability guidance product as a trajectory forecast.

11.3.3. Current

In some regions, oil spill modelers have the capability to import time and spatially varying surface current forecasts from ocean circulation models. These models are updated every few hours in a manner similar to atmospheric models. Figure 11.6 shows the expected movement of a hypothetical spill from a continuous release of oil. In this scenario, there are no winds, or turbulent

TABLE 11.4 Uncertainty for the Surface Wind Forecast

Surface Wind Forecast	Uncertainty
24-hr	Low – Medium
48-hr	Medium
72-hr	Medium – High
96+hr	High

mixing processes. There are only surface currents from five different sources: the Global Navy Coastal Ocean Model,[20] the Global Navy Layered Ocean Model,[21] the Global Hybrid Coordinate Ocean Model,[22] California High Frequency Radar,[23] and the Global Sea Surface Height (SSH 2010) model.[24] The NCOM, NLOM, and HyCOM models have similar physics but were initialized with different data, have different grid resolutions, and different numerical methods. The HFR and SSH model forecast currents from observations. It is interesting to note that the HyCOM and NLOM circulation models move the spill in opposite directions, whereas in the short term, a consensus

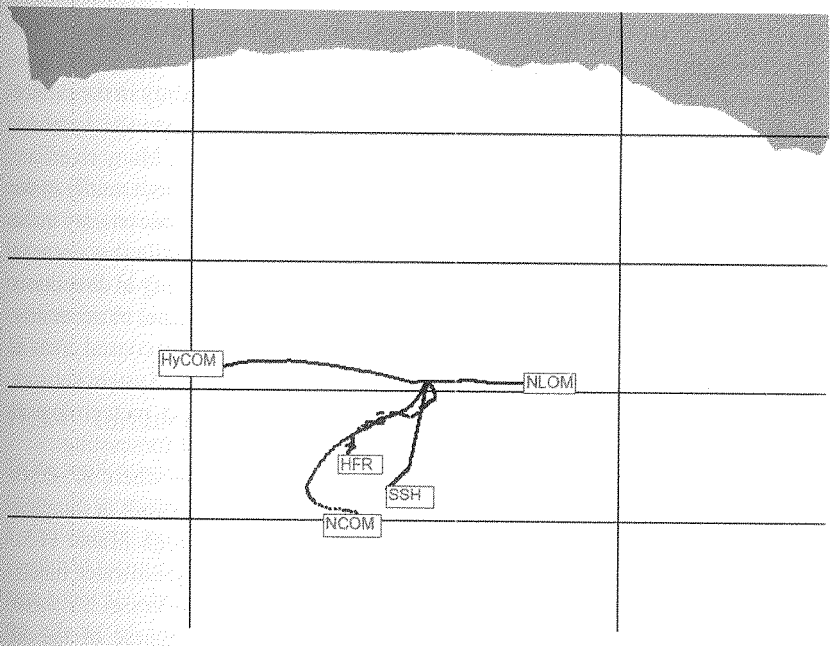

FIGURE 11.6 Particle tracking of a hypothetical spill using multiple current models.

begins to take shape with the HFR, SSH, and NCOM forecasts as the oil is moved offshore. The five-model runs display the uncertainty in the trajectory forecast using just the surface currents from different sources. Further exploration by the forecaster is needed to seek out an explanation of why the model runs differ. Another word of caution: because a model yields results that compare favorably with observations one day or one week, doesn't mean it will do well another day or week. For example, the model may perform better if the surface wind speed is within a specific range. In addition, a model that does well in a certain region may not do well in another region.

In coastal areas without a regional circulation model, simulating the current may become a challenge. Three-dimensional hydrodynamic models will require extensive oceanographic data for input. In a spill response situation, acquiring relevant real-time data is highly unlikely. To work around this problem, modelers may use a combination of real-time observations (e.g., overflights), astronomical tidal predictions, and historical data for the ocean currents, along with a simplified approach to generating currents. All of this takes time to collect and enter into a model. In an emergency response, decision makers need a forecast quickly.

Typically, simplified two-dimensional and one-dimensional models can be more easily calibrated to fit the actual movement of the oil from day to day. It is not unusual that these simple approaches that calibrate currents to daily observations provide better results than large sophisticated models that are difficult to adjust and calibrate. Large, complicated models are often calibrated with historical records that are often short and are collected under environmental conditions very different from those of the spill.

Table 11.5 provides a subjective assessment of the uncertainty in the surface circulation of various water bodies. Closer inspection of a specific hydrodynamic model will likely reveal quantitative error assessment. Many rivers are gauged and controlled by locks and dam systems, so that the uncertainty in the predicted flow is generally low. If the river forecaster provides uncertainty in the flow, this information can be included in the analysis. For spills that occur in tidal-driven estuaries or an ungauged river system, the uncertainty in direction is relatively low (Table 11.5), but the strength of the current may not be accurately known; hence, the overall uncertainty is low to medium. A few coastal areas in the United States have the Physical Oceanographic Real-Time System network that combines real-time monitoring of the water level and meteorological conditions with numerical circulation models for water-level forecasting.

The inner continental shelf extends from the shoreline to where the depth increases to about 120 m. In this area, most of the oil releases result in shoreline impacts, and the uncertainty, unfortunately, is medium to high (Table 11.5). Currents in this zone are dominated by long-shore winds, freshwater runoff, and tides. In the 2002 oil recovery operation of the sunken vessel SS *Jacob Luckenbach*, all of these forces were apparent over the course of the oil removal. The vessel sank in 1953, approximately 30 km southwest of the

TABLE 11.5 Uncertainties in Surface Current

Surface Current	Uncertainty
River	
Gauged	Low
Un-gauged	Low – Medium
Lake	Low – Medium
Shallow water lagoon	Low – Medium
Tidally dominated estuary	Medium
Inner continental shelf	Medium – High
Deep ocean (off continental shelf)	High
Under ice cover	High

Golden Gate Bridge, San Francisco, California. During the course of the operations, when the winds were particularly light, smaller slicks moved to the south and, a few hours later, moved to the north with a weak tide. Without a dominant mechanism forcing the circulation, it became difficult to predict the overall transport of the oil. In contrast to the T/V *Puerto Rican* incident, the inability to predict strong, large-scale forces responsible for the abrupt changes in the current direction and speed resulted in an erroneous forecast on the scale of a few kilometers over the time span of a few hours.

The deep ocean, off the continental shelf, is dominated by drifting oceanic eddies. These density-driven currents have a slow net drift and typically do not affect the currents on the inner shelf. Therefore, their uncertainty is of less importance for most oil spills unless they occur where the shelf is short or nonexistent (e.g., Hawaii). Figure 11.7 shows a snapshot of the SSH-derived currents with large oceanic eddies with current velocity ranging from 5 to 13 cm/s.

11.3.4. Turbulent Diffusion

To the spill modeler, processes smaller than the resolution of the model and timescale motions are most often represented as turbulent mixing and present a challenging problem in oil transport. Virtually all oil spill models use simplified formulas to simulate the horizontal and vertical "mixing" of oil. This term could also be considered the "ignorance coefficient" because it represents the effects of mechanisms that are poorly understood and represented.[26] A common approach is to represent turbulence using a constant diffusion

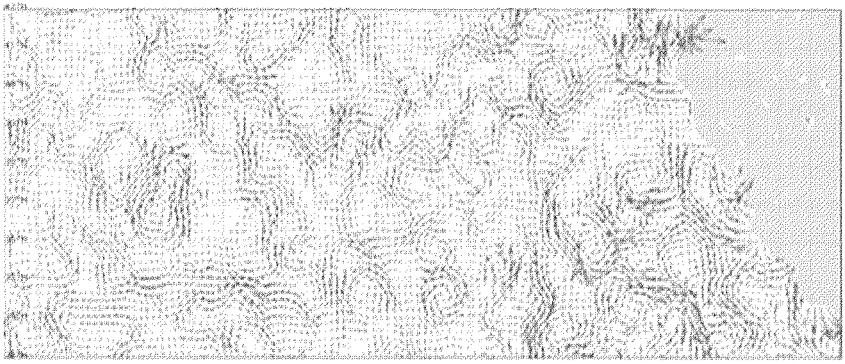

FIGURE 11.7 SSH derived currents. *Modified from CoastWatch.*[24]

coefficient,[26] but there are other options.[27,28] The effects of turbulence will mask small errors in the surface circulation and winds and smooth out the effects of subgrid-scale processes (e.g., Langmuir circulation and convergence zones). The consequence of this turbulent diffusion approach is a loss of resolution that increases over time.

11.3.5. Oil Weathering

The rate and degree with which an oil weathers affects its wind-drift factor (or leeway) and hence, its trajectory. As oil weathers, its chemical properties change. Density will increase as the light fractions evaporate, and both viscosity and density will increase if the oil emulsifies. These property changes will affect wind drift and the oil's ability to disperse. Uncertainty in weathering predictions is generally lower for spills of light refined products, which rapidly dissipate and do not form stable emulsions (e.g., gasoline and diesel). A few crude oils have also been studied, both in the lab and in field trials for weathering behavior. This extra information makes prediction about their behavior more reliable. For other types of oils, such as intermediate fuel oils, where the available data only vaguely characterizes their weathering characteristics, uncertainty is high for the transport, fate, and effects of the oil, and the uncertainty grows over time. For the best estimate trajectory, the modeler may select the oil in the model that best represents the product spilled. To define uncertainty bounds, the oil can be modeled as a conservative quantity, which is neither evaporated nor dispersed into the water column. Field observations can be used to help calibrate weathering of the oil, which in turn will help improve trajectory estimates.

The slick drift factor or leeway changes over time because, initially, the spill appears as a large cohesive film but eventually tears apart into smaller patches or tarballs. Table 11.6 shows different wind drifts for various oils and the

TABLE 11.6 Wind Drift Uncertainty and Distance Traveled for Various Oils

Oil Type	No. of Hours	Wind Velocity (m/s)	Wind Drift or Leeway (%)	Vector Contribution (km)
Gasoline	24	7.7	3 to 4	22–30
Diesel	24	7.7	3 to 4	22–30
Fresh IFO	24	7.7	3	22
Fresh crude oil	24	7.7	3 to 4	22–30
Weathered IFO	24	7.7	2 to 3	13–22
Emulsified oil	24	7.7	1 to 2	5.5–13
Scattered tarballs	24	7.7	0.5 to 2	3.7–13

distance likely to travel with a 7.7 m/s wind for 24 hours. The drift factors are estimates based on the modeler's experience matching visual observations of the slick with the trajectory forecast. For oils with ranges, like the scattered tarballs, this represents the uncertainty in the wind drift and can be modeled by randomly selecting a slick drift between 0.5 and 2% of the wind speed for each patch of oil at each model time step. Since the wind speed is not likely constant, this modeling technique can also simulate wind gusts.

Weathering of oil will also determine the type and severity of impacts expected from the oil spill and, consequently, the amount of response personnel and equipment. For example, if the expected impact from a spill were scattered coin-sized tarballs every 10 m along the shoreline, the cleanup response effort would be very different than that for a spill resulting in a 2-m-wide band of emulsified oil. Therefore, it is important to not only forecast where and when oil will go but what type of impact to expect. Any uncertainty related to the fate of the oil should be conveyed with the trajectory forecast.

11.3.6. Ensemble Forecasting

The 1976 *Argo Merchant* grounding off Nantucket Island, Massachusetts, was one of the most studied oil spills in history with over 200 scientists participating in the response effort. Five independent research teams provided operational forecasting of the oil distribution.[29,30] The on-scene commander was presented with five forecasts; each displaying different trajectories. This was the beginning of ensemble forecasting in spill response. Ensemble forecasting involves generating a collection of forecasts based on varying initial conditions, model parameters, and physics. The forecasts can be a compilation of outputs from different models[31] or from the same model using different boundary conditions

and data choices[32,33]. Ensemble forecasting has developed into the primary means of presenting trajectory forecast uncertainties.

The results of ensemble forecasting must be communicated so that the decision maker can interpret and understand the information. Figure 11.8A shows an example a visual graphic of the trajectory forecast that uses the best available input data. Here, particles simulating oil movement are converted so that darker contours indicate a higher concentration of particles.[4] The forecast provides only one prediction of the future, with no information about uncertainty. Decision makers are likely to move much of the available oil recovery and protection resources to the area where the contour contacts the shoreline. This is often the type of forecast requested by emergency responders to support operational decisions, even though it is not the complete picture needed for optimum response.

Figure 11.8B shows a visual representation of ensemble forecasting. The confidence limit represents the output from a series of trajectory forecasts. In addition to output from multiple models, the forecaster may have used his or her subjective judgment and considered other plausible, what-if, scenarios. The scenarios may have included what if the weather forecast of a frontal passage is off by 12 hours; the release time is off by 1 hour, and the surface current speed off by 20 cm/ s? How would this affect the oil movement? The confidence limit is a visual cue to the decision maker that represents the boundary of the output from multiple models and/or output from multiple runs from one model. The product conveys the likely locations of oil and provides responders with not only a best estimate trajectory, but also other possibilities that could result in a significant threat.

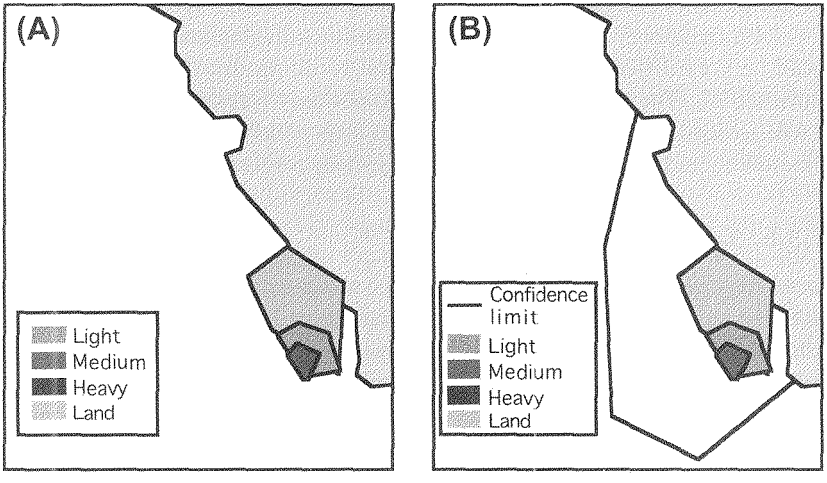

FIGURE 11.8 Examples of a trajectory forecast without uncertainty (A) and with uncertainty (B).

11.3.7. Communicating Trajectory Forecast Uncertainty

Communicating the uncertainty of the trajectory forecast is critical to users. It allows them to make decisions based on the reliability of the forecast and the consequences from inaccuracies in the forecast. The general public is familiar with probabilities associated with forecasts thanks in large part to National Oceanic and Atmospheric Administration's (NOAA's) National Weather Service producing forecasts for hurricanes, tornadoes, and precipitation in terms of probabilities. However, for spill movement, it is not possible to compute the uncertainty probabilities for where and when the oil will come ashore. The number of spills with adequate field observations is not sufficient for statistical analysis. Well-documented marine oil spills with robust data sets are the exception, and experimental spills in the ocean are quite few in number. Ocean-surface current drifter studies cannot provide probabilities of the oil movement for any given day, under any given condition. Given the environmental variability and model shortcomings, there is not enough data to generate probabilities for oil spill trajectory forecast. As a result, the oil spill trajectory forecast uncertainty must be conveyed in a way other than with probabilities.

Galt proposed a digital standard that presents uncertainty of the trajectory forecast that alleviates the "language of probabilities" problem.[4] The trajectory model is first used with the best available input data. It is then run a second time to set the uncertainty or confidence bounds. In the uncertainty model run, each of the particles can be thought of as a centroid of an independent spill and is assigned its own wind and current data. The resultant spread of the particles represents an ensemble of spills. The distribution is not related to oil concentration but represents an ensemble of different spills. However, to make this work, the expert forecaster needs to specify uncertainty bounds for the currents, winds, and other various inputs parameters. A standardized method does not exist, and the approach relies on the forecaster's subjective judgment. Figure 11.9 shows an example of the NOAA standard for visually representing uncertainty. The graphic is designed to express the amount of complexity and uncertainty in a particular forecast without presenting probabilities. Post-processing software, independent of the oil spill model, was used to generate the graphic. The product includes a base map, contoured particles, and an outer confidence limit. The bottom of Figure 11.8 contains a scale with eight patterns of oil distribution. By looking at the scale bar, emergency responders can quickly determine how the light, medium, and heavy contours relate to the oil distribution observed on-scene and, from this, develop response options.

Regardless of the way uncertainty is expressed to the decision maker, it needs to be done. To do this successfully, the forecaster realistically expresses uncertainty for every input parameter as well as the numerical uncertainty inherent with the model. This is a daunting task, particularly for estimating uncertainty with oil type, oil volume, spill location, spill time, and oil slick observational data.

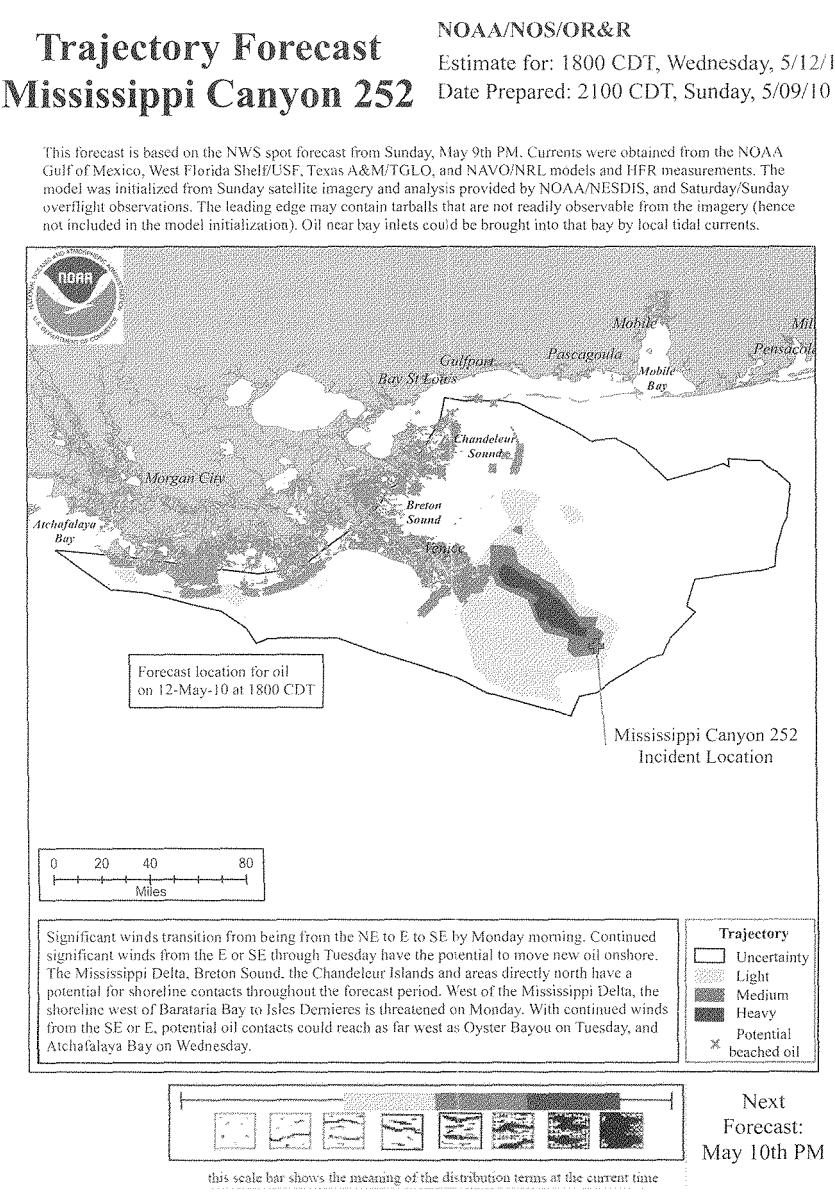

FIGURE 11.9 Sample trajectory forecast product.

11.4. TRAJECTORY FORECAST VERIFICATION

How accurate are oil spill models? The question is an obvious one but difficult to answer. The back-of-the-envelope calculation presented in Section 2 is a good place to start. For demonstration purposes, the hypothetical calculation

or forecast indicates that the oil spill remains offshore. Field observation data is needed for verification, and for this demonstration, the location of every piece of oil is known. Suppose the field data indicates the bulk of the oil remained offshore and only a small amount of oil came ashore. Was the model or, in this case, the calculation accurate? The skills of a trained forecaster in this process are important. The forecaster can make multiple calculations or multiple models runs and include uncertainty. If the small amount of oil onshore was within the uncertainty of the calculation, then the forecast was accurate.

Model errors can occur for various reasons and are not consistent over time or space; therefore, it is important to have a skilled forecaster verify the model output. Oil spill models cannot precisely predict the movement of every patch of oil. Some models may perform better than others under different conditions, but, inevitably, oil spill models will be wrong. Quantifying the model's error is not easy due to the constraints found at most oil spill incidents (e.g., observations of surface oil that are both temporally and spatially incomplete). This contrasts with forecasting in other fields. For example, NOAA's National Hurricane Center has precise metrics to measure hurricane forecasts versus observations. At this time, precise metrics to measure oil spill trajectory forecasts do not exist. Ideally, a formal methodology would be developed for the comparison of the trajectory forecast with observed field data. Such a comparison would provide a means for assessing the model's performance relative to other spill models. A challenge for the oil spill trajectory forecaster is determining whether a model, despite its uncertainties, can be used to make a useful forecast. The challenge for decision makers is to determine how to use the forecast and its inherent uncertainties to make an informed decision. This section provides a brief description within which a forecaster and decision maker can determine a model's performance for accurately predicting the oil movement.

Field observation data are the basis of model verification. However, collecting data from field experiments and during an emergency response is not simple. It is extremely difficult and often illegal or impossible to stage experimental oil spills in the open ocean. If permission is granted, the experiments are small-scale and conducted over a short time period: usually hours, not the days needed for characterizing a specific set of conditions. This makes it difficult to test models against field data due to the varying environmental conditions and a mismatch between model scales and experiment scales. Attempts to use data from emergency response are always problematic because the on-scene observations of the oil distribution contain significant errors. It is not always known how much of the oil was spotted by the observer or what part of the slick was seen. Overflights of the spill may not be conducted due to poor weather or aircraft availability resulting in large time gaps between observations. Observational errors can also result from observers reporting "false positives" such as kelp beds, silt plumes, algae, and jellyfish, to name but a few. Remote-sensing techniques are imperfect as well because of limitations of the

sensor, availability of assets (aircraft and satellite), and weather conditions. Due to these constraints, other approaches need to be developed to evaluate the performance of oil spill models.

A common approach for evaluating an oil spill model's performance is a hindcast. In a hindcasting, the release details of wind and current data at the time of the incident are entered into a model to see how well the output matches the reported location of oil. If the hindcast accurately shows the oil movement as known to have occurred, the model is considered successful. The comparison between the hindcast and observations mostly consist of visual inspection rather than statistical evaluation due to the problems with collecting oil observation data.[34-37] Hence, there is a need for an experienced forecaster who understands the uncertainty associated with oil fate and observations.

Oil observations can be used to make model adjustments so that the hindcast matches the observed distribution of the oil. This is model calibration, and an example can be found in Turrell.[38] Parameters within the model are calibrated to match the movement of the spill. Again, the process is subject to error due to problems in collecting field observations and requires a knowledgeable forecaster who knows which model parameters to modify for a best fit. Other approaches are to compare model estimates and measurements to field data on a spill-by-spill basis and then calibrate a model with that comparison.[17,39] However, caution is needed in this approach to avoid using a calibrated model for different geographic locations and environmental conditions. Every spill is a unique event, and every location has its own environmental challenges.

The remaining technique for evaluating oil spill model performance that appears in the literature is validation. Oil spill trajectory models can never be conclusively validated because they never completely simulate reality.[40] In general, validated models are those that have shown correspondence to experimental data. A more accepted approach is a model evaluation process in which the results of the model are determined to be sufficient and, that despite the uncertainties, can be used in decision making.[41] In all cases, the model's documentation should provide clear understanding of why and how the model can be used.

11.4.1. Diagnostic Verification

Forecast verification is an integral part of the forecast process in an emergency response as the spill situation and environmental conditions can change very rapidly. As an example, the vessel(s) involved in the accident may be unstable. A submerged pipeline may have a small continuous leak with a potential for a much larger release of oil. The weather is constantly changing, and the currents are changing with tides and coastal events. Therefore, the model results need to be continuously compared to observed data by a skilled forecaster during a spill response. The forecaster needs to compare the predictions with field reports and decide if the model parameters are sufficiently correct or

require modifications to match the field data. Calibrating the model(s) with the previous day's overflight observations does not ensure that the forecast will match the next day's overflight, but it will give the forecaster an idea of which model parameters to monitor. During the T/V *Puerto Rican* incident, discussed in Section 1, daily adjustments were made to the model, but the forecasters never anticipated a reversal in the surface current, not even with a predicted wind shift.

The more serious the consequence of forecast error, the more important monitoring and collection of field data. Essentially, the forecaster is calibrating the model to the spill during the response. Figure 11.10A shows an example of a map of the oil distribution for an oil spill. The map was used to verify the spill model. The model is run from the start of the spill and stopped at the time of the overflight observation. Since no model can simulate reality perfectly, visual inspection of the overflight map and the model run likely indicates differences in the oil location. Adjustments are likely made to model parameters so that the model matches the overflight map. The calibrated model can then be used to generate a forecast (Figure 11.10B). In a spill, forecast verification is an integral part of the forecast process.

11.5. SUMMARY AND CONCLUSIONS

In this chapter, the fundamentals of uncertainty related to oil spill fate and transport forecasting were presented. The T/V *Puerto Rican* incident was used as an example of the importance of uncertainty in the trajectory forecast. This event showed that an estimate of the uncertainty in the forecast provides more information than a single best estimate that uses the initial model input data. Decision makers, who only consider the single best estimate and largely ignore the forecast uncertainty, tend to make less than optimal decisions. If an incident similar to the T/V *Puerto Rican* were to occur today, close monitoring of the spill by field observations (e.g., overflights, surface current buoys, and remote sensing) and communicating the trajectory forecast uncertainty will help responders make more informed decisions and avoid problems.

Presenting both the best estimate and the uncertainty in the trajectory forecast provides the decision maker the opportunity to support a minimum-regret decision-making strategy.[42] At nearly every spill, there is always a limited amount of resources available for shoreline protection and cleanup. With both the best estimate and uncertainty, decision makers can weigh the wisdom of directing the cleanup toward the most likely spot for oil as opposed to defending less likely but more environmentally important locations.[43,44] Overflight operations can conduct more intelligent surveillance, using uncertainty or confidence forecast boundaries to determine their flight paths and prevent any oil from sneaking past the response efforts. The public can be provided with a more realistic representation of what is known about the slick location, avoiding false expectations concerning trajectory accuracy.

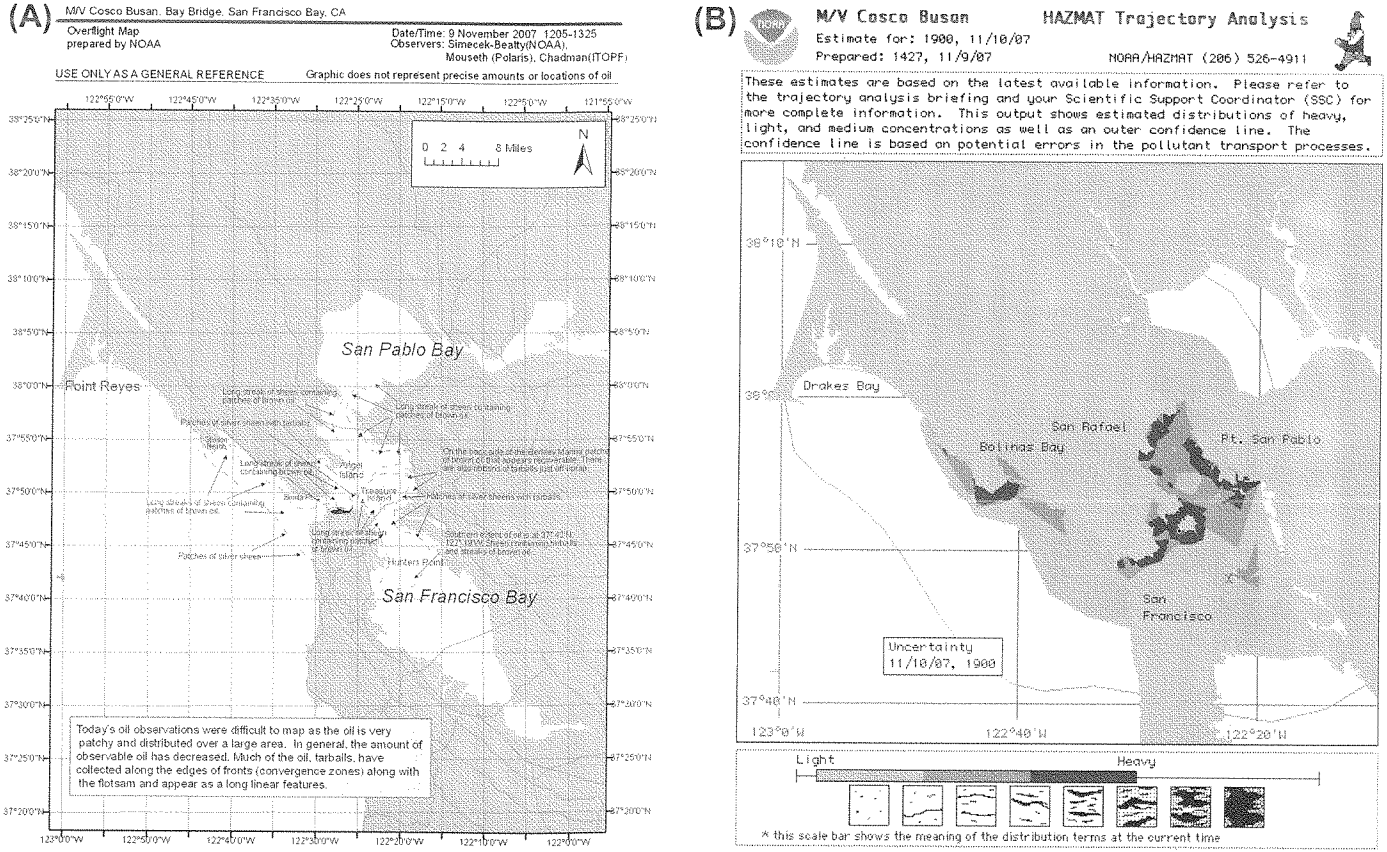

FIGURE 11.10 Map of oil distribution (A) and oil spill trajectory forecast (B).

The conclusions from this chapter are simple but important. Oil spill fate and transport forecasting contains errors and, under certain circumstances very large errors. As a result, it is important to convey uncertainty bounds with the forecast. Good field data and a skilled forecaster are needed to adequately calculate, portray, and communicate the uncertainty in the predictions.

ACKNOWLEDGMENTS

The findings and conclusions in this chapter are those of the author and do not necessarily represent the views of the National Oceanic and Atmospheric Administration (NOAA). This chapter arose from a series of training conducted by NOAA for the U.S. Coast Guard. We hope this chapter performs the function of introducing relevant principles of modeling uncertainty to the next generation of spill responders. The author would like to acknowledge Glen Watabayashi, Dr. Alan Mearns, and Mark Dix for their assistance in preparing this chapter. Thanks also to Jeffery Lankford for kindly providing Figure 11.1.

REFERENCES

1. PRBO (Point Reyes Bird Observatory). *The Impacts of the T/V Puerto Rican Oil Spill on Marine Bird and Mammal Populations in the Gulf of Farallones.*
2. *FMSA (Farallones Marine Sanctuary Association), Coastal Ecosystem Curriculum: Oil Spills.* http://www.farallones.org/documents/education/oilspills.pdf, 2002.
3. Breaker LC, Bratkovich A. Coastal—Ocean Processes and Their Influences on the Oil Spilled of San Francisco by the M/V Puerto Rican. *Mar Environ Res* 1993;**1003**.
4. Galt JA. Uncertainty Analysis Related to Oil Spill Modeling. *Spill Sci Techn Bull* 1998;**231**:4.
5. Lehr WJ. *Personal Communication to Debra Simecek-Beatty*; February 8, 2010.
6. Smith CL. Determination of the Leeway of Oil Slicks. In: Wolfe DA, Anderson JW, Button DK, Malins DC, Roubal T, Varanasi U, editors. *Fate and Effects of Petroleum Hydrocarbons in Marine Ecosystems and Organisms*, **351**. New York: Pergamon Press; 1976.
7. Huang J. A Review of the State-of-the-art of the Oil Spill Fate/Behavior Models. *IOSC* 1983;**313**.
8. Wu J. Sea-Surface Drift Currents Induced by Wind and Waves. *J Phys Oceanogr* 1983;**1441**.
9. Fallah MH, Stark RM. Random Drift of an Idealized Oil Patch. *Ocean Eng* 1976;**89**.
10. Lehr WJ, Simecek-Beatty D. The Relation of Langmuir Circulation Processes to the Standard Oil Spill Spreading, Dispersion and Transport Algorithms. *Spill Sci Tech Bull* 2000;**247**.
11. Leibovich S. *Surface and Near-surface Motion of Oil in the Sea,* Contract 14-35-00001-30612, Minerals Management Service, U.S. Department of Interior; 1997.
12. Yapa PD, Shen HT. Modeling River Oil-Spills—A Review. *J Hydr Res* 1994;**765**.
13. ASCE Task Committee on Oil Spills. State-of-the-Art Review of Modeling Transport and Fate of Oil Spills. *J Hydraulic Eng* 1996;**594**.
14. Cekirge HM, Palmer SL. Mathematical Modeling of Oil Spilled into Marine Waters. In: Brebbia CA, editor. *Oil Spill Modeling and Process*. Southhampton, UK: WIT Press; 2001.
15. French-McCay DP. Oil Spill Impact Modeling: Development and Validation. *Environ Toxicol Chem* 2004;**2441**.
16. USCG, *United States Coast Guard National Search and Rescue Manual*, Vol. II: Planning Handbook; 1991.

17. French-McCay D. Development and Application of Damage Assessment Modeling: Example Assessment for the North Cape Oil Spill. *Mar Poll Bull* 2003;**341**.
18. Beegle-Krause CJ. Advantages of Separating the Circulation Model and Trajectory Model: GNOME Trajectory Model Used with Outside Circulation Models. *AMOP* 2003;**825**.
19. Kalnay E. *Atmospheric Modeling, Data Assimilation, and Predictability.* Cambridge, UK: Cambridge Univ. Press 2003.
20. *NCOM (Navy Coastal Model), Naval Research Laboratory.* http://www7320.nrlssc.navy.mil/global_ncom, 2010.
21. *NLOM (Global Navy Layered Model), Naval Research Laboratory.* http://www7320.nrlssc.navy.mil/global_nlom, 2010.
22. *HyCom (Global Hybrid Coordinate Ocean Model), National Ocean Partnership Program.* http://www.hycom.org/, 2010.
23. *HFR (California High Frequency Radar), Southern California Coastal Ocean Observing System.* http://sccoos.org/data/hfrnet, 2010.
24. *CoastWatch.* http://coastwatch.noaa.gov/, 2010.
25. NRC (National Research Council). *Principles for Evaluating Chemicals in the Environment.* National Academy of Sciences; 1975.
26. Okubu A. *Diffusion and Ecological Problems: Mathematical Models.* Dordrecht, Holland: Springer-Verlag; 1980.
27. Elliot AJ, Dale AC, Proctor R. Modeling the Movement of Pollutants in the UK Shelf Seas. *Mar Poll Bull* 1992;**614**.
28. Thibodeaux L. *Chemodynamics: Environmental Movement of Chemicals in Air, Water, and Soil.* New York, NY: John Wiley & Sons; 1979.
29. Grouse PL, Mattson JS. *The Argo Merchant Oil Spill, National Oceanic and Atmospheric Administration.* Boulder, CO: Environmental Research Laboratory; 1977.
30. Pollack AM, Stolzenbach KD, *Investigations in Response to the Argo Merchant Oil Spill, Sea Grant Program, Report No. MITSG 78-8.* Cambridge, MA: Crisis Science; 1978.
31. Daniel P, Dandin P, Josse P, Skandrani C, Benshila R, Tiercelin C, et al. Towards Better Forecasting of Oil Slick Movement at Sea Based on Information from the Erika. In: *Proc. Third R&D Forum on High-Density Oil Spill Response.* Brest, France: Int'l. Maritime Org; 2002.
32. Sebastiao P, Guedes Soares C. Uncertainty in Predictions of Oil Spill Trajectories in a Coastal Zone. *J Mar Sys* 2006;**257**.
33. Sebastiao P, Guedes Soares C. Uncertainty in Predictions of Oil Spill Trajectories in Open Sea. *Ocean Eng* 2007;**576**.
34. Venkatesh S. Model Simulations of the Drift and Spread of the *Exxon Valdez* Oil Spill. *Atmosphere-Ocean* 1990;**90**.
35. Venkatesh S, Crawford WR. Spread of Oil from the *Tenyo Maru*, off the Southwest Coast of Vancouver Island. *Natural Hazards* 1993;**75**.
36. Proctor R, Elliot AJ, Flather RA. Forecast and Hindcast Simulations of the *Braer* Oil Spill. *Mar Pollut Bull* 1994;**219**.
37. WDOE (Washington Department of Energy), *Puget Sound Trajectory Analysis Planner (TAP) Technical Documentation.* Spill Prevention, Preparedness, and Response Program, Publication#03-08-007; 2003.
38. Turrell WR. Modeling the *Braer* Oil Spill—A Retrospective view. *Mar Pollut Bull* 1994;**4**.
39. Vethamony PK, Sudheesh MT, Babu S, Jayakumar R, Manimurali AK, Saran LH, et al. Trajectory of an Oil Spill of Goa, Eastern Arabian Sea: Field Observations and Simulations. *Environ Pollut* 2007;**438**.

40. Anderson MG, Bates PD. *Model Validation Perspectives in Hydrological Science*. New York, NY: John Wiley & Sons; 2001.
41. Pascual P, Stiber N, Sunderland E. *Draft Guidance on the Development, Evaluation, and Application of Regulatory Environmental Models*. U.S. Environmental Protection Agency, http://www.epa.gov/crem/knowbase; 2003.
42. Galt JA. The Integration of Trajectory Models and Analysis into Spill Response Information Systems. *Spill Sci Tech* 1997;**23**.
43. Wirtz KW, Liu X. Integrating Economy and Uncertainty in an Oil-Spill. DSS: The Prestige Accident in Spain. *Estuar Coast Shelf Sci* 2006;**525**.
44. Wirtz KW, Baumberger N, Adam S, Liu X. Oil Spill Impact Minimization Under Uncertainty: Evaluating Contingency Simulations of the Prestige Accident. *Ecolog.l Econ* 2007;**417**:61.